Evidenze astrofisiche e cosmologiche della materia oscura

Paolo de Bernardis

Dipartimento di Fisica, Università La Sapienza, Roma

Pomeriggio di discussione su materia oscura

INFN Sezione di Roma - Sapienza

20/gennaio/2014

INFN Istituto Nazionale di Fisica Nucleare SEZIONE DI ROMA

Dark Matter

In astrophysics and cosmology **two** types of dark matter are considered :

a) Dark because it has not been detected yet, using electromagnetic radiation, but **is** electromagnetically interacting (the so-called *missing baryons*)

b) Dark because it **does not** interact electromagnetically (the so-called *non-baryonic dark matter*, e.g. massive neutrinos, or WIMPs)

Here we will focus on b), which might account for >20% of the mass-energy density in the Universe.

Galaxies, all the way down !

What is a galaxy made of

- Stars and their remnants (mass estimated from stellar evolution and luminosity measurements)
- Interstellar gas and dust (mass estimated from absorption and emission)
- A large halo of ionized gas (mass estimated from absorption of X-rays coming from other galaxies) see e.g. Gupta et al. 2012, ApJ, 756, L8
- Is this baryonic mass all what is needed ?

Dark matter in galaxies

- The mass density of baryons in galaxies is not large enough to explain their dynamics.
- Stars in galaxies orbit :
  - Circular orbits in the disk of spiral galaxies
  - Randomly oriented orbits in elliptical galaxies
- Orbital velocities can be measured and compared to theory (Newton's dynamics) to infer galaxy masses.


NGC3198


NGC3198

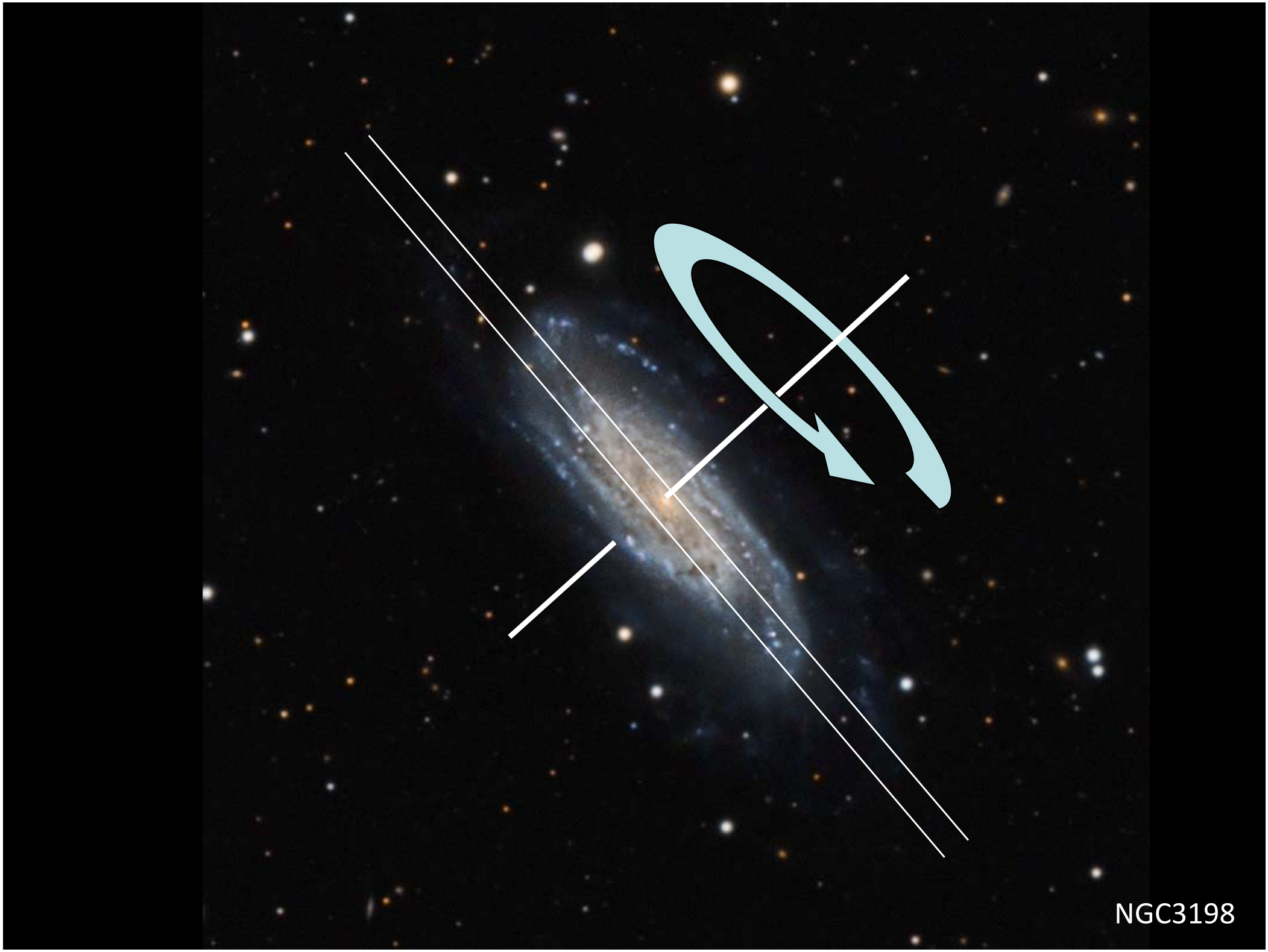
NGC3198

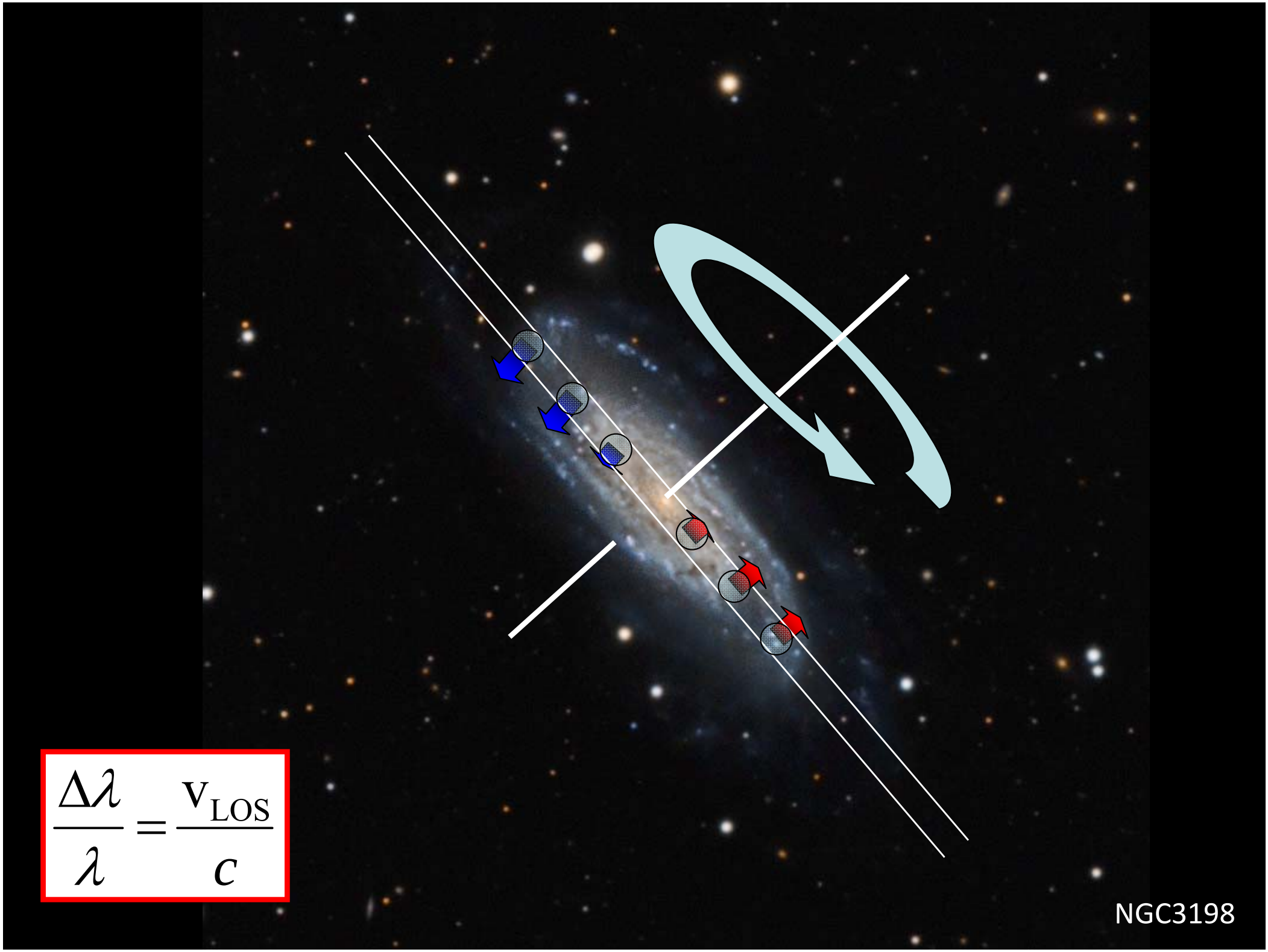
$\frac{\Delta\lambda}{\lambda} = \frac{v_{LOS}}{c}$
NGC3198

$$v_{LOS} = c\frac{\Delta\lambda}{\lambda}$$

Edge-on spiral galaxy :

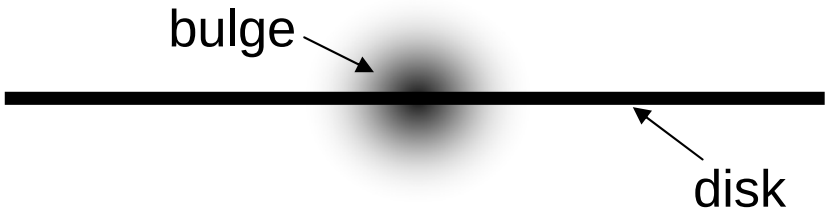

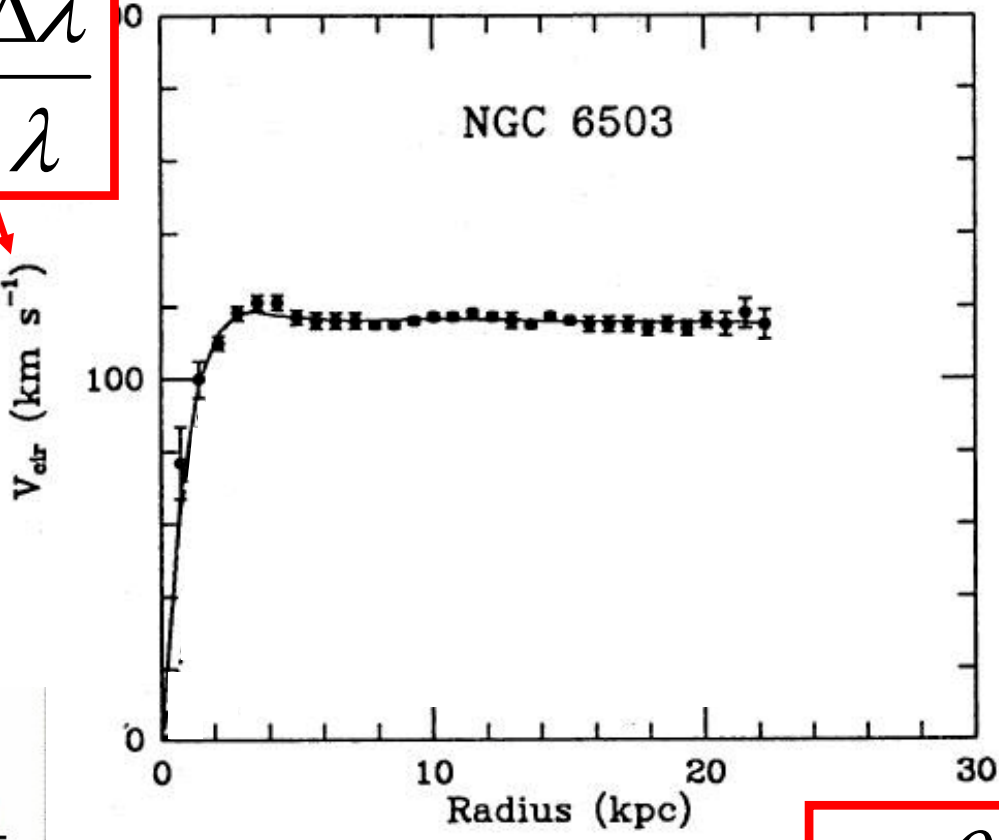

$$r = \theta D$$

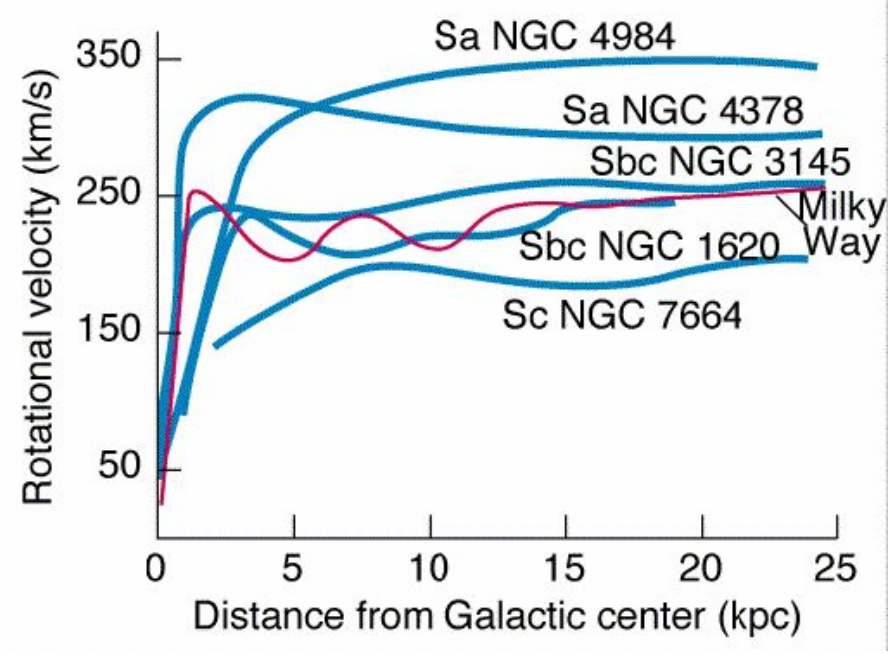

• All the rotation curves share the same basic trend (linear rise in the bulge region, approximately constant at larger distances)

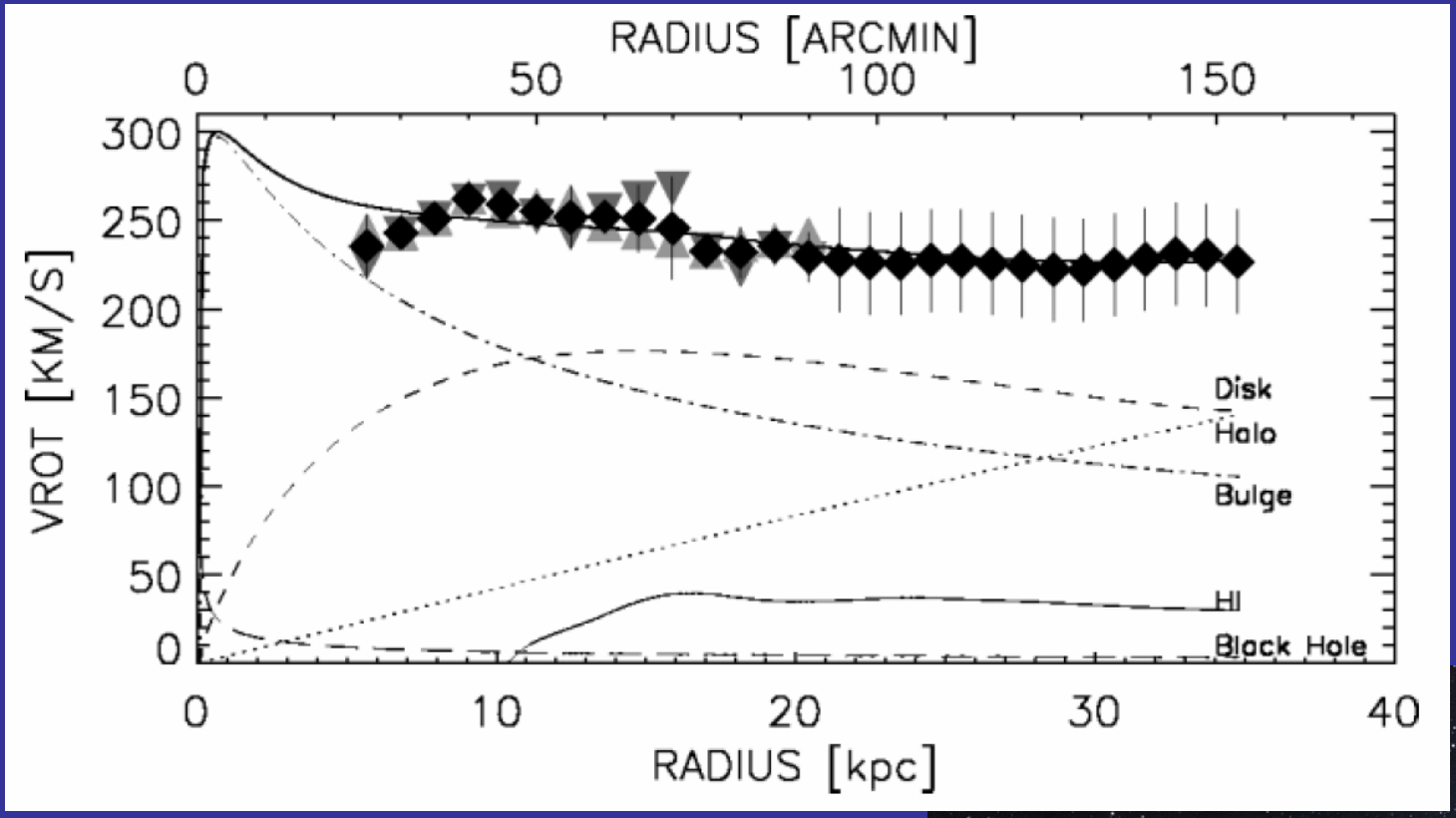

M31

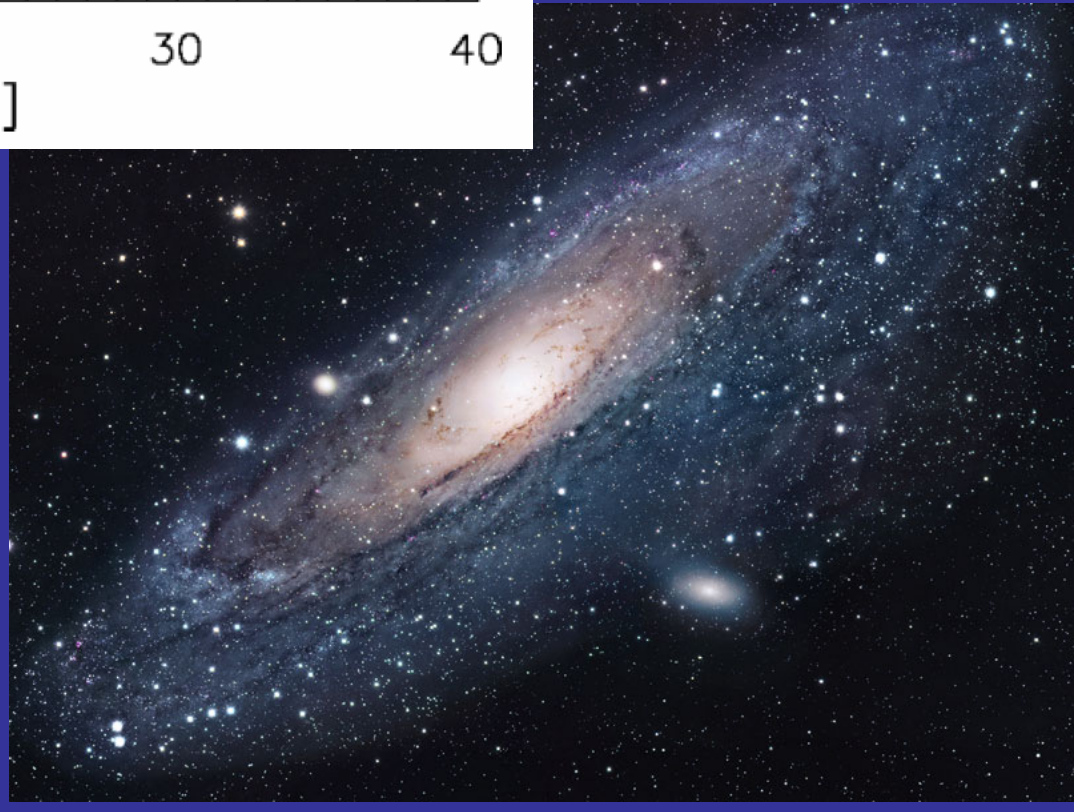

• Using 21 cm radiation the constant trend at large distances is confirmed at radii >> than the optical radius.

Edge-on galaxy :

$$v = c\frac{\Delta\lambda}{\lambda}$$

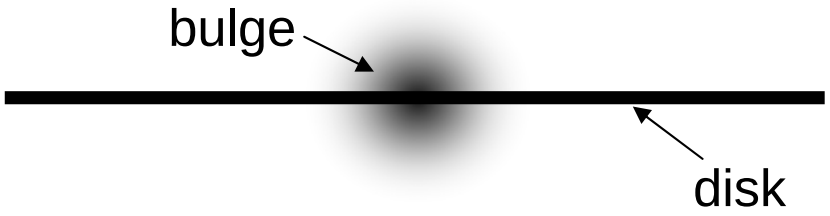

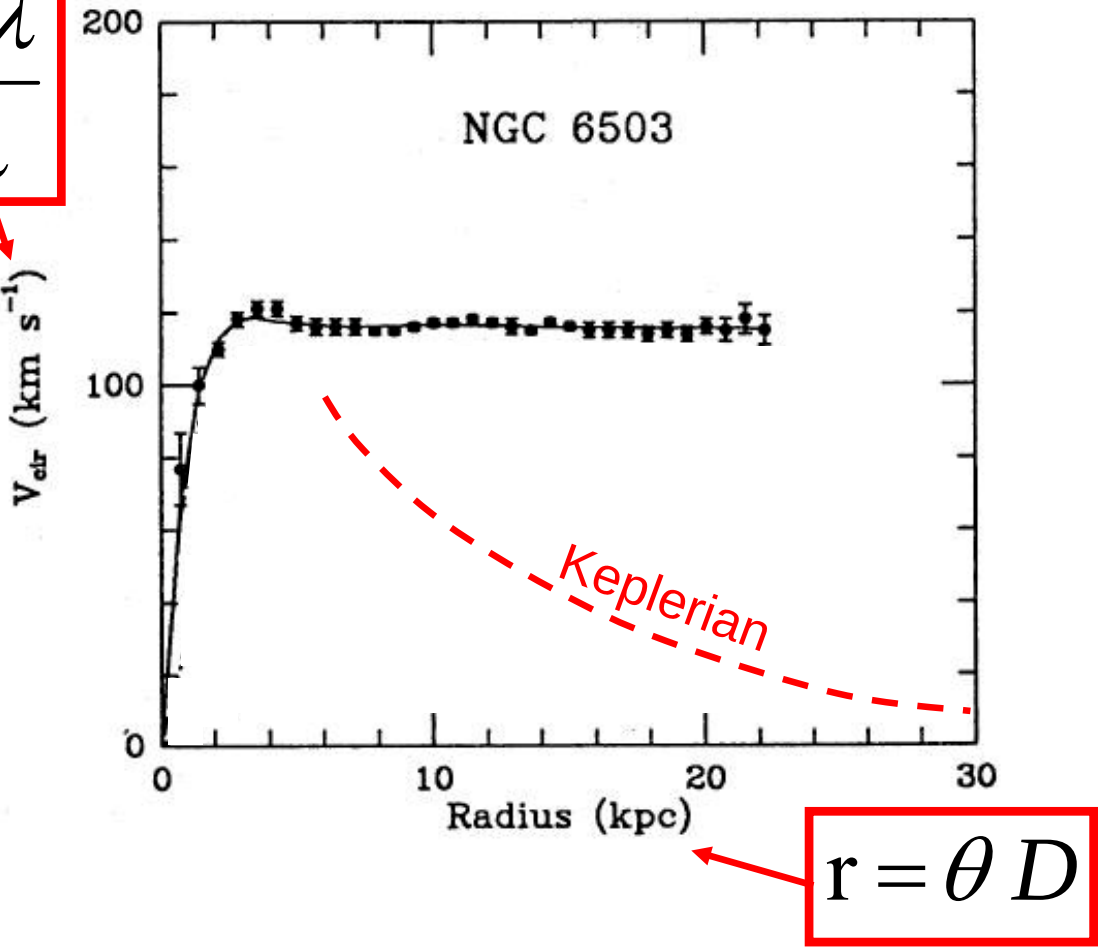

$$r = \theta D$$

If the mass density has a spherical symmetry (as in the bulge of the galaxy)

$$v = \sqrt{\frac{GM(<r)}{r}}$$

From the bulge only, the velocity of a test star at $r > r_b$ would be Keplerian

$$v = \sqrt{\frac{GM_b}{r}}$$

Edge-on galaxy :

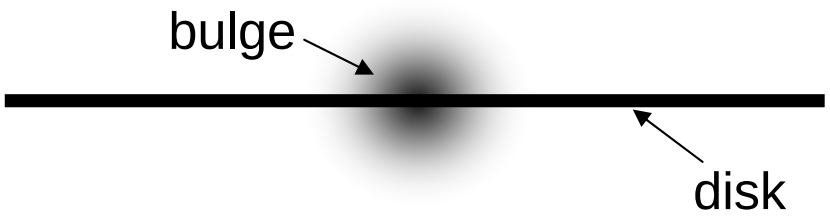

$$v = c\frac{\Delta\lambda}{\lambda}$$

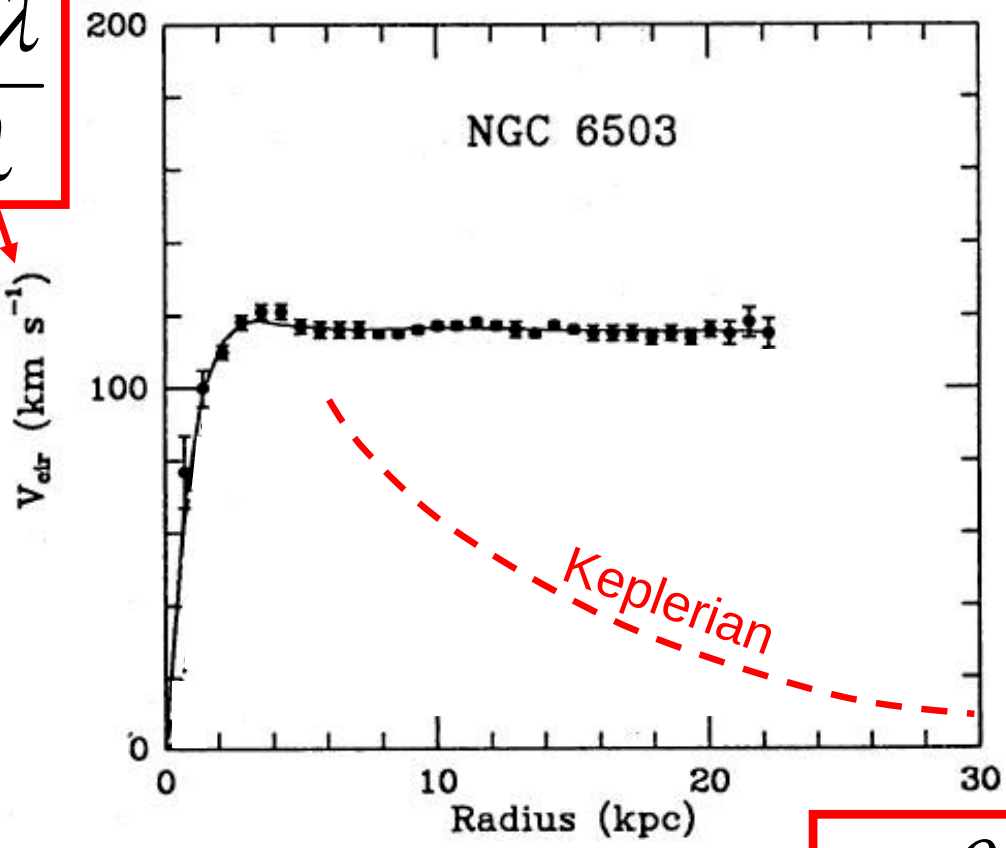

$$r = \theta D$$

If the mass density has a spherical symmetry (as in the bulge of the galaxy)

$$v = \sqrt{\frac{GM(<r)}{r}}$$

From the bulge only, the velocity of a test star at $r > r_b$ would be Keplerian

$$v = \sqrt{\frac{GM_b}{r}}$$

It can be shown that in the presence of an exponential disk with scale radius r_d the combined effect of bulge + disk is still Keplerian :

$$v \approx \frac{1}{\sqrt{r}} \; ; \quad r > 3r_d$$

Edge-on galaxy :

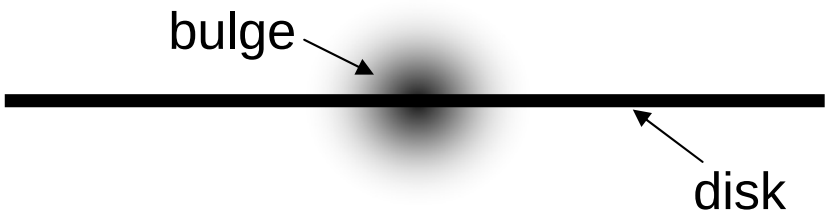

$$v = c\frac{\Delta\lambda}{\lambda}$$

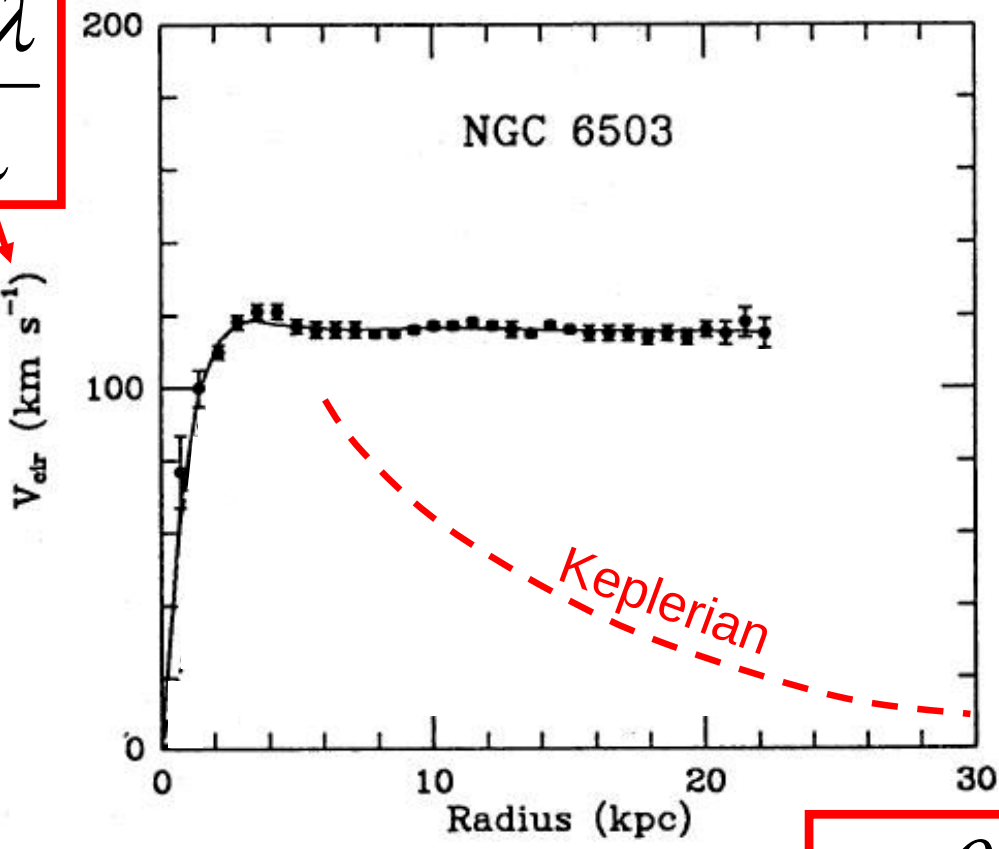

$$r = \theta D$$

If the mass density has a spherical symmetry (as in the bulge of the galaxy)

$$v = \sqrt{\frac{GM(<r)}{r}}$$

From the bulge only, the velocity of a test star at $r > r_b$ would be Keplerian

$$v = \sqrt{\frac{GM_b}{r}}$$

It can be shown that in the presence of an exponential disk with scale radius r_d the combined effect of bulge + disk is still Keplerian :

THIS DOES NOT FIT THE MEASURED DATA !

$$v \approx \frac{1}{\sqrt{r}} \; ; \quad r > 3r_d$$

- Two main interpretations:
  - The mass of the galaxy is dominated by an approximately spherical dark halo, much larger than the optical radius, and with density falling as $1/r^2$ at large radii. In fact, in this case

$$M(<r) = \int_0^r 4\pi r^2 \rho(r) dr \propto r$$

$$\longrightarrow \quad \mathrm{v}(r) = \sqrt{\frac{GM(<r)}{r}} \propto \text{constant}$$

  - Gravity deviates from Newton's law at extremely low accelerations (i.e. at large distances in galaxies) (Milgrom, MOND theory).


Blue = dark halo

Dark Matter

- The luminosity of spiral galaxies falls off exponentially wirh r ; the luminosity of elliptical galaxies falls off as $1/r^4$.
- So, luminous matter cannot produce the observed constant rotation curves at large radii.
- The total luminous mass is much less than the mass required from the relation

$$v = \sqrt{\frac{GM(<r)}{r}} \quad \rightarrow \quad M(<r_{\max}) = \frac{r_{\max} v_{\max}^2}{G}$$

- Typical numbers (confirmed also by the analysis of the motion of satellite galaxies):

$$M(<200\,kpc) \approx 2\times 10^{12} M_{sun} \qquad L \approx 2\times 10^{10} L_{sun}$$

$$\Rightarrow \quad \gamma = \frac{M_{Sp}}{L_{Sp}} \approx 100 \frac{M_{sun}}{L_{sun}} = 100\gamma_{sun}$$

- Stars in spiral galaxies have an average mass to light ratio $\gamma < 5\gamma_{sun}$. So the required mass has to be **dark**.
- Luminous matter can account for at most 5% of the total mass.

Additional evidence for dark matter in galaxies

- Motion of globular clusters
- Motion of small satellite galaxies
- MACHOs (could be baryonic)
- Gravitational lensing
- ….

Gravitational deflection of light

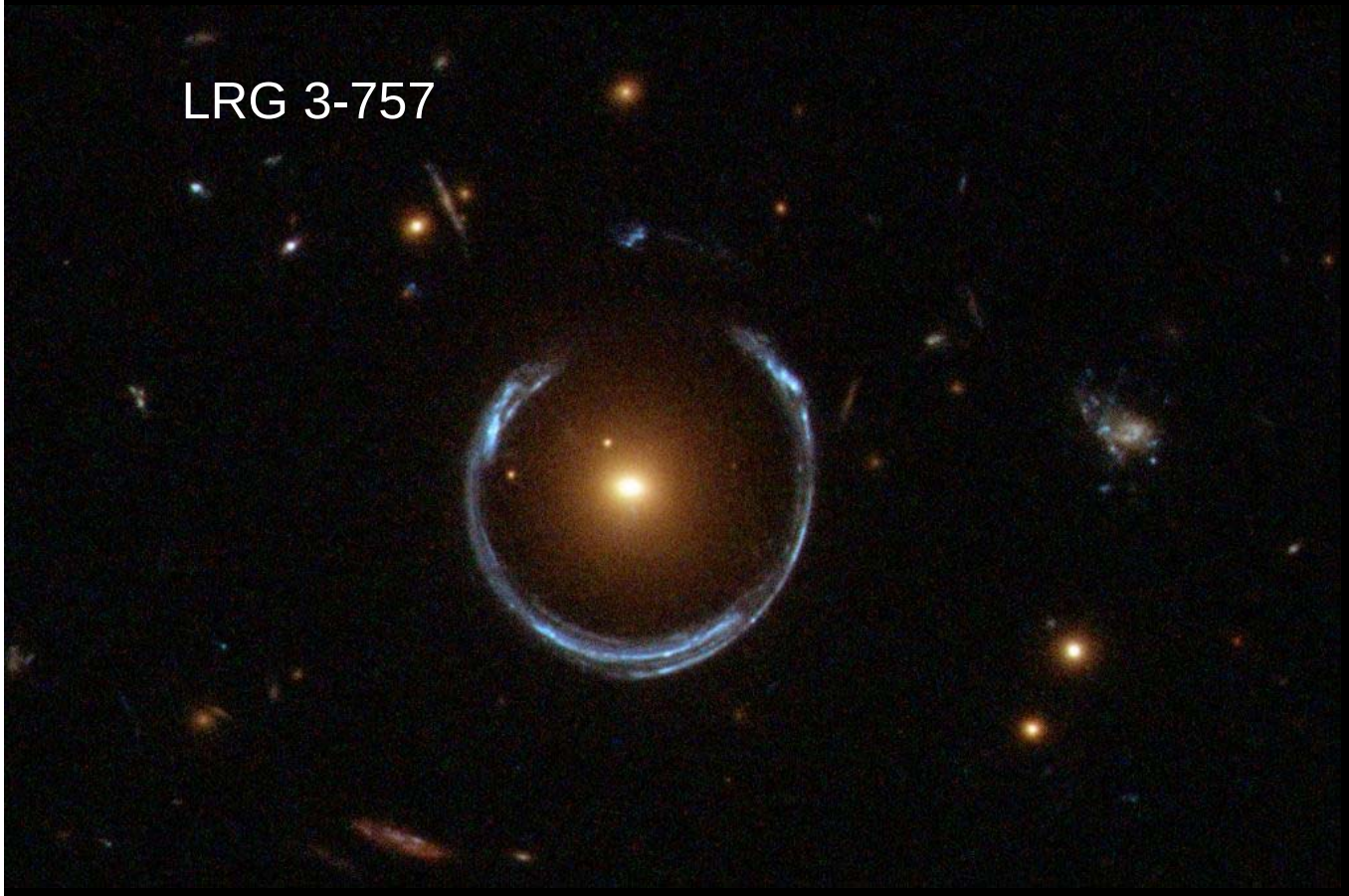

$$\theta_E = \sqrt{\frac{4GM_L}{c^2}\frac{d_{LS}}{d_L d_S}}$$

M_L can be computed from measured data :

Angular diameter distances are estimated from the measured redshifts of L and S

θ_E is estimated from the image

$$M_L = 5\text{x}10^{12}\ M_{sun}$$

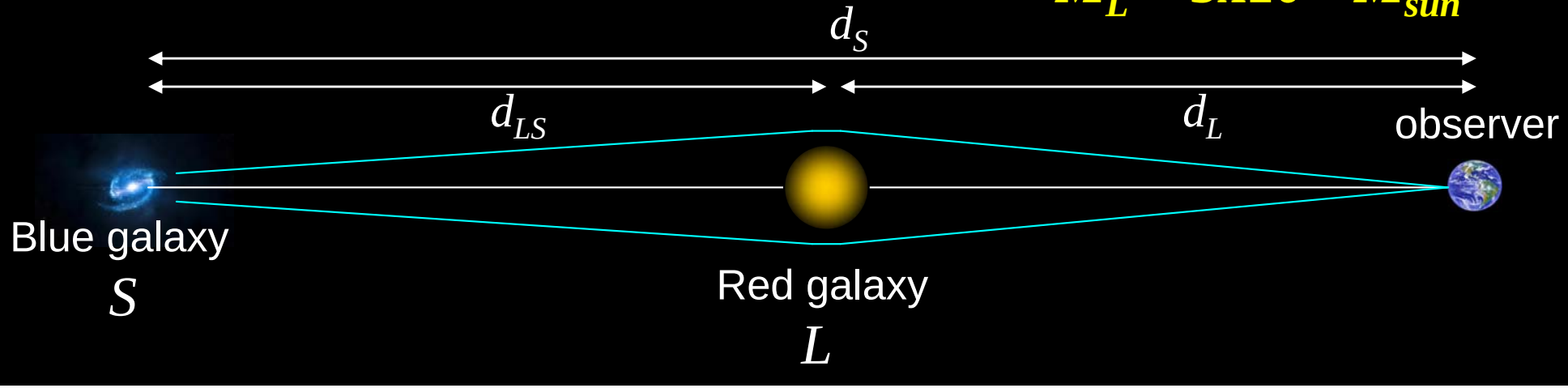

Fukujita + Silk - The Astrophysical Journal , 616 : 643–668 , 2004

TABLE 1

THE COSMIC ENERGY INVENTORY

Ω_i

Category	Parameter	Components[a]	Totals[a]
1....			
1.1			
1.2			
1.3			
2....			
2.1			
2.2			
2.3....	Prestellar nuclear binding energy	$-10^{-4.1 \pm 0.6}$	
3....	Baryon rest mass: From Primordial nucleosynthesis: all kinds		0.045 ± 0.003
3.1....	Warm intergalactic plasma	0.040 ± 0.003	
3.1a....	Virialized regions of galaxies	0.024 ± 0.005	
3.1b....	Intergalactic	0.016 ± 0.005	
3.2....	Intracluster plasma	0.0018 ± 0.0007	
3.3....	Main-sequence stars: spheroids and bulges	0.0015 ± 0.0004	
3.4....	Main-sequence stars: disks and irregulars	0.00055 ± 0.00014	
3.5....	White dwarfs	0.00036 ± 0.00008	
3.6....	Neutron stars	0.00005 ± 0.00002	
3.7....	Black holes	0.00007 ± 0.00002	
3.8....	Substellar objects	0.00014 ± 0.00007	
3.9....	H I + He I	0.00062 ± 0.00010	
3.10....	Molecular gas	0.00016 ± 0.00006	
3.11....	Planets	10^{-6}	
3.12....	Condensed matter	$10^{-5.6 \pm 0.3}$	
3.13....	Sequestered in massive black holes	$10^{-5.4}(1 + \epsilon_n)$	

- In summary, for galaxies: $M_{luminous} << M_{baryons} << M_{dark}$

  ~1% ~10% ~90%

Census of baryons in galaxies - ——— = luminous

Dark Matter in Clusters of Galaxies

- Clusters are very large concentrations of auto-gravitating galaxies (100-1000+ members)
- In addition to galaxies, large masses X-ray emitting of diffuse, ionized gas.
- Independent evidence for dark matter from
  - Dynamics of galaxies in clusters
  - X-ray brightness of clusters
  - Gravitational lensing of field galaxies
  - Merging clusters
  - ….


Coma : formed by about 1000 identified galaxies

Coma Cluster

Figure 4.10— The distribution of radial velocities of all 583 identified Coma cluster galaxies ($4000 < cz < 10000$ km s^{-1}). The solid curve is a Gaussian with mean 6977 ± 53 km s^{-1} and standard deviation 950 ± 39 km s^{-1}. The dotted curve is the sum of two Gaussians with $\overline{cz_1} = 7501 \pm 187$ km s^{-1}, $\sigma_1 = 650 \pm 216$ km s^{-1} and $\overline{cz_2} = 6640 \pm 470$ km s^{-1}, $\sigma_2 = 1004 \pm 120$ km s^{-1} and gives a better fit to the observed distribution. The radial velocities of the three dominant galaxies are indicated.

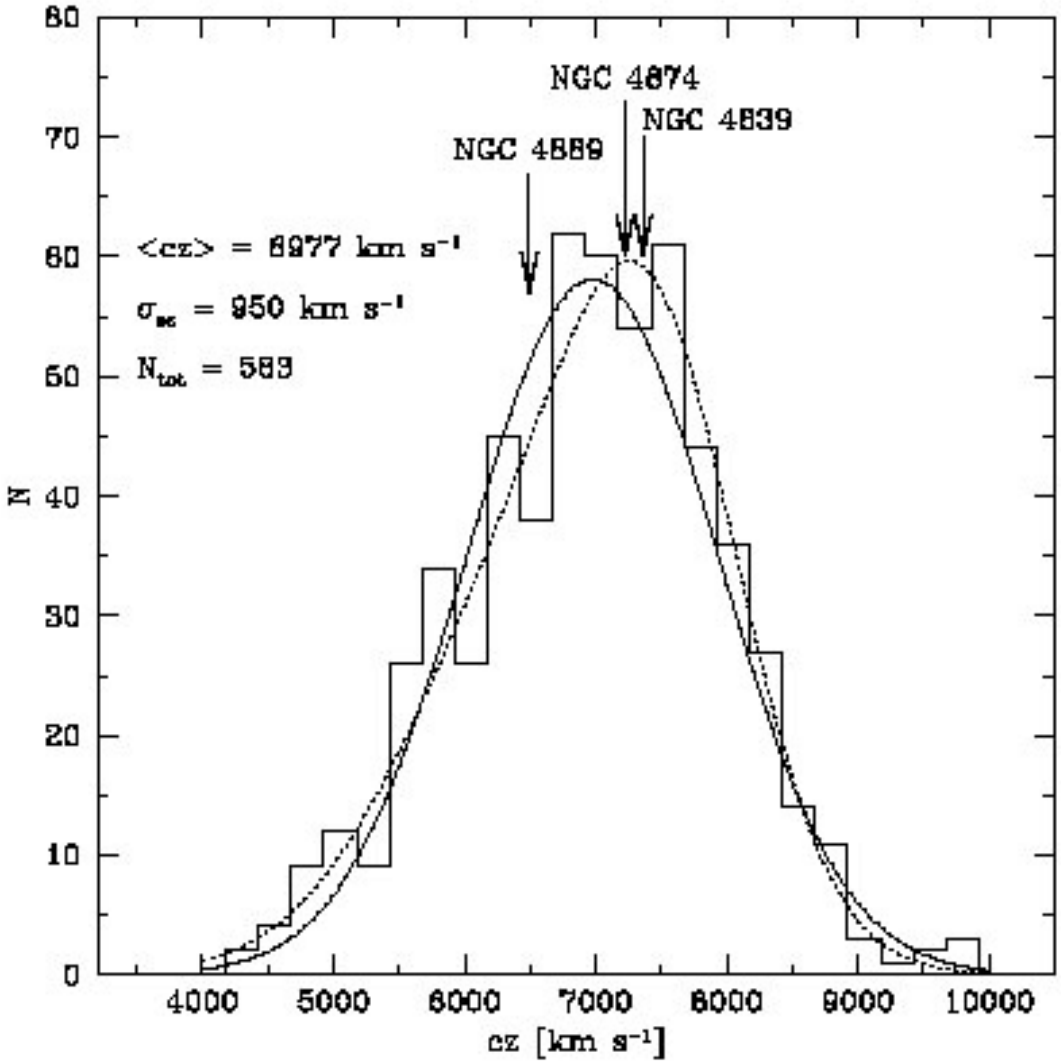

http://www.ub.rug.nl/eldoc/dis/science/m.beijersbergen/c4.pdf

Galaxies in a cluster as a self-gravitating system

$$K = \frac{1}{2} M \left\langle \mathrm{v}^2 \right\rangle \qquad M = \sum_i m_i$$

For spherical symmetry

$$U = -\frac{GM^2}{R_e}$$

Where R_e is the effective average radius of the system, and depends on the radial density distribution

For a virialized system

$$\frac{U}{2} = -K$$

$$M \left\langle \mathrm{v}^2 \right\rangle = \frac{\alpha G M^2}{R_e} \quad \rightarrow \quad M = \frac{\left\langle \mathrm{v}^2 \right\rangle R_e}{G}$$

$$\boxed{M = \frac{3\sigma_{LOS}^2 R_e}{G}}$$

σ_{LOS} = dispersion of velocities projected along the line of sight – can be measured with the Doppler effect ;
R_e can be estimated assuming that the luminosity profile tracks the mass density.

$$M_{coma} = 3.3 \times 10^{15} M_{sun} \quad \Longleftrightarrow \quad L_{coma} = 1.4 \times 10^{13} L_{sun}$$

$$\left.\frac{M}{L}\right|_{\text{Coma}} = \gamma_{\text{Coma}} = \frac{3.36\times10^{15} M_{sun}}{1.4\times10^{13} L_{sun}} = 240\frac{M_{sun}}{L_{sun}} = 240\gamma_{\text{sun}}$$

- The mass to light ratio in clusters is in general >> than for the sun.
- However, stars in galaxies have an average mass to light ratio $\gamma<6.5\gamma_{\text{sun}}$. So

$$\gamma_{cluster} = \frac{\sum_{i=1}^{N} \gamma_i L_i}{\sum_{i=1}^{N} L_i}$$

cannot be >100 if there are only stars.

- **Dark Matter is needed.**

Cluster	γ
A2390	173
MS0016+16	202
MS0302+16	157
MS0440+02	218
MS0451+02	250
MS0451-3	275
MS0839+29	200
MS0906+11	560
MS1006+12	204
MS1008-12	154
MS1224+20	148
MS1231+15	123
MS1358+62	138
MS1455+22	412
MS1512+36	164
MS1612+26	106

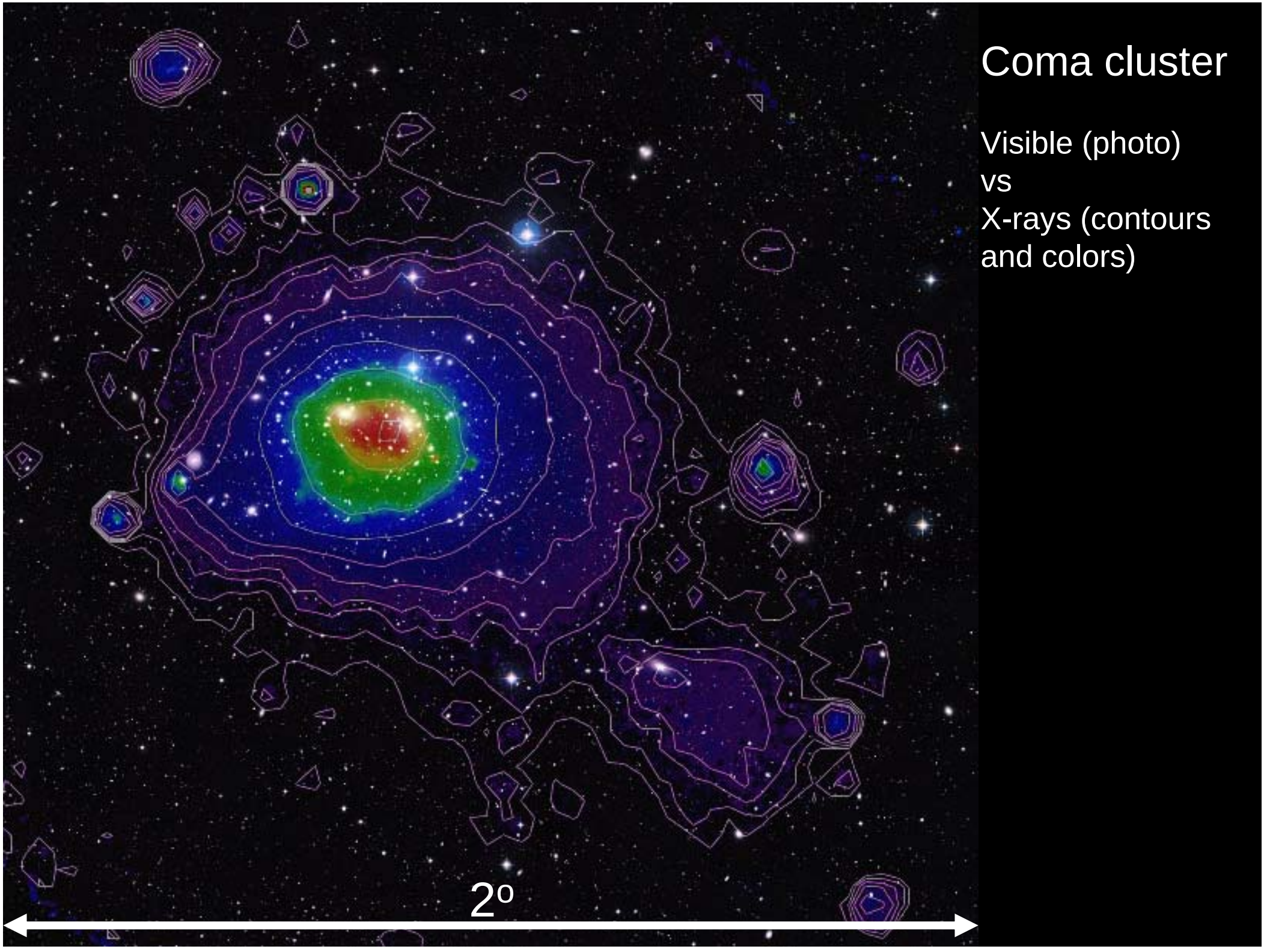

Coma cluster

Visible (photo)
vs
X-rays (contours and colors)

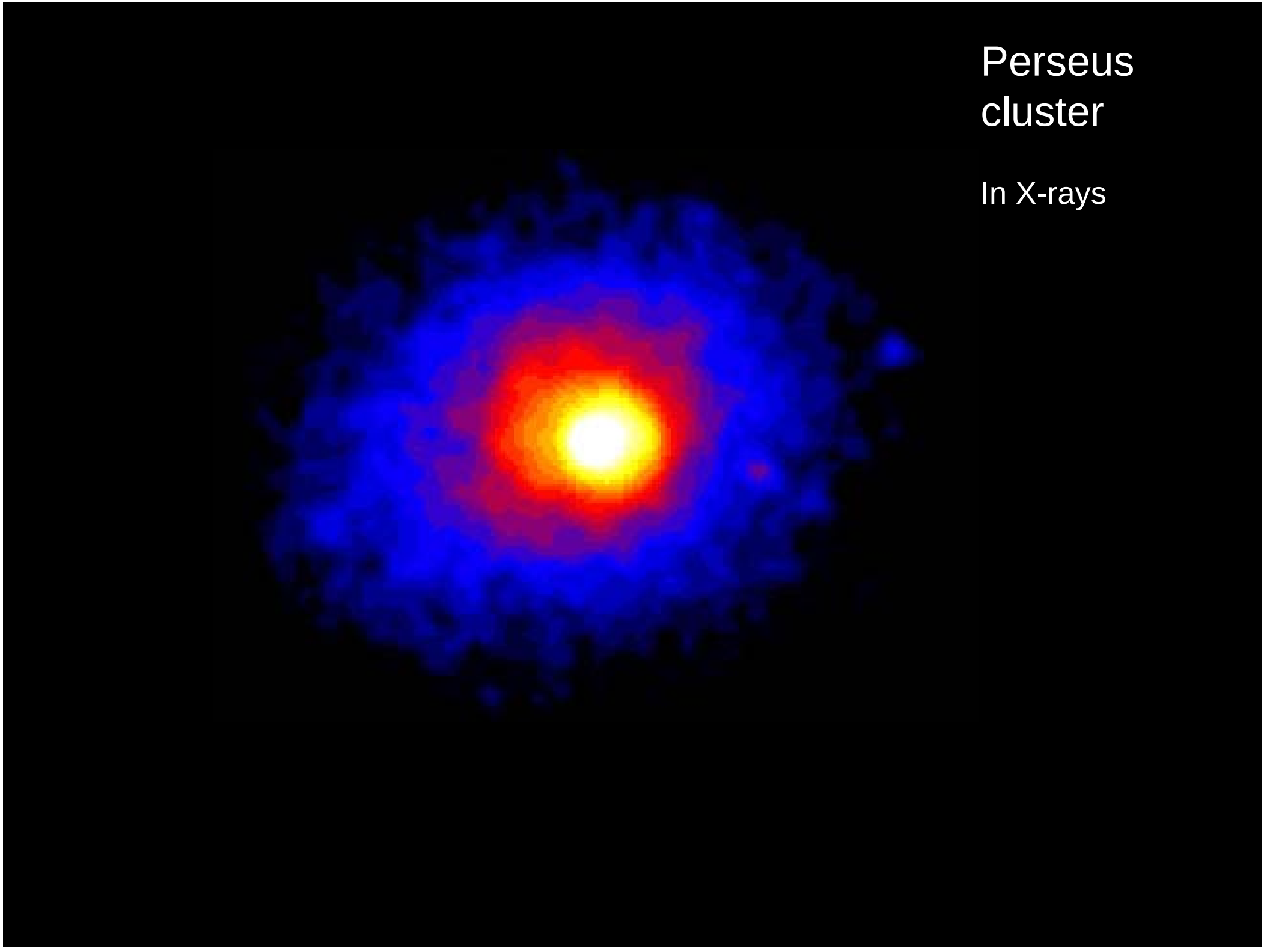
Perseus
cluster
In X-rays

A2029

X-rays vs. visible

CHANDRA X-RAY

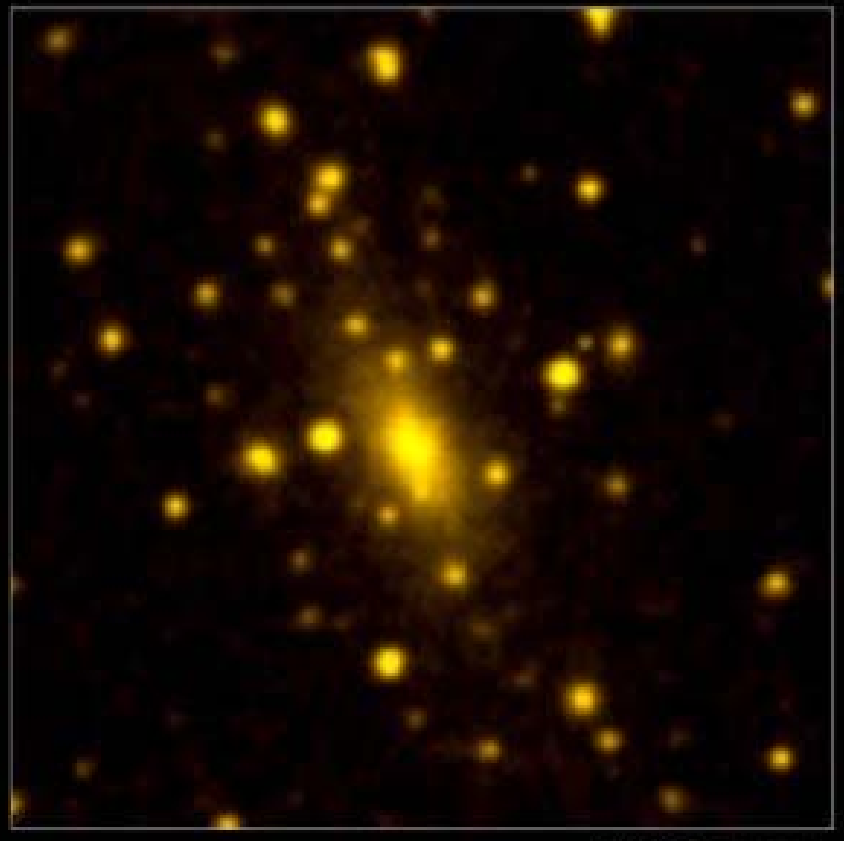

DSS OPTICAL

CHANDRA (NASA)

X-ray Observatories

XMM (ESA)

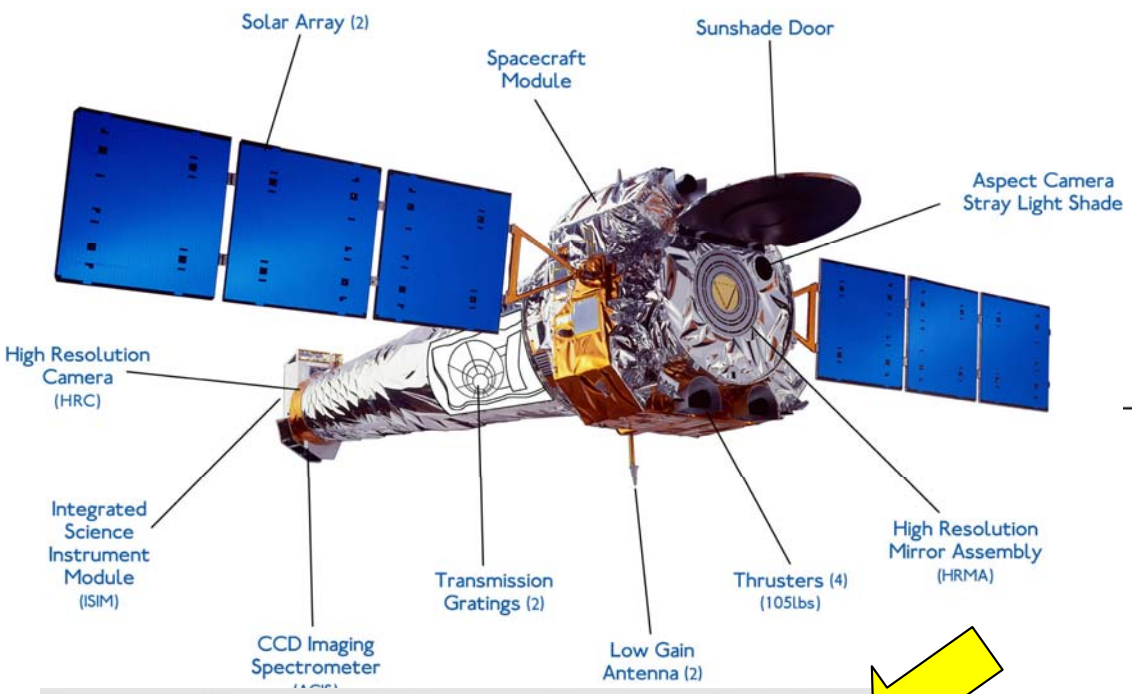

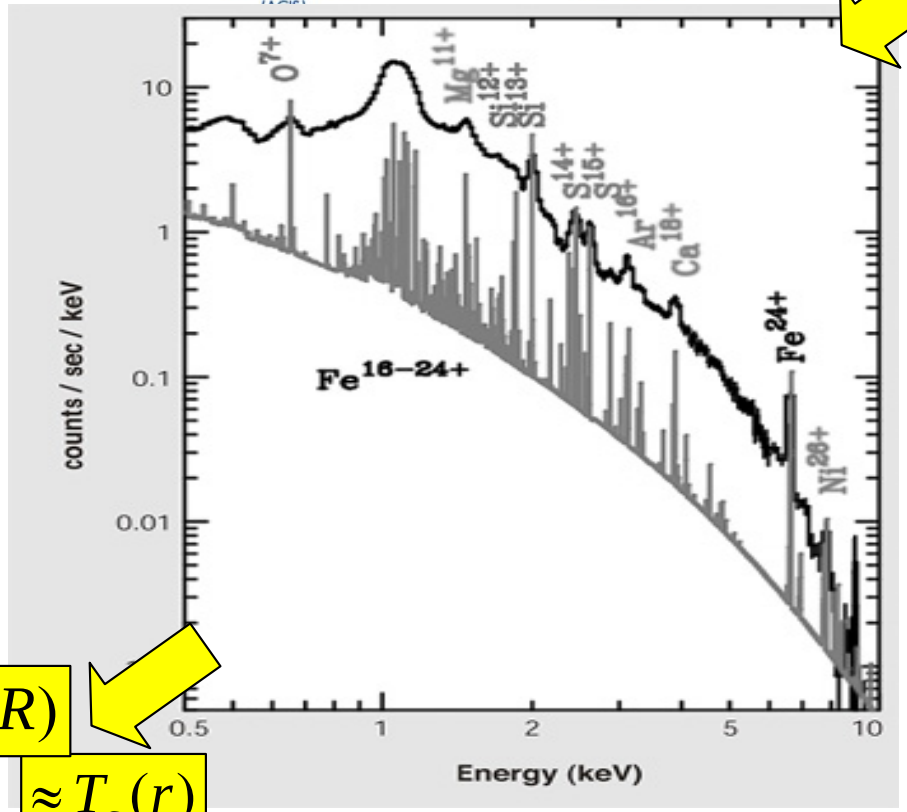

$I_X(R)$

$\approx T_g(r)$

xmm observatory system

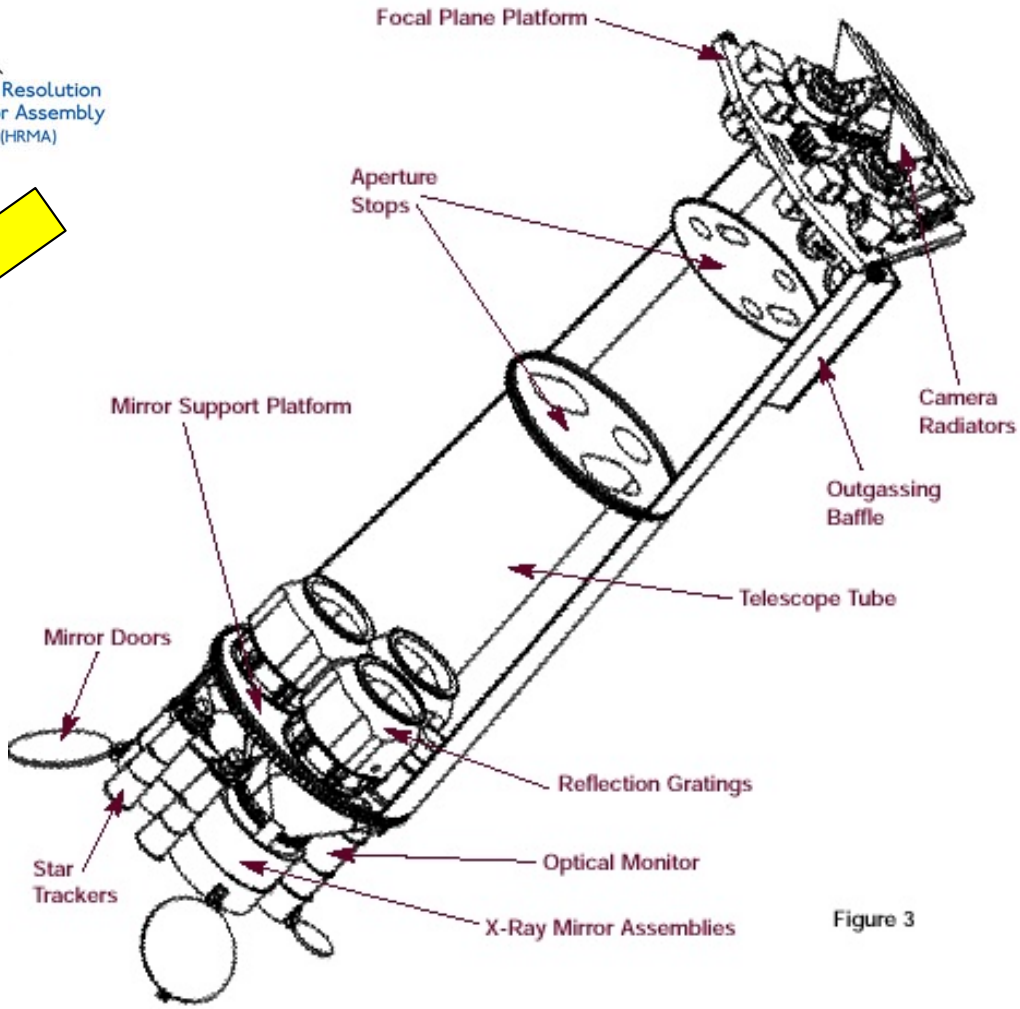

Figure 3

Bremsstrahlung from ionized gas

For regular clusters (spherical symmetry)

- Observed brightness: $I_X(R) = I_{X,0}\left[1+\left(\frac{R}{a_X}\right)^2\right]^{-3\beta+\frac{1}{2}}$
- Luminosity density: $j_X(r) = j_{X,0}\left[1+\left(\frac{r}{a_X}\right)^2\right]^{-3\beta}$
- Polytropic gas, spherical symmetry: $T_g \propto n_g^{\gamma-1}$
- Gas density: $n_g(r) = \sqrt{\frac{j_X(r)}{L(T_g(r))}} = n_{g,0}\left[1+\left(\frac{r}{a_X}\right)^2\right]^{-6\beta/(\gamma+3)}$
- Temperature profile: $T_g(r) = T_{g,0}\left[1+\left(\frac{r}{a_X}\right)^2\right]^{-6\beta(\gamma-1)/(\gamma+3)}$

Bremsstrahlung from ionized gas

Hydrostatic equilibrium:

$$\frac{dp}{dr} = -\rho\frac{d\Phi}{dr} = -\frac{GM(<r)}{r^2}\rho \quad \rightarrow M(<r) = -\frac{r^2}{\rho G}\frac{dp}{dr}$$

Ideal gas, other masses pressureless:

$$p = \frac{kT_g}{m}n_g \quad \rightarrow \quad \frac{dp}{dr} = \frac{k}{m}\left(\frac{\partial n_g}{\partial r}T_g + \frac{\partial T_g}{\partial r}n_g\right)$$

$$M(<r) = -\frac{kT_g}{Gm}\left(\frac{\partial \ln n_g}{\partial \ln r} + \frac{\partial \ln T_g}{\partial \ln r}\right)r \Rightarrow$$

All mass

$$M(<r) \cong \frac{12\beta\gamma a_X}{\gamma+3}\frac{kT_{g,0}}{Gm}\left(\frac{r}{a_X}\right)^3\left[1+\left(\frac{r}{a_X}\right)^2\right]^{-\left[1+\frac{6\beta(\gamma-1)}{(\gamma+3)}\right]}$$

Gas mass

$$M_g(<r) = 4\pi\int_0^r r^2 n_g(r)dr = \frac{2\pi(\gamma+3)n_{g,0}a_X^3}{\gamma+3-6\beta}\left[1+\left(\frac{r}{a_X}\right)^2\right]^{1-\frac{6\beta}{(\gamma+3)}}$$

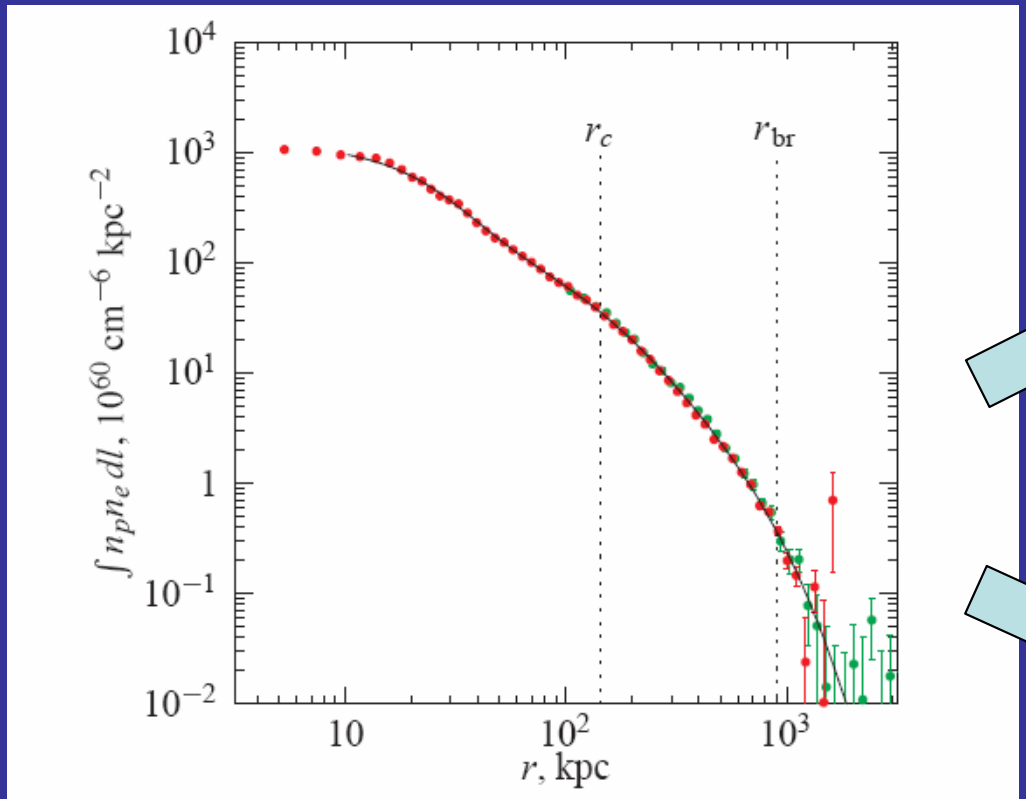

F . 2.— Observed projected emissivity profile for A133. *Chandra* and *ROSAT* PSPC data are shown in red and green, respectively. Solid line shows the best fit to the 3D gas density model (eq. [3]). The slope of the emissivity profile steepens by 1 at radius $r_{\rm br} = r_s(\varepsilon - 1)^{-1/\gamma}$.

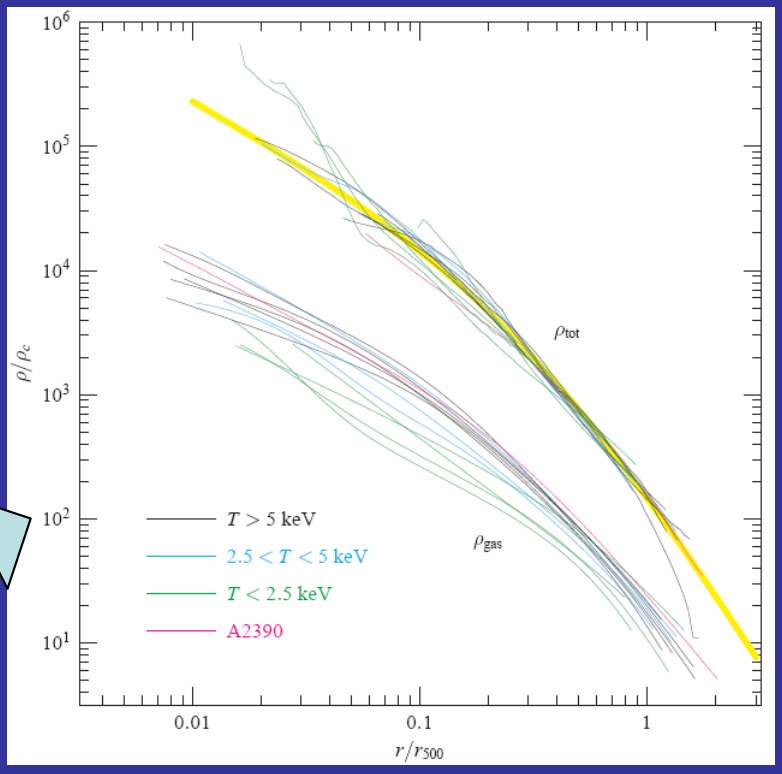

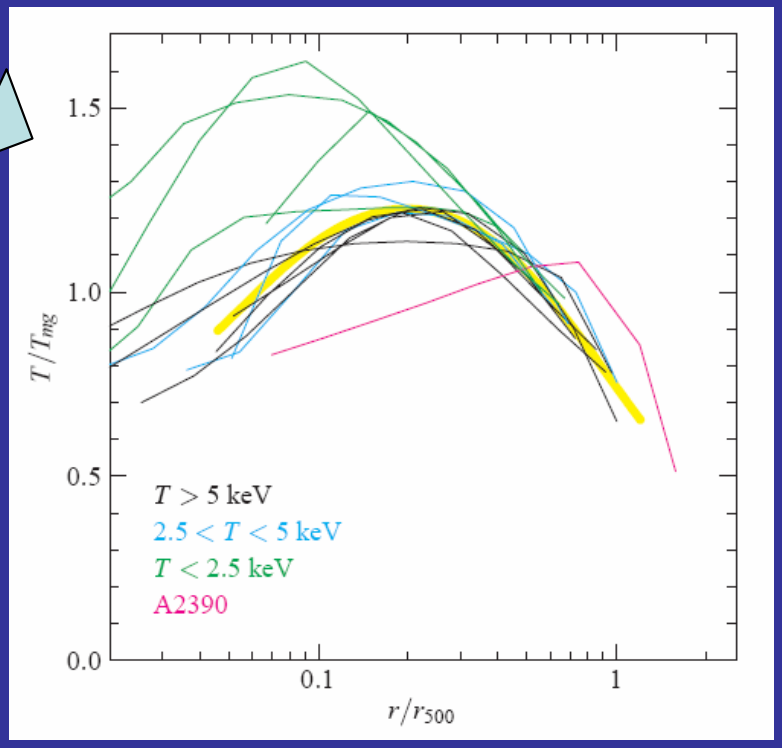

http://arxiv.org/abs/astro-ph/0507092

Bremsstrahlung from ionized gas

- From observations (CHANDRA, XMM, …) of $I_X(R)$ and $T_g(R)$, good best-fit estimates of the parameters a_X, β, γ.
- Using the $M(<r)$ and $M_g(<r)$ equations one finds, for a range of γ (γ=0 isothermal, γ=5/3 adiabatic, …) and other uncertainties

$$f = \frac{M_g}{M} = 0.12...0.18$$

- Note that M_{stars}=*0.02-0.03 M* :
- *A galaxy cluster is made of dark matter, with ionized gas and stars as minor components :* $\boldsymbol{M_{stars} < M_g < M}$

SZE

- Where does a cluster end ?
- Bremsstrahlung goes as n_g^2, rapidly falling to zero in the outskirts of the cluster
- CMB photons crossing the cluster undergo inverse Compton scattering against electrons in the plasma of the cluster.
- The signal has a very specific spectral signature, and is proportional to n_g, i.e. is more sensitive to the gas in the periphery of the cluster than the X-ray signal.

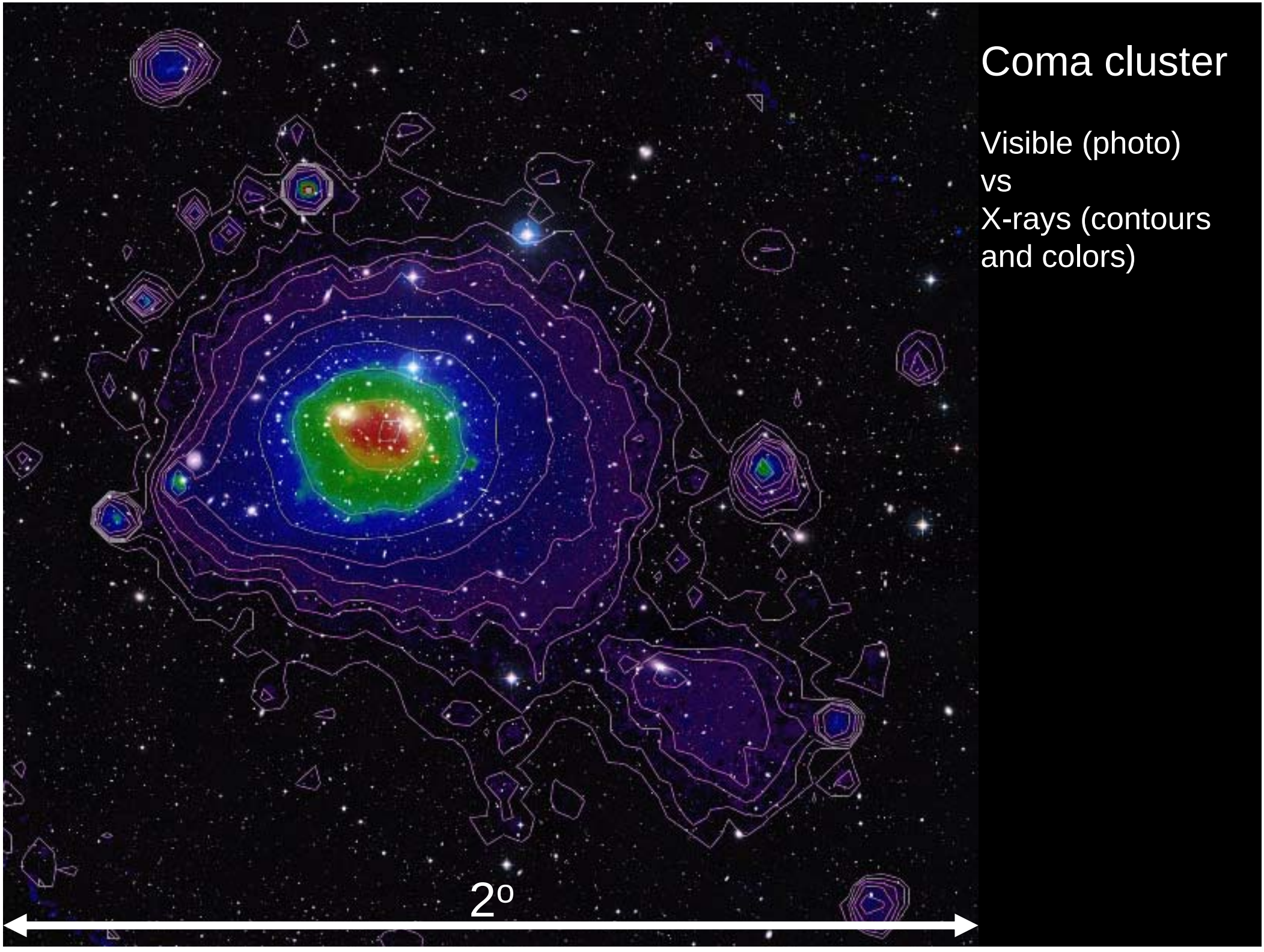

Coma cluster

Visible (photo)
vs
X-rays (contours and colors)

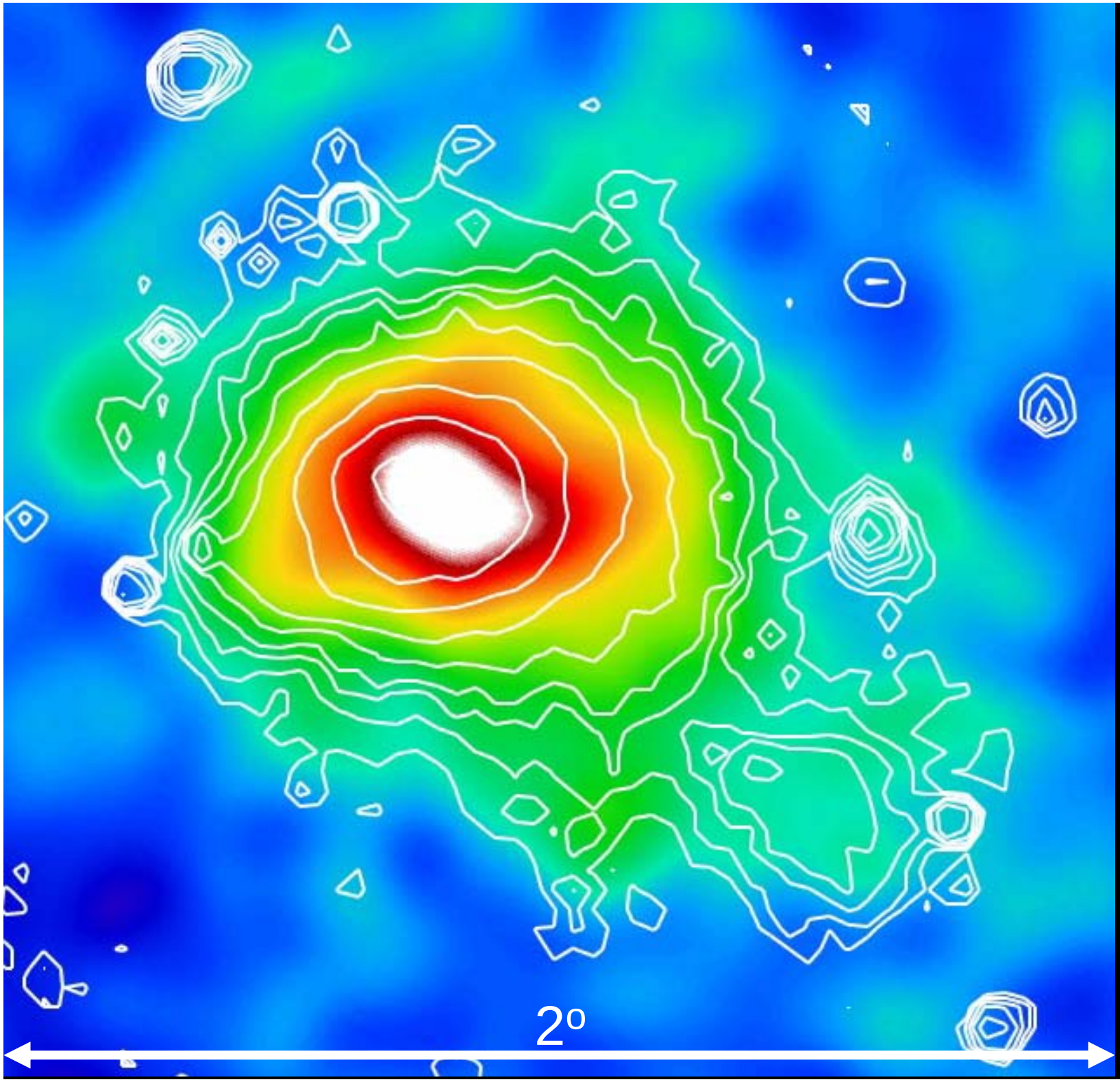

Coma cluster

Mm-waves
(Planck, colors)
vs
X-rays (contours):
bremsstrahlung
from hot gas.

Gravitational deflection of light

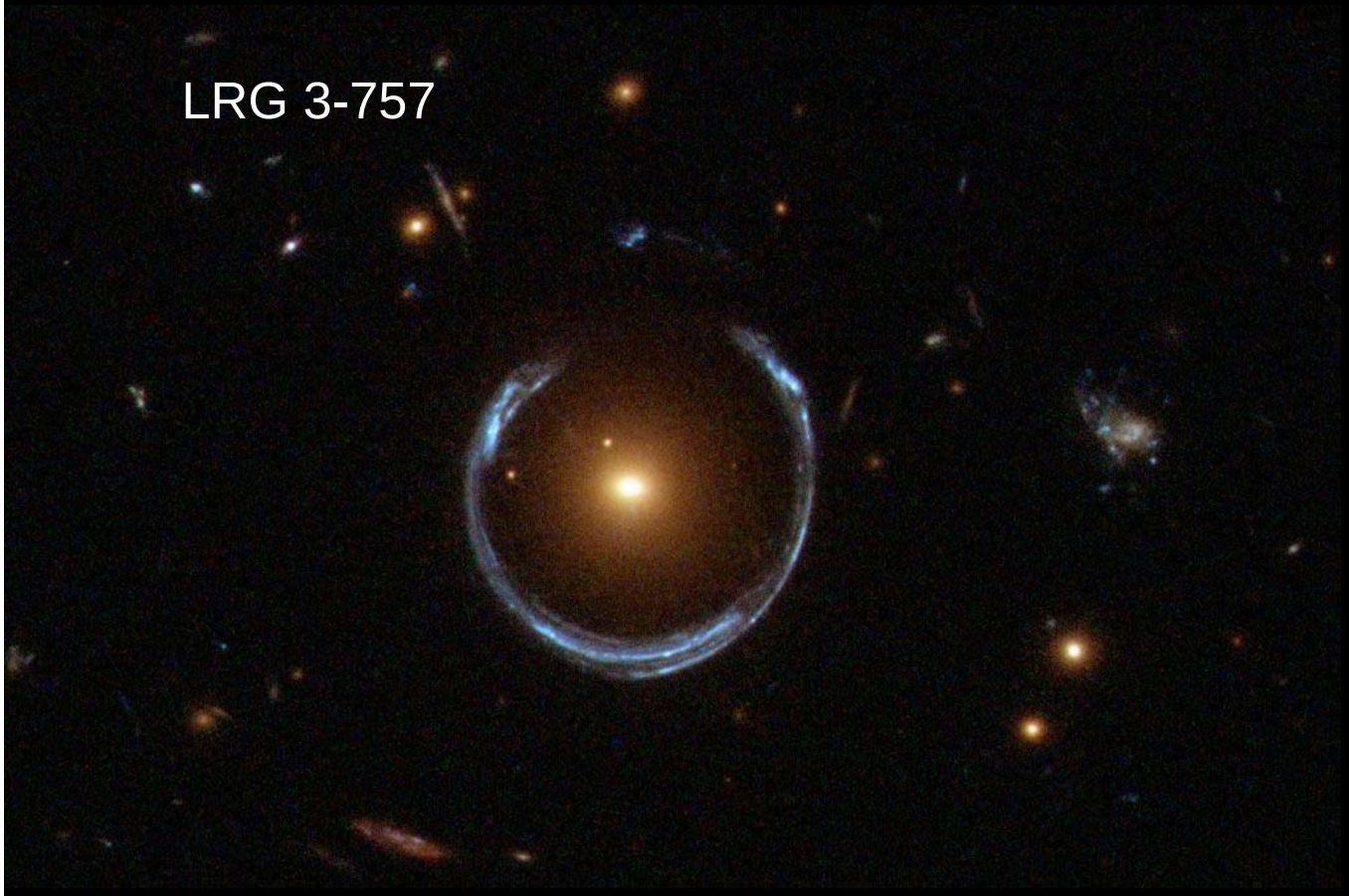

$$\theta_E = \sqrt{\frac{4GM_L}{c^2}\frac{d_{LS}}{d_L d_S}}$$

M_L can be computed from measured data :

Angular diameter distances are estimated from the measured redshifts of L and S

θ_E is estimated from the image

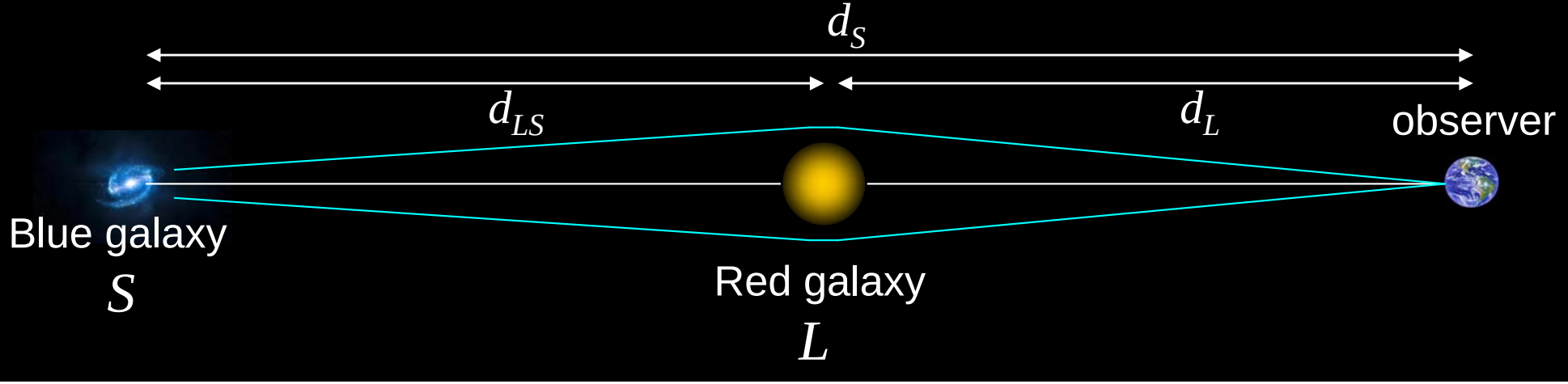

If the lens is a galaxy cluster, the symmetry is broken, and multiple arc-images are produced.
STRONG LENSING (A2218)
Information mainly on central mass

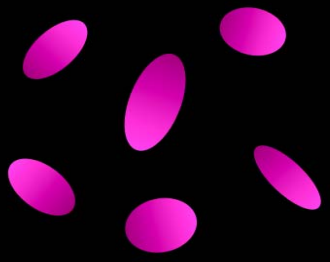

Galaxies randomly distributed

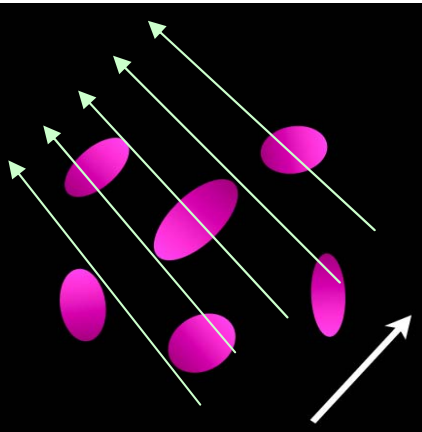

Slight alignment

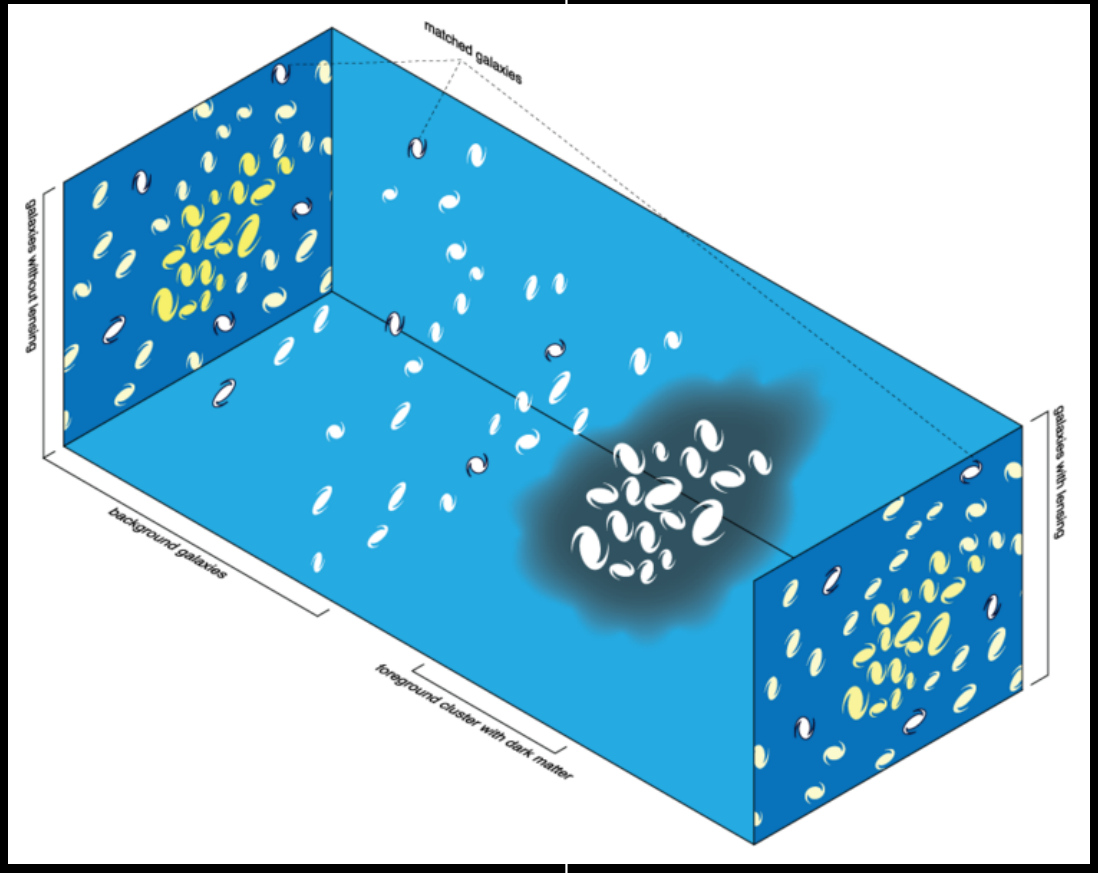

Field galaxies :

In deep ground-based suverys: 10-20 galaxies/arcmin^2. Even more for HST

In the absence of large mass concentrations, orientations are randomly distributed

Near a mass concentration, gravitational lensing stretches the images preferentially in one direction, producing a change in the observed ellipticity of each galaxy, and a weak alignement of the major axes of galaxies experiencing the same gravitational potential. **WEAK LENSING**.

The lensing potential can be reconstructed from the observed alignment.

A2390

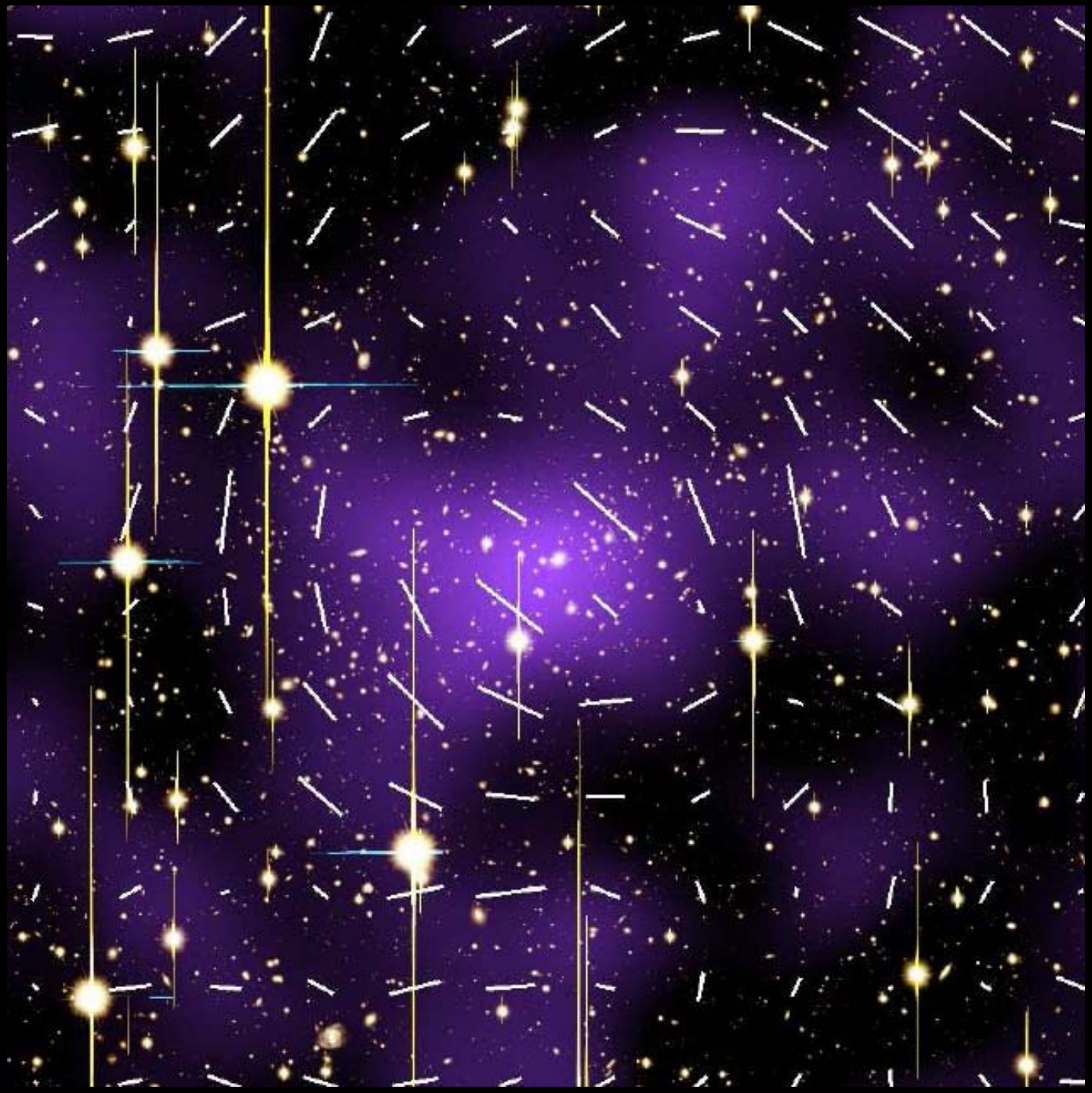

Sticks: shear field averaged over 1’ pixels.

Colors: reconstructed mass distribution

Photo: galaxies and stars

ADDITIONAL EVIDENCE FOR DARK MATTER IN CLUSTERS

see astro-ph/1303.3274

Oguri M., Takada M., Okabe N., Smith G. P., 2010, MNRAS, 405, 2215

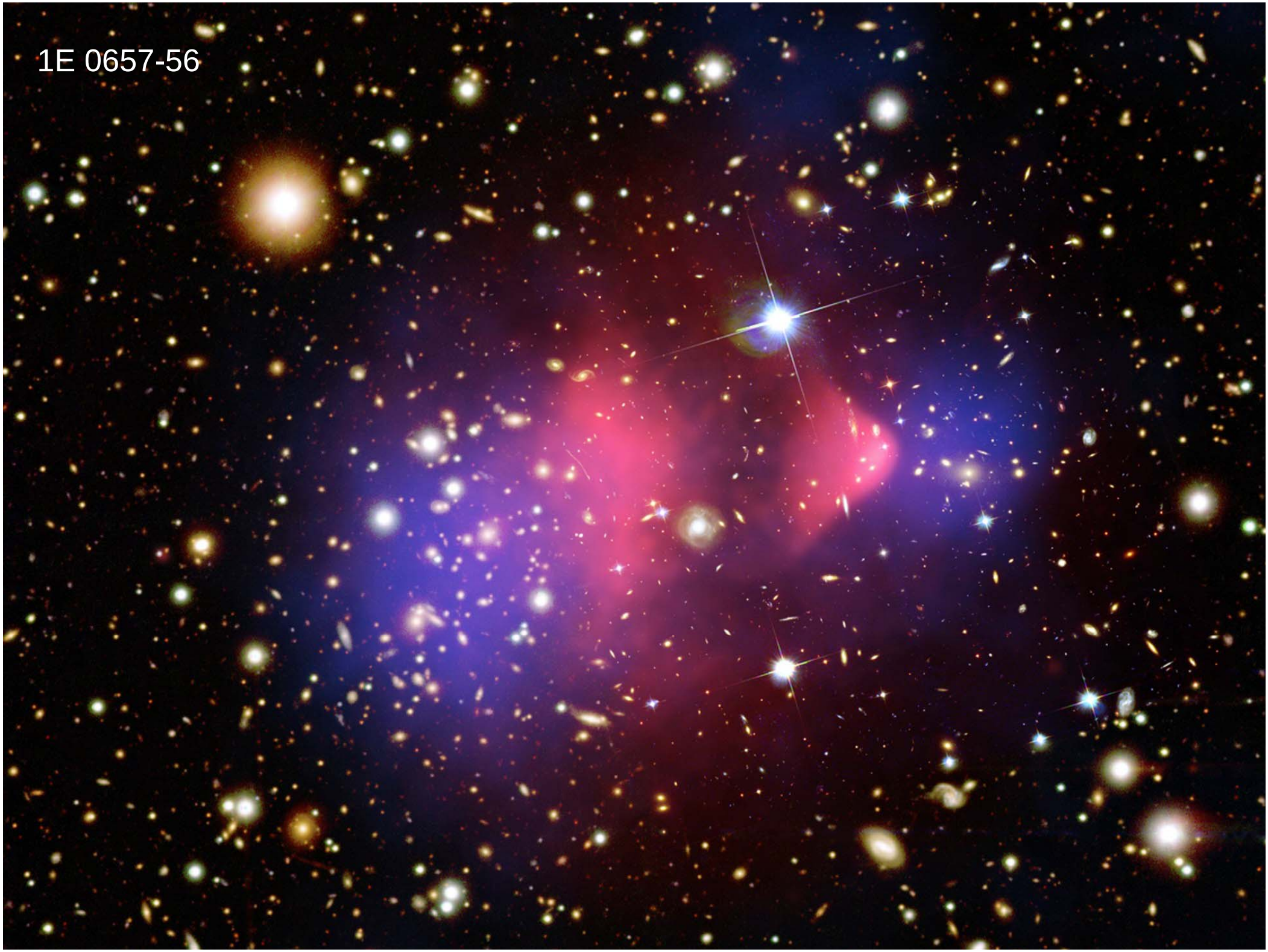
1E 0657-56

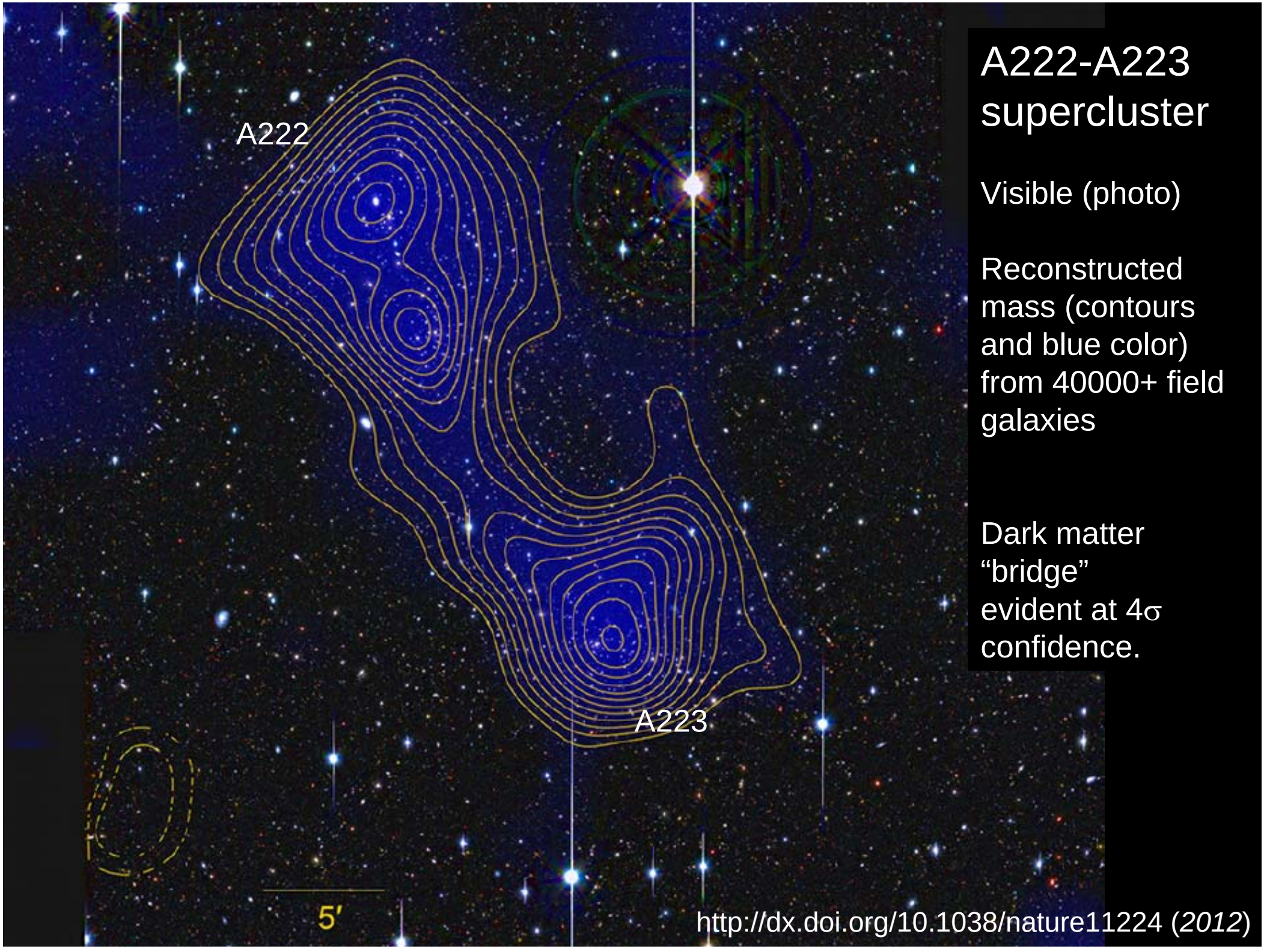

A222-A223 supercluster

Visible (photo)

Reconstructed mass (contours and blue color) from 40000+ field galaxies

Dark matter “bridge” evident at 4σ confidence.

http://dx.doi.org/10.1038/nature11224 (*2012*)

Which kind of dark matter ?

- Self-interaction cross-section: upper limits from bullet cluster (Markevitch et al. 2004, $\sigma/m<1cm^2/g$)

- Mass profiles of clusters depend on the nature of DM
- Cold dark matter clusters following the so-called NFW profile (NFW 1996), or the Einasto profile.
- Stacking analysis of 50 regular clusters: NFW and Einasto both OK. Isothermal excluded (astro-ph/1302.2728)

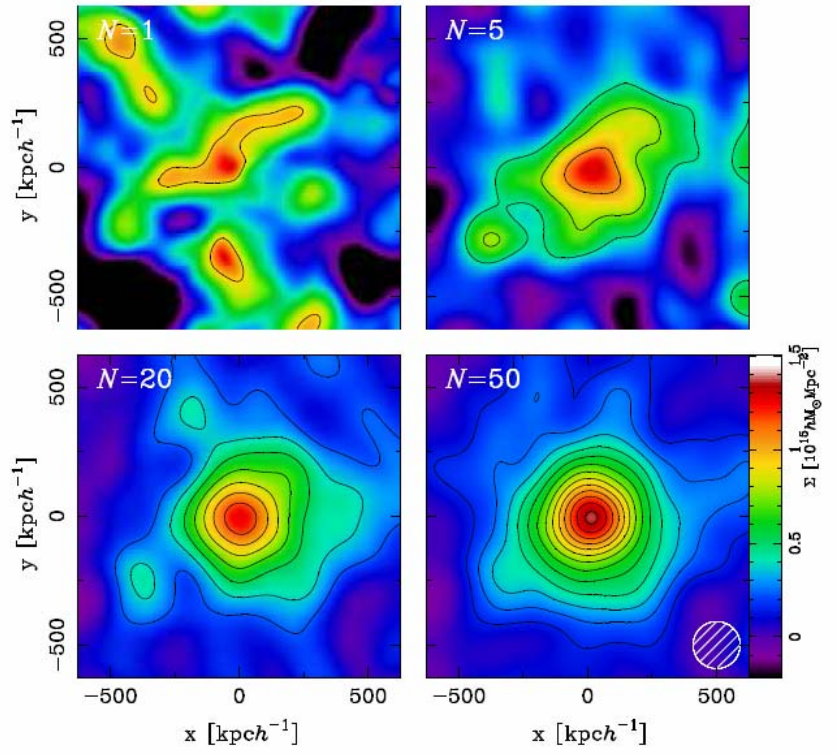

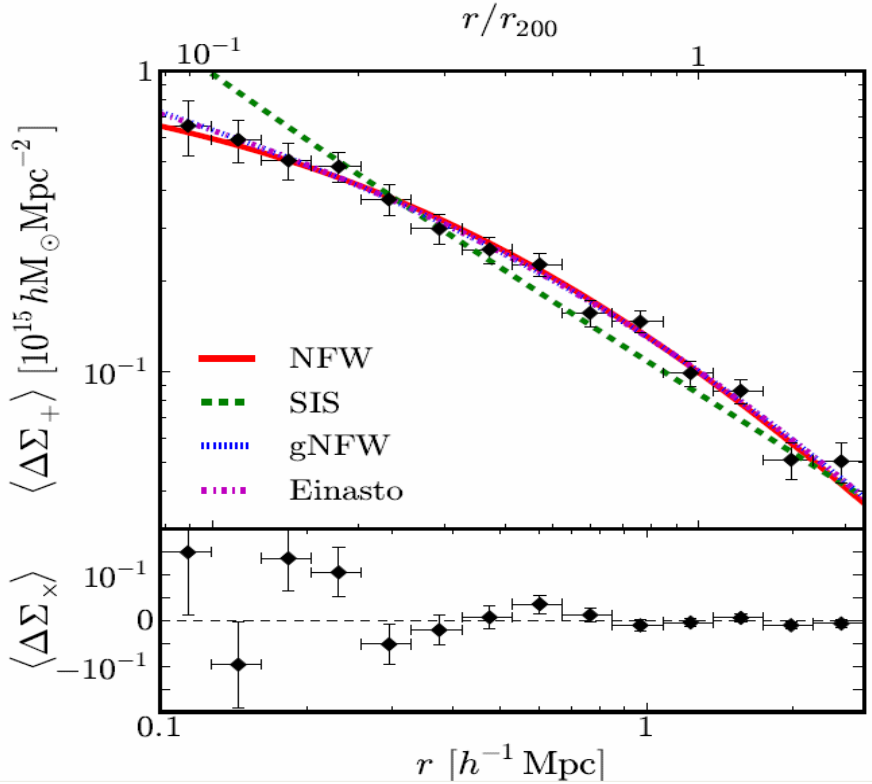

Dark Matter
and large-scale structure

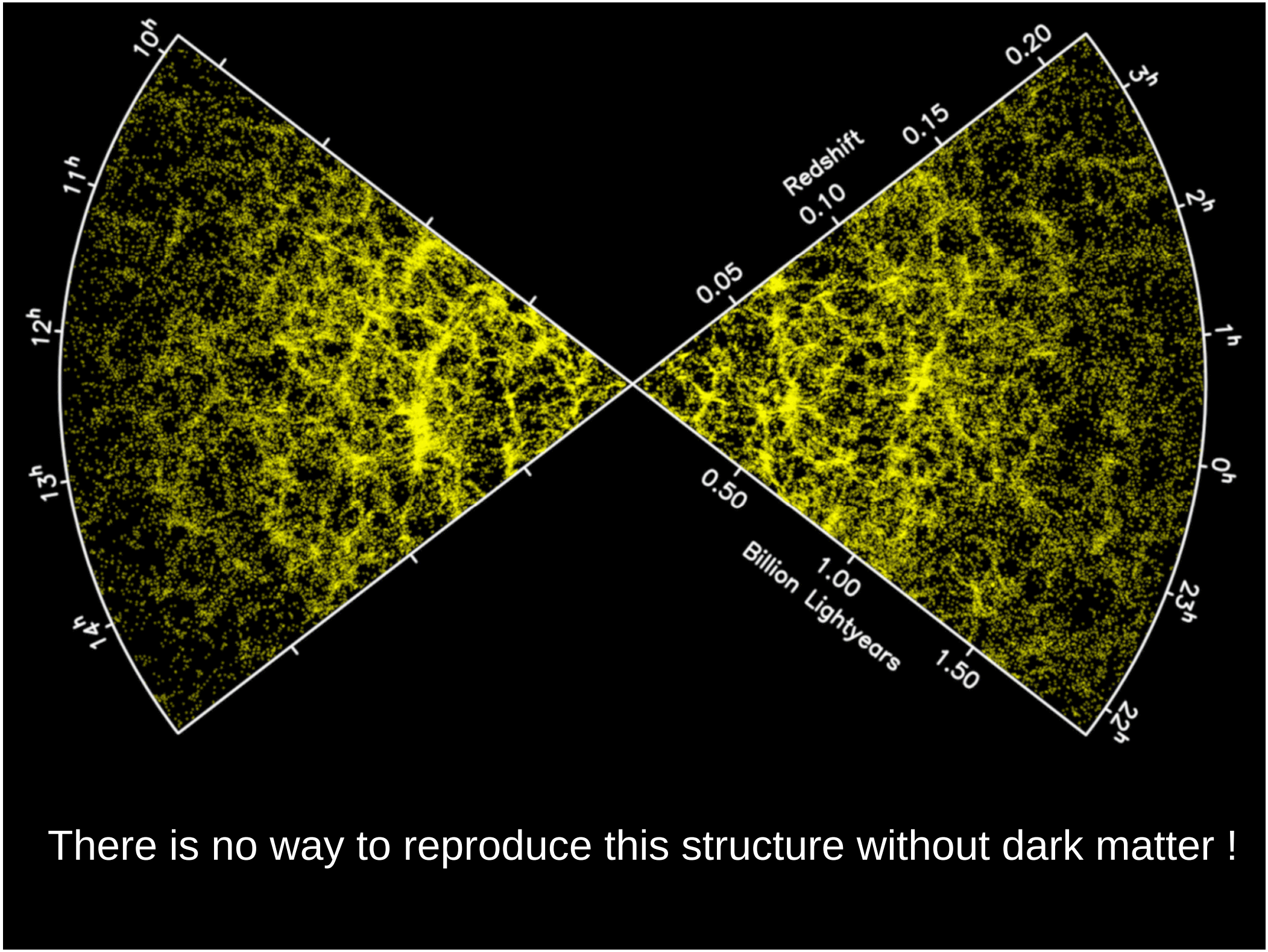

There is no way to reproduce this structure without dark matter !

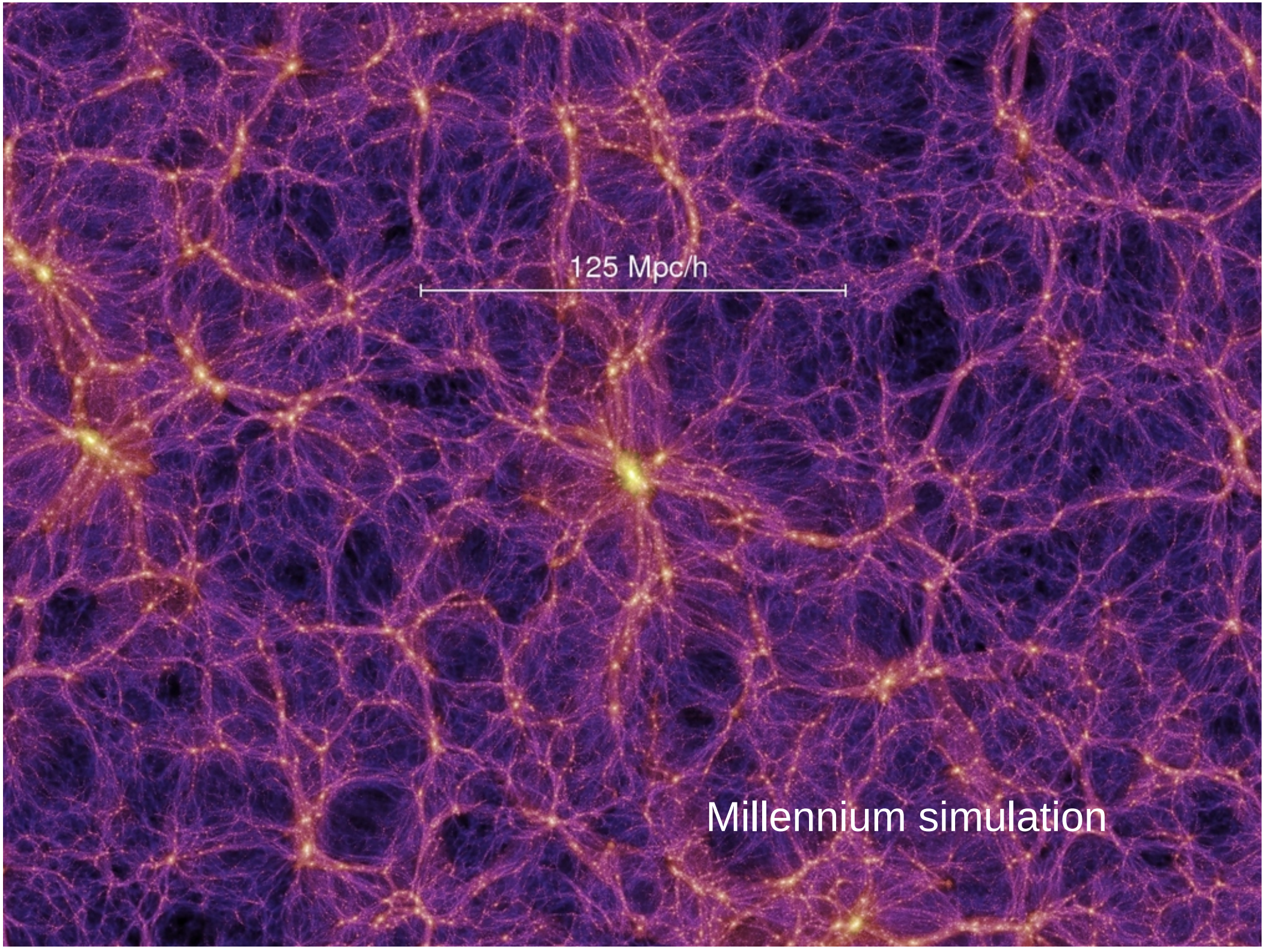
125 Mpc/h
Millennium simulation

Dark Matter
in the Early Universe

What is the CMB

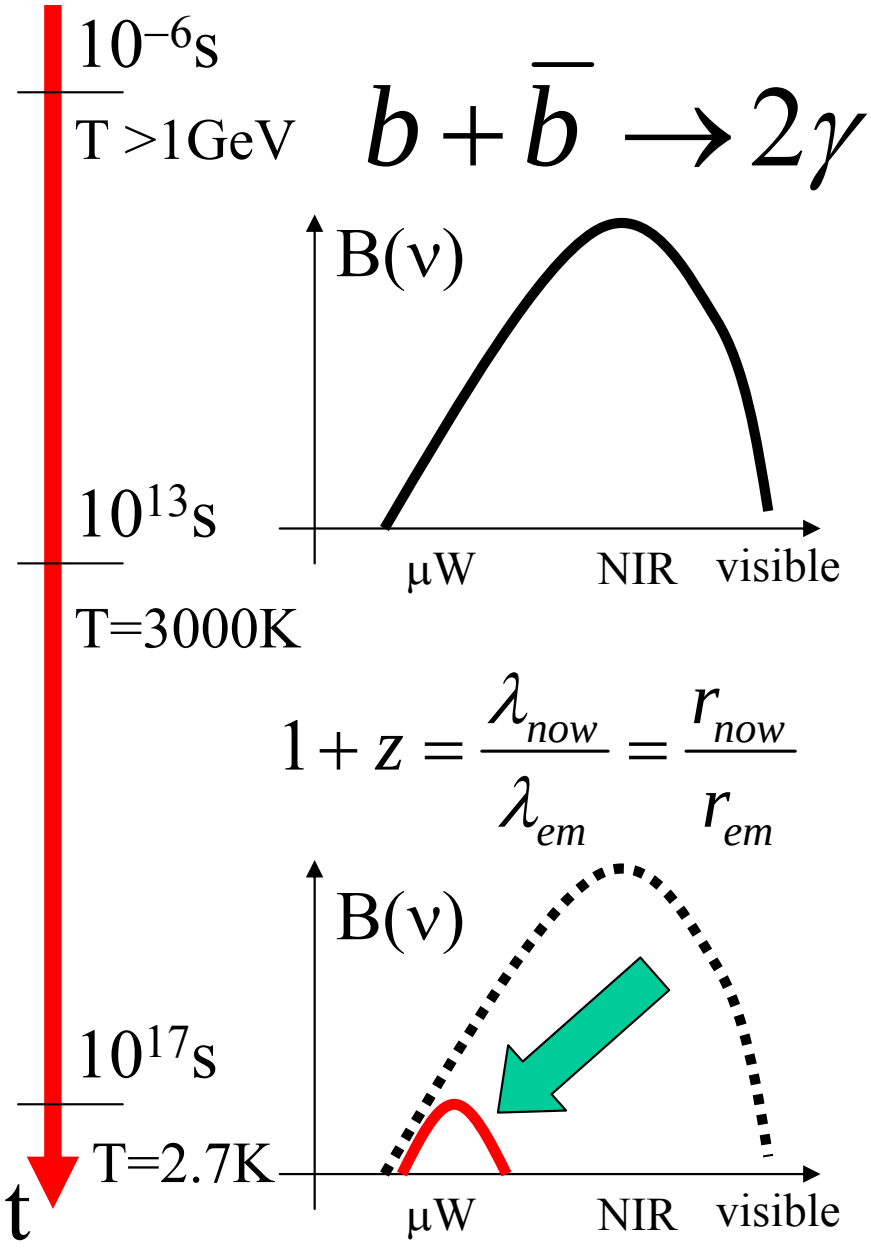

According to modern cosmology:

An abundant background of photons filling the Universe.

- **Generated** in the very early universe, less than 4 μs after the Big Bang ($10^9\gamma$ for each baryon)
- **Thermalized** in the primeval fireball (in the first 380000 years after the big bang) by repeated scattering against free electrons
- **Redshifted** to microwave frequencies **and diluted** in the subsequent 14 Gyrs of expansion of the Universe
- **Today: 410γ/cm³, ~1 meV**

These photons carry
significant information
on the structure, evolution and
composition of our universe

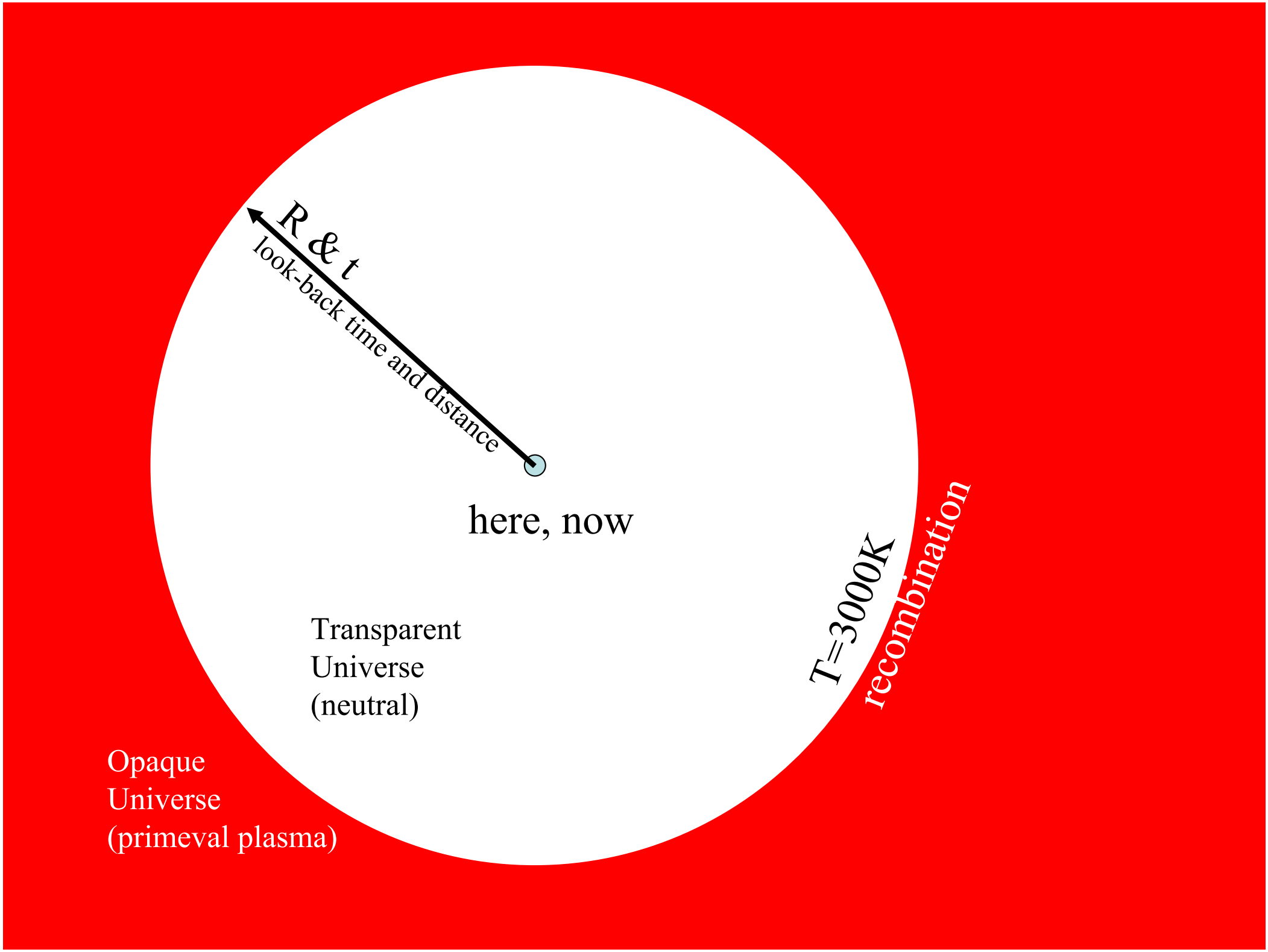
R & t
look-back time and distance
here, now
Transparent
Universe
(neutral)
T=3000K
recombination
Opaque
Universe
(primeval plasma)

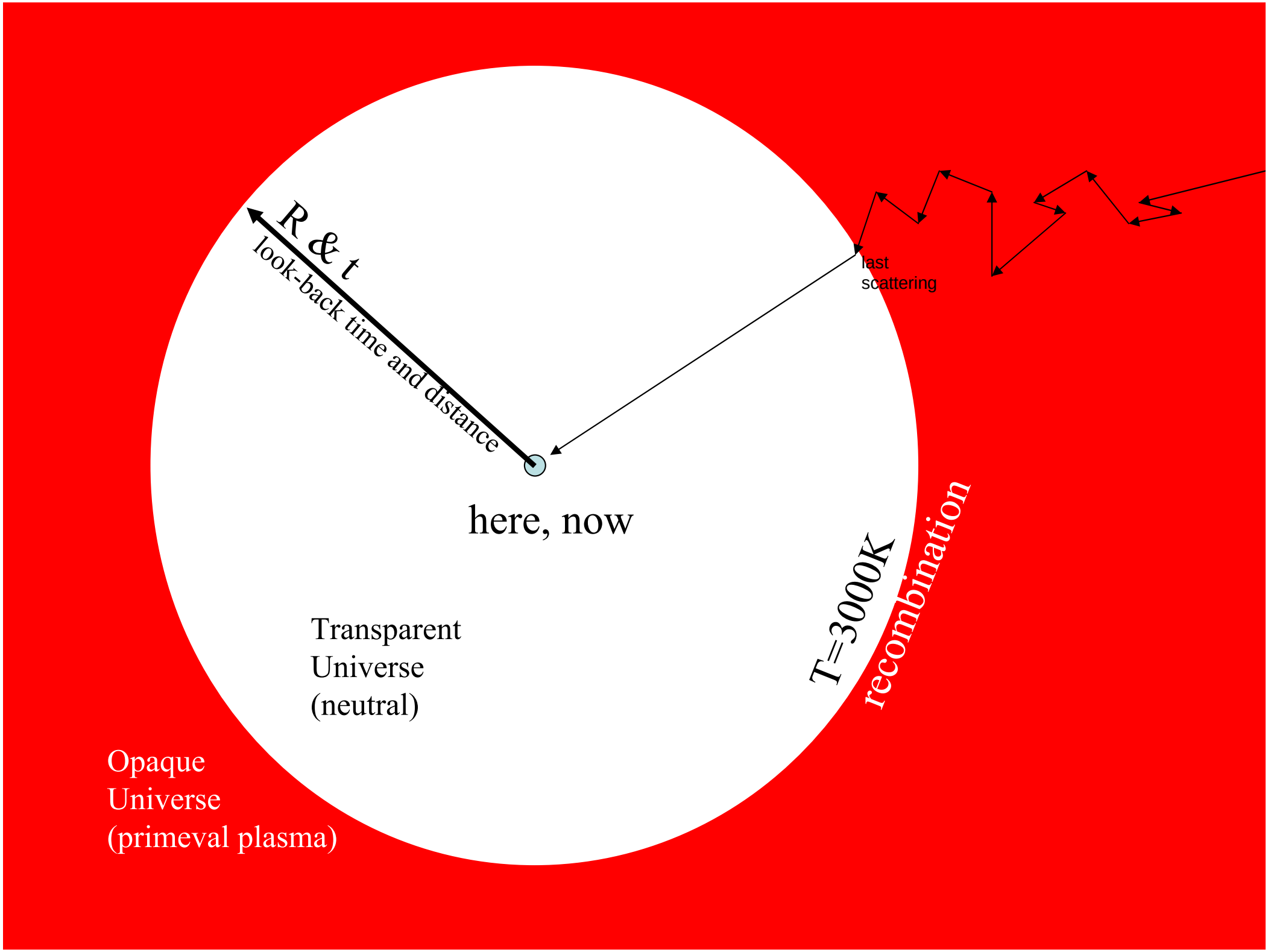
R & t
look-back time and distance
last
scattering
here, now
Transparent
Universe
(neutral)
T=3000K
recombination
Opaque
Universe
(primeval plasma)

CMB anisotropy (intrinsic)

- Different physical effects, all related to the *small* density fluctuations $\delta\rho/\rho$ present 380000 yrs after the big bang (recombination) produce CMB Temperature fluctuations:

$$\frac{\delta T}{T} = \frac{1}{3}\frac{\delta\varphi}{c^2} + \frac{1}{4}\frac{\delta\rho_\gamma}{\rho_\gamma} - \frac{\vec{v}}{c}\cdot\vec{n}$$

Sachs-Wolfe (gravitational redshift) | Photon density fluctuations | Doppler effect from velocity fields

- Scales larger than the horizon are basically frozen in the pre-recombination era. Flat power spectrum of $\delta T/T$ at large scales.
- Scales smaller than the horizon undergo acoustic oscillations during the primeval fireball. Acoustic peaks in the power spectrum of $\delta T/T$ at sub-degree scales.

CMB anisotropy (intrinsic)

- The primeval plasma of photons and matter oscillates :
- self-gravity vs radiation pressure.
- We can measure the result of these oscillations as a weak anisotropy pattern in the image of the CMB.
- Statistical theory: all information encoded in the angular power spectrum of the image.

Density perturbations ($\Delta\rho/\rho$) were **oscillating** in the primeval plasma (as a result of the opposite effects of gravity and photon pressure).

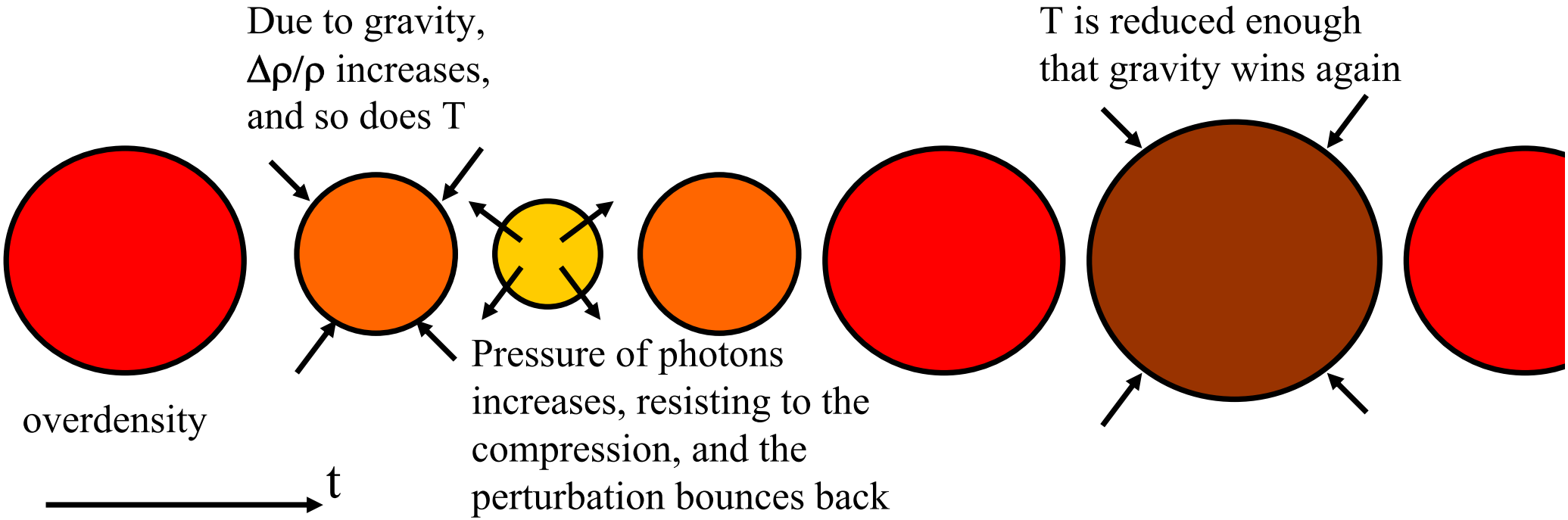

Before recombination $T > 3000$ K

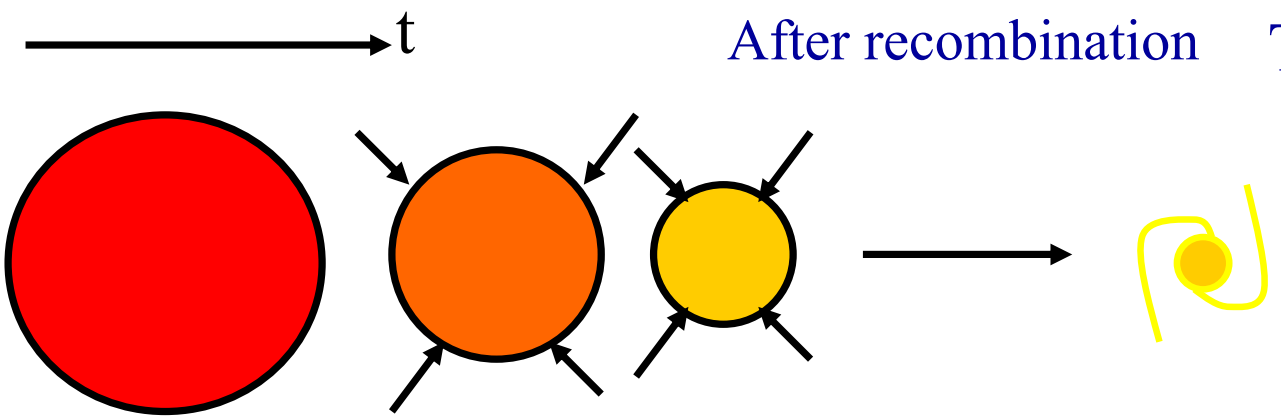

After recombination $T < 3000$ K

Here photons are not tightly coupled to matter, and their pressure is not effective. Perturbations can grow and form Galaxies.

After recombination, density perturbation can **grow** and create the hierarchy of structures we see in the nearby Universe.

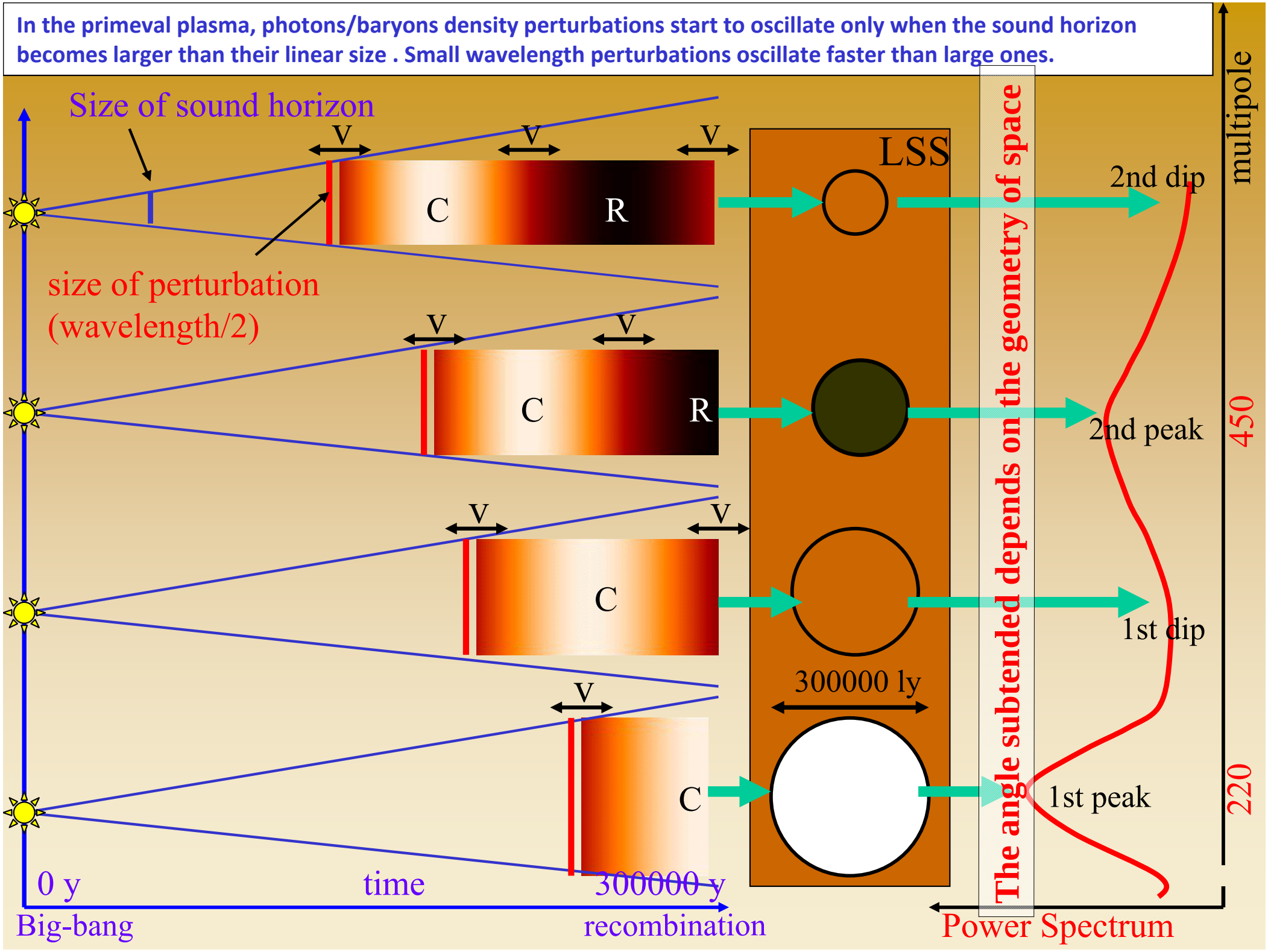
In the primeval plasma, photons/baryons density perturbations start to oscillate only when the sound horizon becomes larger than their linear size . Small wavelength perturbations oscillate faster than large ones.
Size of sound horizon
size of perturbation
(wavelength/2)
V
C
R
LSS
300000 ly
0 y
time
300000 y
Big-bang
recombination
The angle subtended depends on the geometry of space
multipole
450
220
2nd dip
2nd peak
1st dip
1st peak
Power Spectrum

Expected power spectrum:

$$\Delta T(\theta,\varphi) = \sum_{\ell,m} a_{\ell m} Y_\ell^m(\theta,\varphi)$$

$$c_\ell = \left\langle a_{\ell m}^2 \right\rangle$$

$$\left\langle \Delta T^2 \right\rangle = \frac{1}{4\pi} \sum_\ell (2\ell+1) c_\ell$$

See e.g. http://camb.info to compute c_ℓ for a given cosmological model

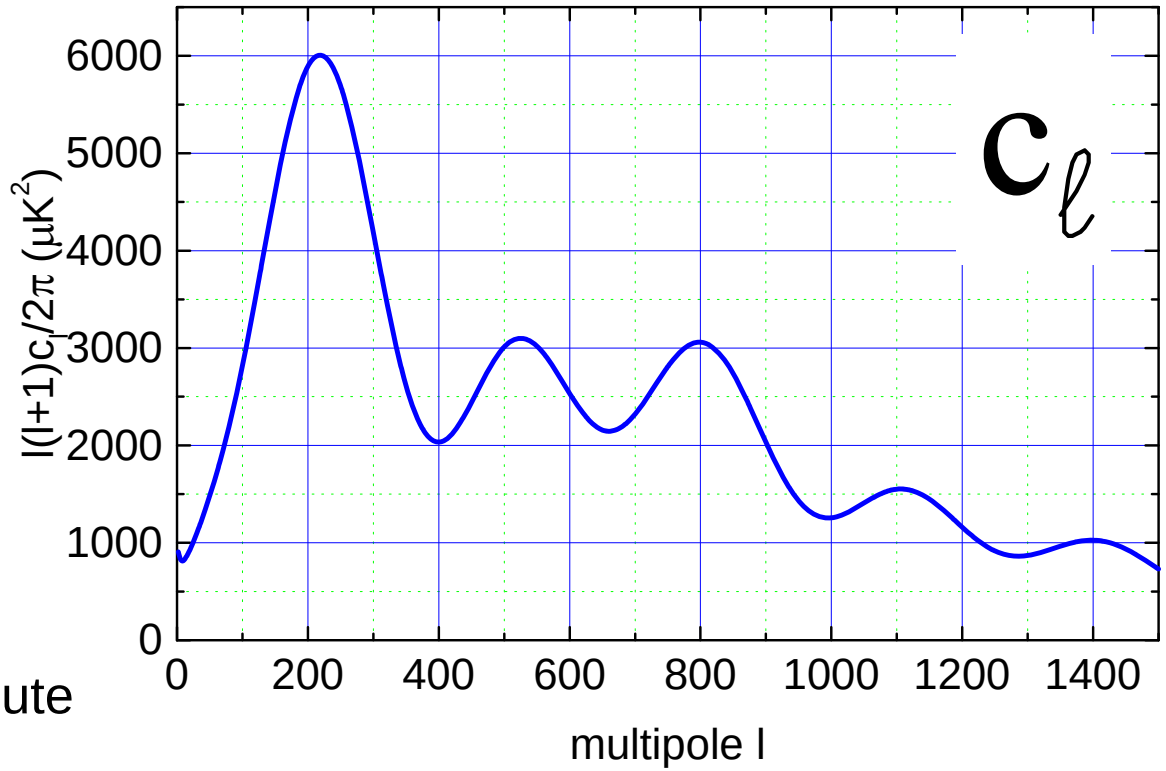

An instrument with finite angular resolution is not sensitive to the smallest scales (highest multipoles). For a gaussian beam with s.d. σ:

$$w_\ell^{LP} = e^{-\ell(\ell+1)\sigma^2}$$

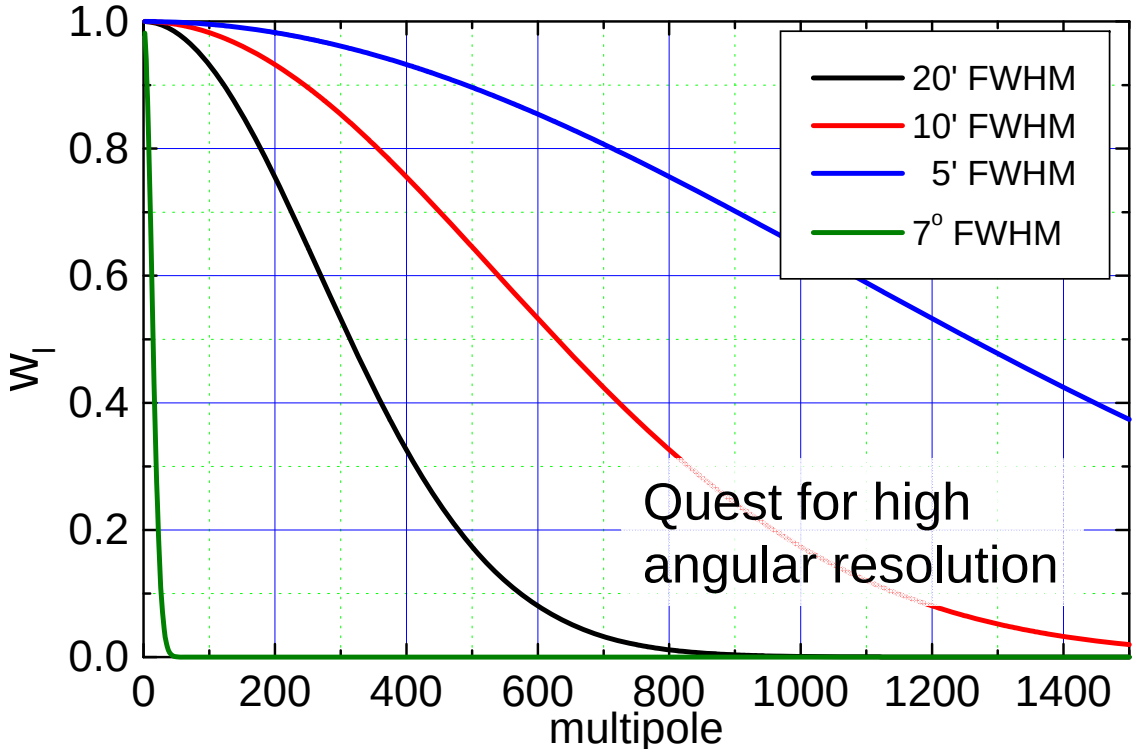

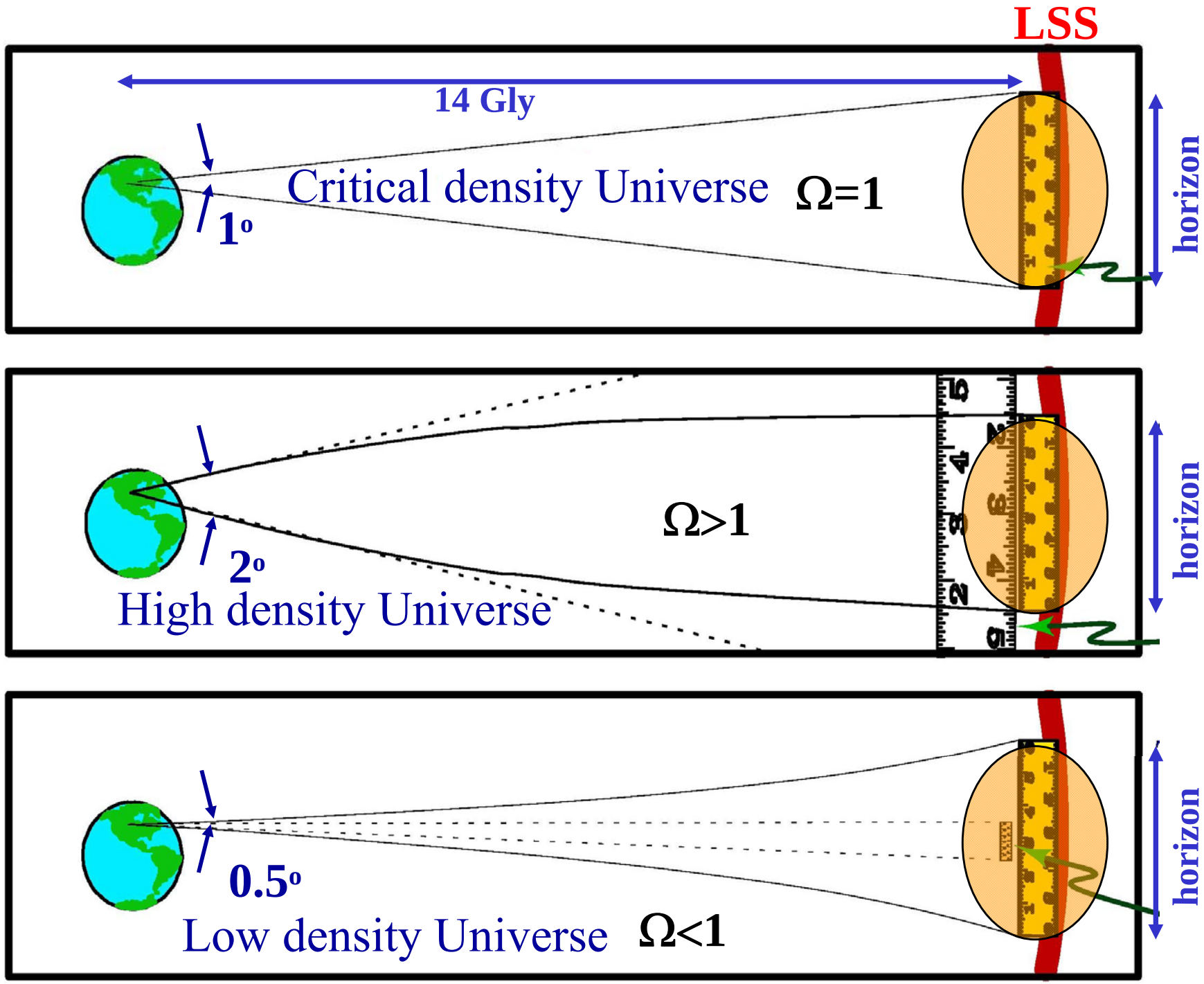

The image and PS are modified by the geometry of the universe

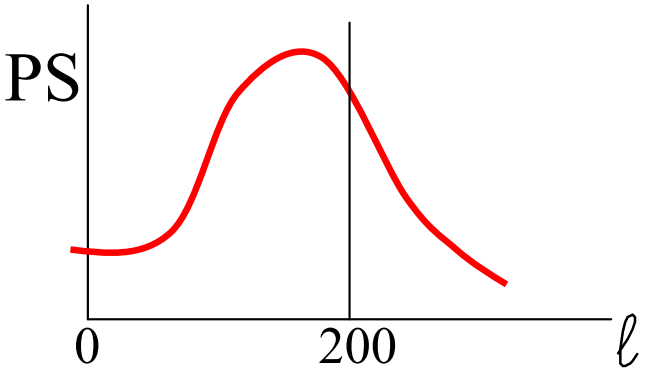

High density Universe

$\Omega>1$

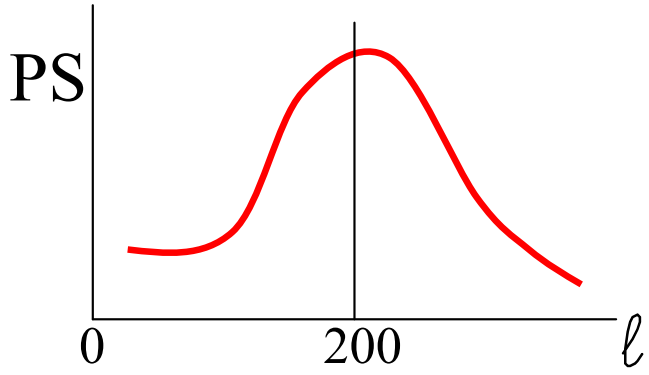

Critical density Universe

$\Omega=1$

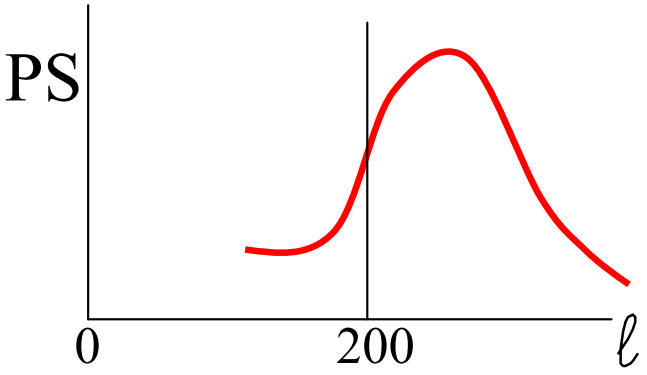

Low density Universe

$\Omega<1$

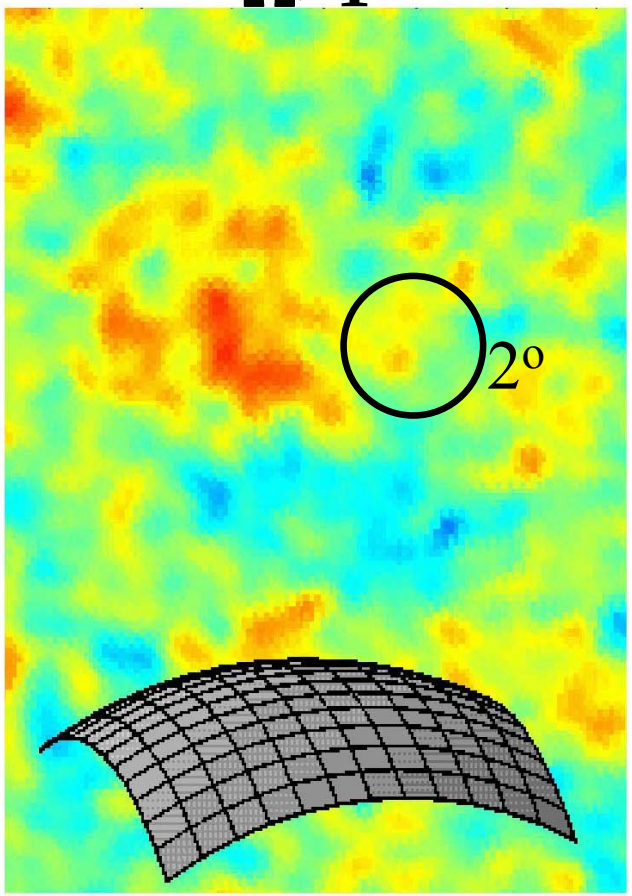

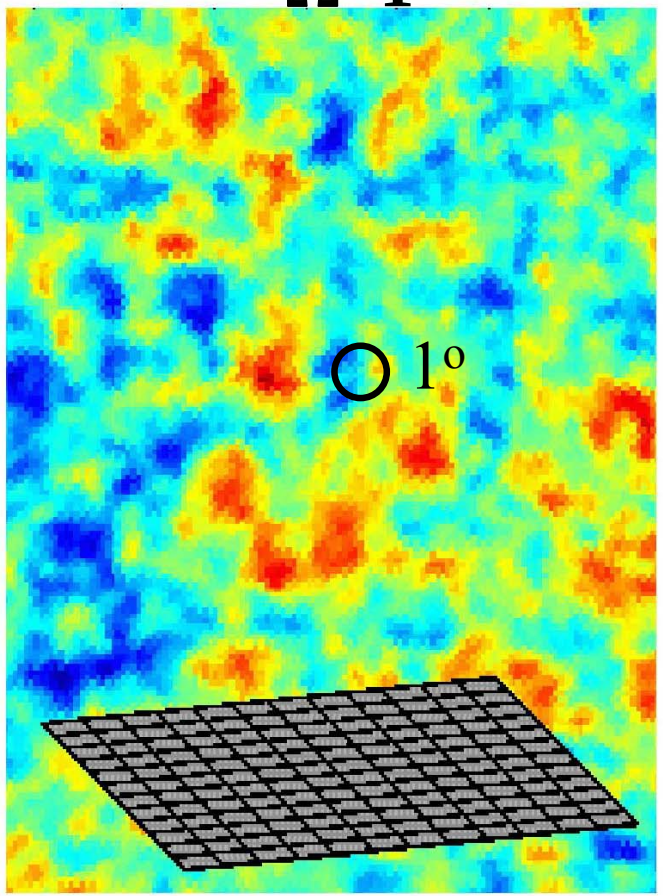

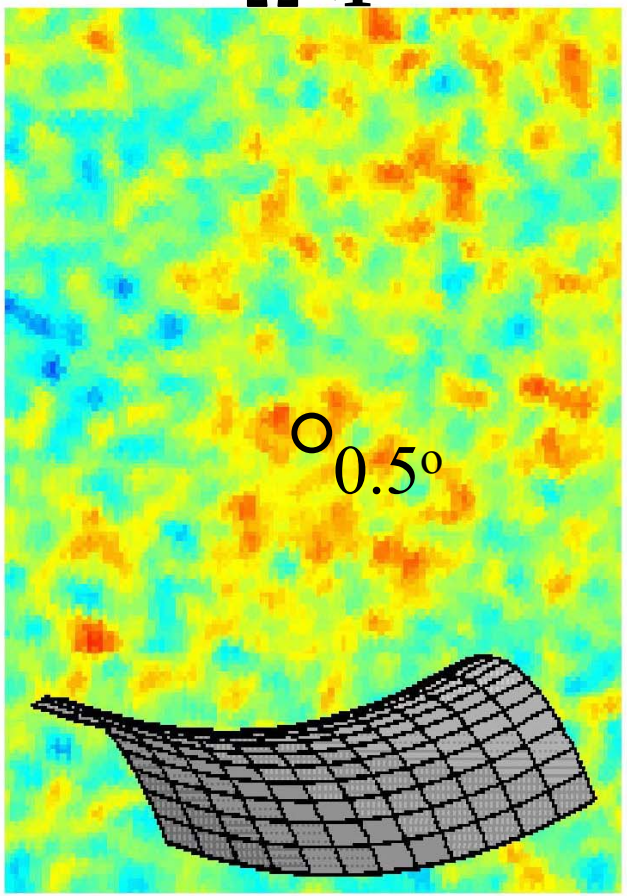

The mass-energy density of the Universe can be measured in this way.

Composition

- The composition of the universe (baryons, dark matter, dark energy) affects the shape of the power spectrum.
- Accurate measurements of the power spectrum allow to constrain the energy densities of the different components of the universe.

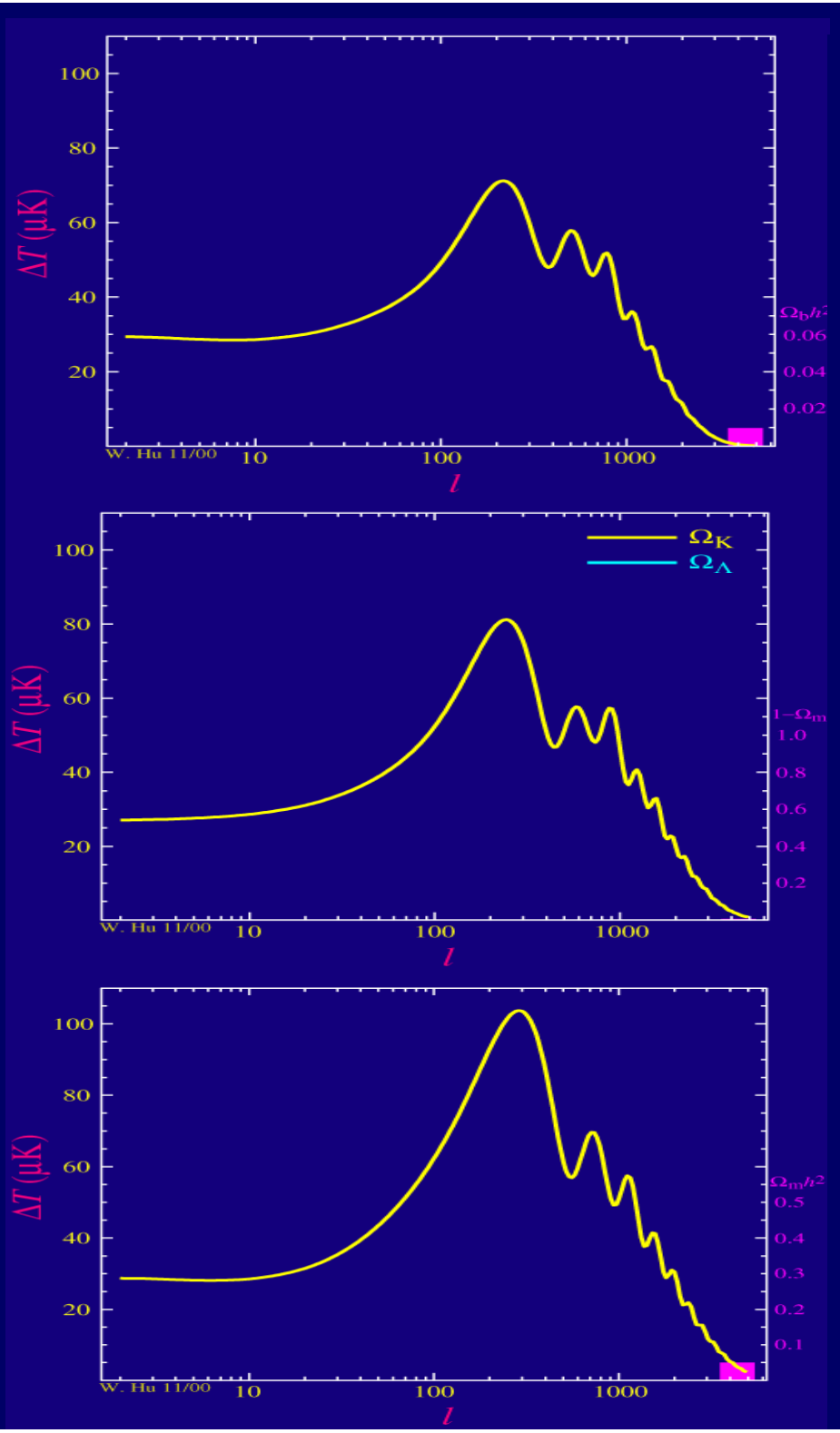

Baryons-photons fluid oscillations

- The fluid sits in the potential well due to the (mainly dark) matter distribution.
  - Gravity compresses the fluid
  - Radiation resists compression
- The equation describing the oscillation is formally the equation of a mass on a spring falling under gravity.
  - The spring compression represents radiation pressure
  - The position of the mass represents fluid mass (energy) density
  - The potential well follows the distribution of dark matter.

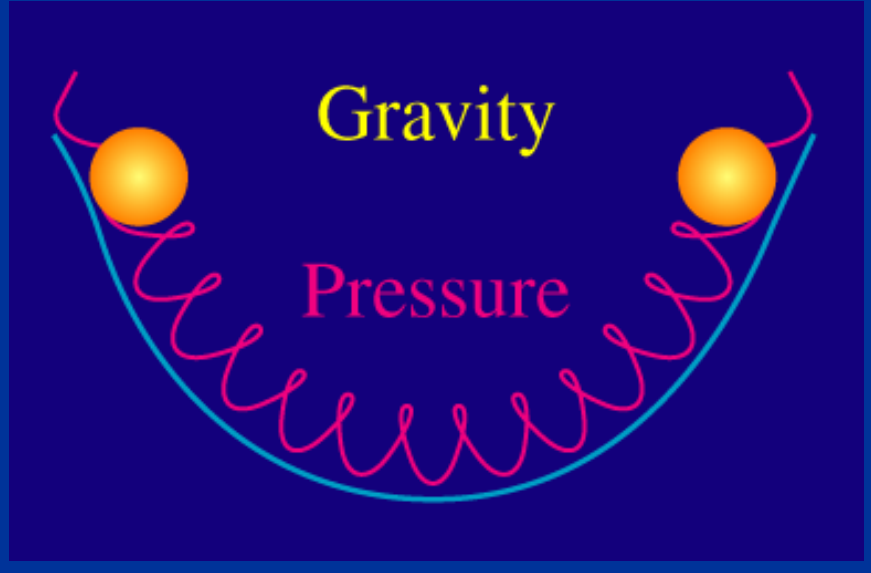

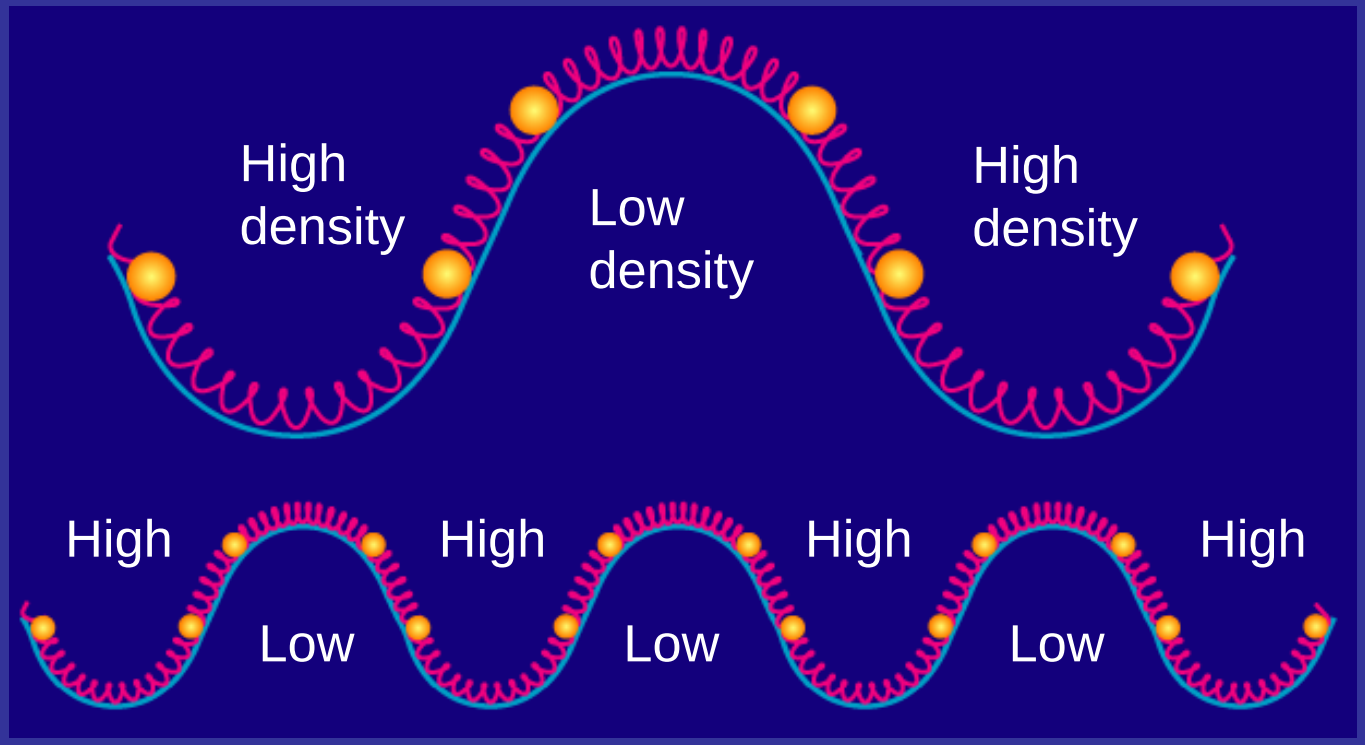

Fluctuations of different size (wavelength) oscillate at different speed ($\omega=kc_s$) And arrive at recombination with different phase.

Sound waves stop oscillating at recombination. Extrema in density (i.e. enhanced CMB anisotropy) correspond to multiples of the fundamental (sound horizon scale)

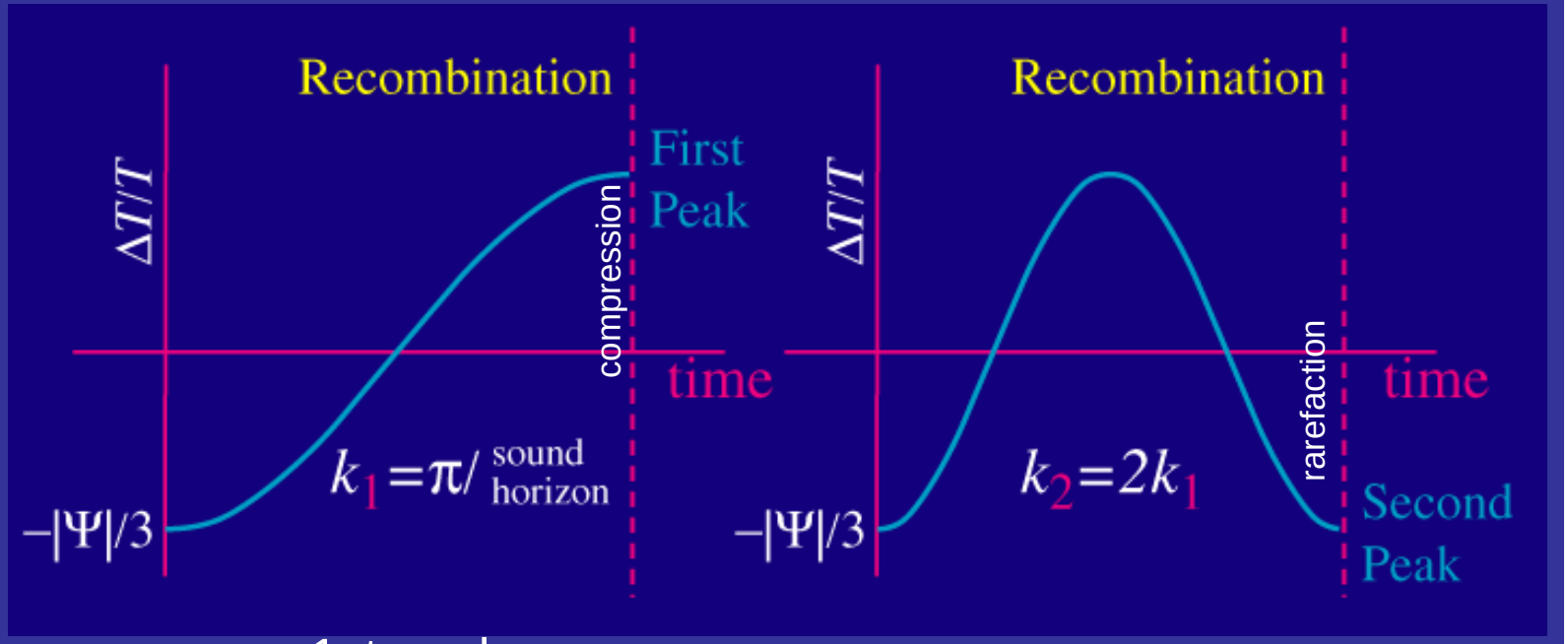

1st peak

2nd peak ….

Baryons load down the photon-baryon plasma and add inertial (and gravitational) mass to the oscillating system.

Odd numbered (first, third, fifth...) acoustic peaks are associated with how far the plasma "falls" into gravitational potential wells (how much the plasma compresses), They are enhanced by an increase in the amount of baryons in the universe.

The even numbered peaks (second, fourth, sixth) are associated with how much the plasma rarefies.

Thus with the addition of baryons the odd peaks are enhanced over the even peaks. The more baryons the more the second peak is *relatively* suppressed.

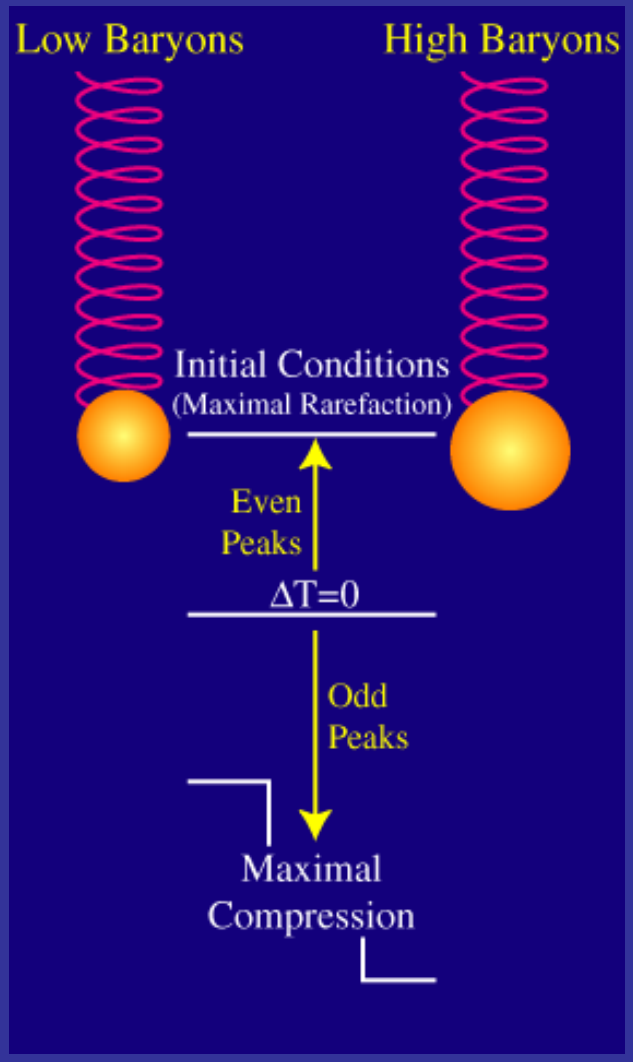

http://background.uchicago.edu/~whu/intermediate/harmonic.html

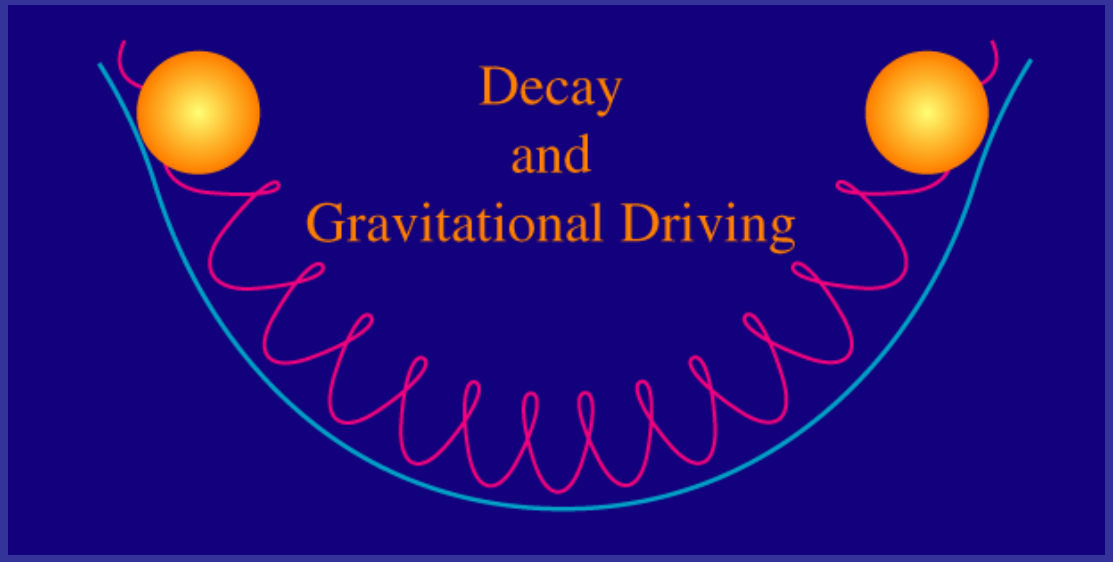

These fluctuations do not oscillate in a fixed gravitational well, since radiation is very important expecially in the radiation dominated era.

As pressure stops the radiation from further compression, the density fluctuation stabilizes leaving the gravitational potential to decay with the expansion of the universe. The decay happens when the fluid is in its most compressed state. The fluid now sees no gravitational potential to fight against as it bounces back and the amplitude of the oscillations goes way up.

However, if the dark matter density is high, this effect is reduced. So we expect a reduction of the amplitude of all peaks when matter density is increased.

http://background.uchicago.edu/~whu/intermediate/baryons.html

Including all the effects :

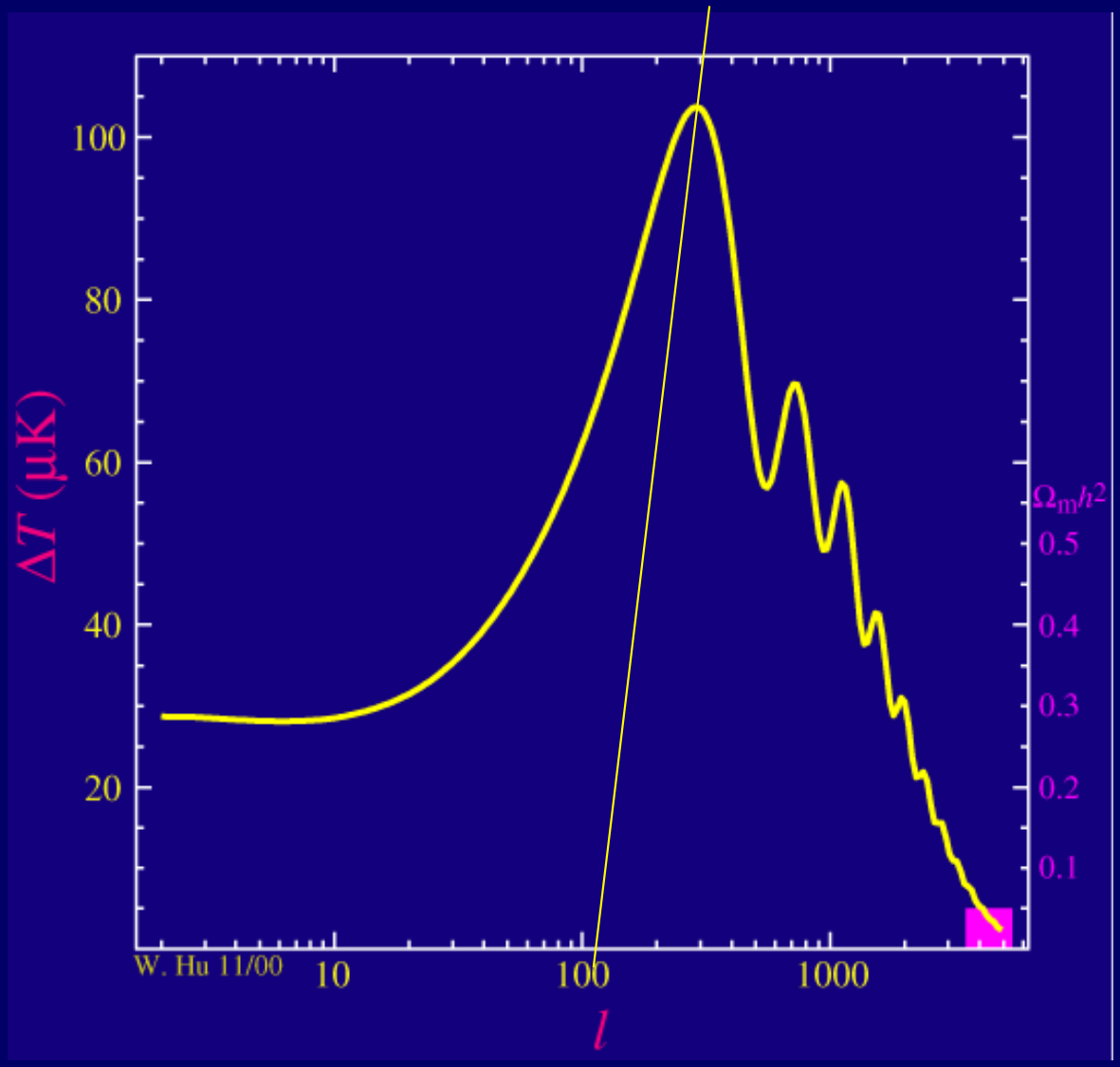

http://background.uchicago.edu/~whu/intermediate/baryons.html

Planck is a very ambitious experiment.

It carries a complex CMB experiment (the state of the art, a few years ago) all the way to L2,

improving the sensitivity wrt WMAP by at least a factor 10,

extending the frequency coverage towards high frequencies by a factor about 10

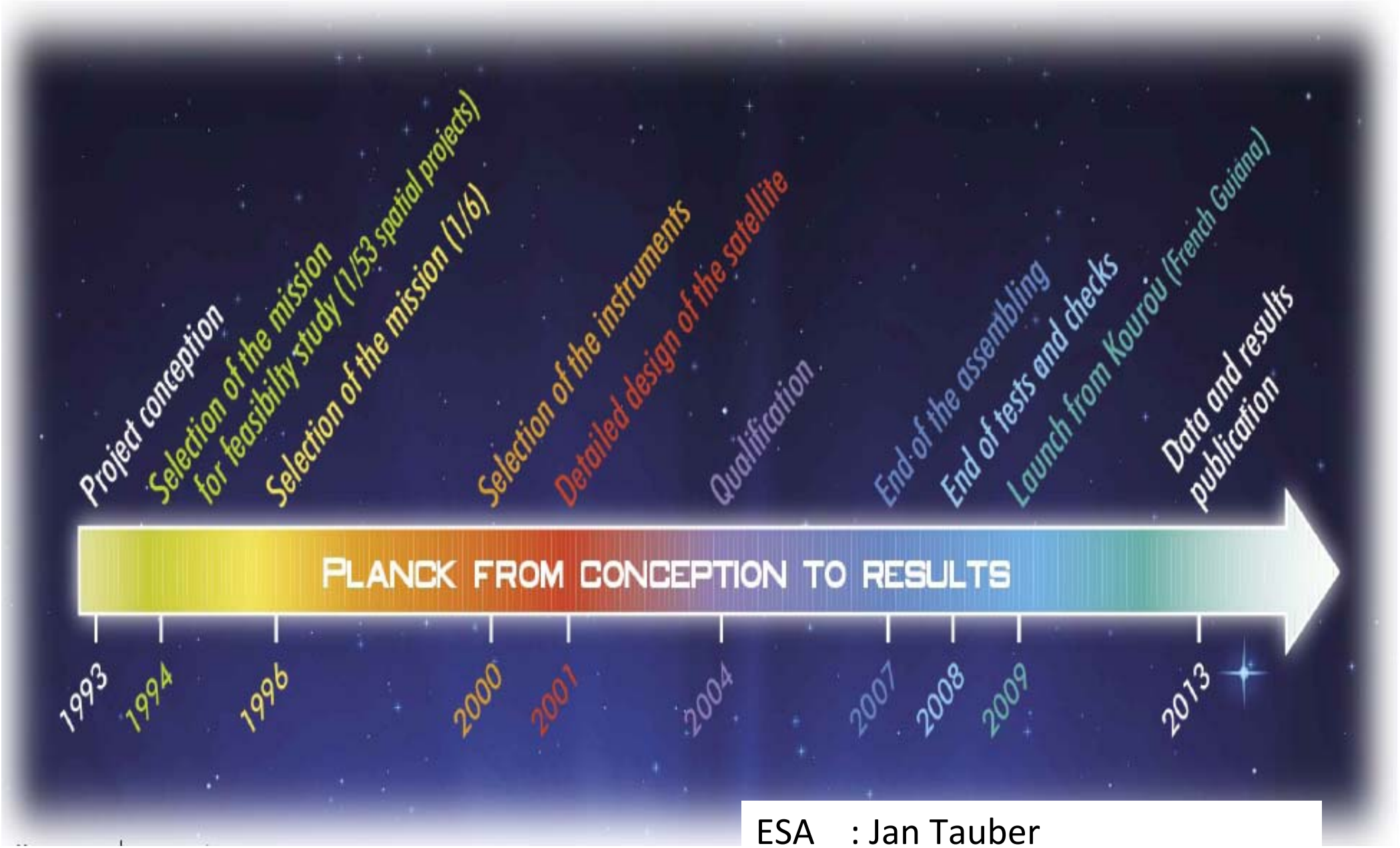

Almost 20 years of hard work of a very large team, coordinated by:

ESA : Jan Tauber
HFI PI : Jean Loup Puget (Paris)
HFI IS : Jean Michel Lamarre (Paris)
LFI PI : Reno Mandolesi (Bologna)
LFI IS : Marco Bersanelli (Milano)

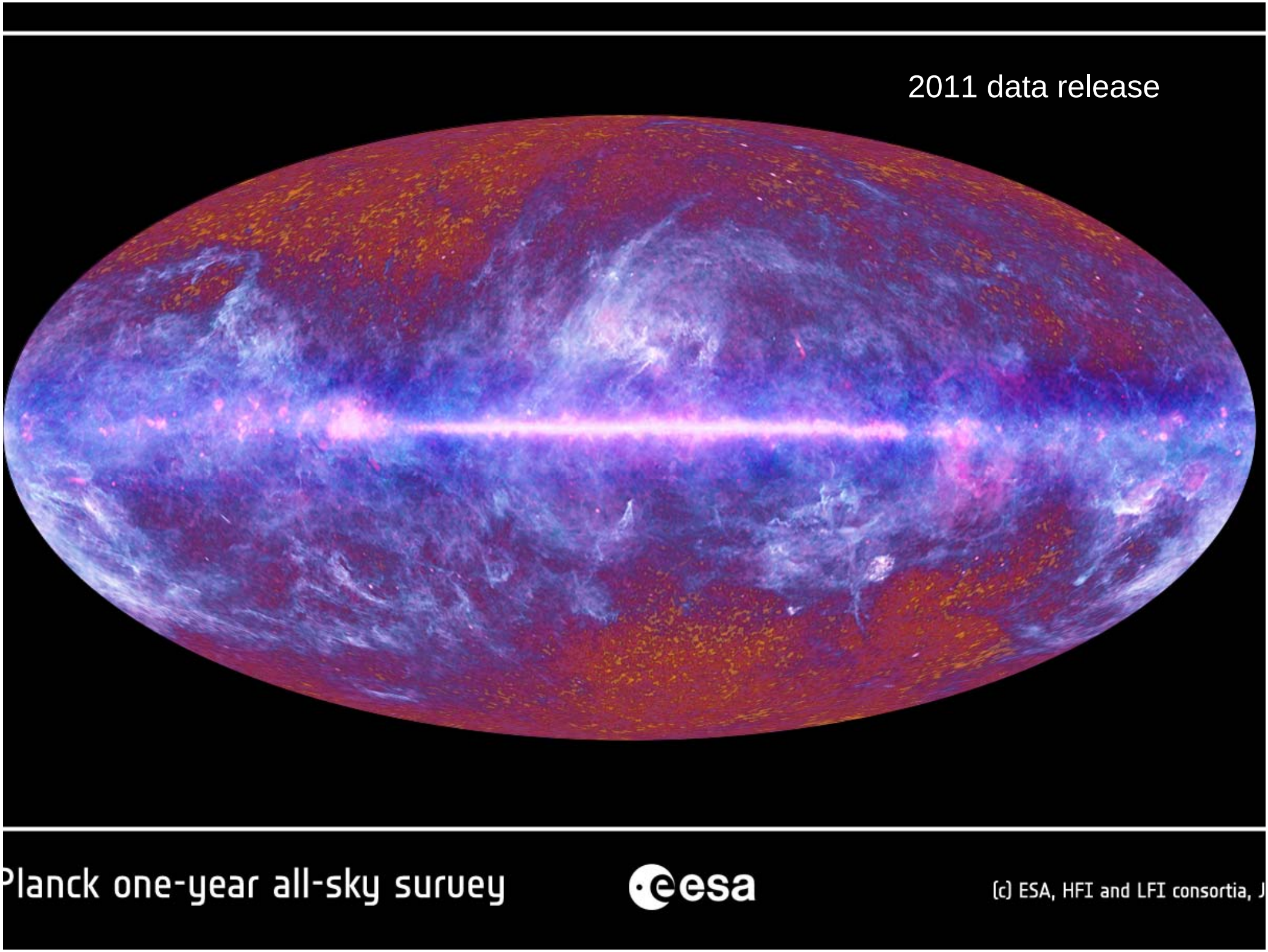
2011 data release
Planck one-year all-sky survey
esa
(c) ESA, HFI and LFI consortia, J

The 2013 Planck results

- Planck 2013 results. I. Overview of products and results
- Planck 2013 results. II. Low Frequency Instrument data processing
- Planck 2013 results. III. LFI systematic uncertainties
- Planck 2013 results. IV. LFI beams
- Planck 2013 results. V. LFI calibration
- Planck 2013 results. VI. High Frequency Instrument data processing
- Planck 2013 results. VII. HFI time response and beams
- Planck 2013 results. VIII. HFI calibration and mapmaking
- Planck 2013 results. IX. HFI spectral response
- Planck 2013 results. X. HFI energetic particle effects
- Planck 2013 results. XI. Consistency of the data
- Planck 2013 results. XII. Component separation
- Planck 2013 results. XIII. Galactic CO emission
- Planck 2013 results. XIV. Zodiacal emission
- Planck 2013 results. XV. CMB power spectra and likelihood
- Planck 2013 results. XVI. Cosmological parameters
- Planck 2013 results. XVII. Gravitational lensing by large-scale structure
- Planck 2013 results. XVIII. The gravitational lensing-infrared background correlation
- Planck 2013 results. XIX. The integrated Sachs-Wolfe effect
- Planck 2013 results. XX. Cosmology from Sunyaev- Zeldovich cluster counts
- Planck 2013 results. XXI. All-sky Compton-parameter map and characterization
- Planck 2013 results. XXII. Constraints on inflation
- Planck 2013 results. XXIII. Isotropy and statistics of the CMB
- Planck 2013 results. XXIV. Constraints on primordial non-Gaussianity
- Planck 2013 results. XXV. Searches for cosmic strings and other topological defects
- Planck 2013 results. XXVI. Background geometry and topology of the Universe
- Planck 2013 results. XXVII. Special relativistic effects on the CMB dipole
- Planck 2013 results. XXVIII. The Planck Catalogue of Compact Sources
- Planck 2013 results. XXIX. The Planck catalogue of Sunyaev-Zeldovich sources
- Planck 2013 results. Explanatory supplement

29 papers (+1 to come on CIB);
800+ pages
1 Explanatory Supplement
all products available online

The 2013 Planck results

- Planck 2013 results. I. Overview of products and results
- Planck 2013 results. II. Low Frequency Instrument data processing
- Planck 2013 results. III. LFI systematic uncertainties
- Planck 2013 results. IV. LFI beams
- Planck 2013 results. V. LFI calibration
- Planck 2013 results. VI. High Frequency Instrument data processing
- Planck 2013 results. VII. HFI time response and beams
- Planck 2013 results. VIII. HFI calibration and mapmaking
- Planck 2013 results. IX. HFI spectral response
- Planck 2013 results. X. HFI energetic particle effects
- Planck 2013 results. XI. Consistency of the data

Instruments, processing, systematic effects

- Planck 2013 results. XII. Component separation
- Planck 2013 results. XIII. Galactic CO emission
- Planck 2013 results. XIV. Zodiacal emission

Components separation

- Planck 2013 results. XV. CMB power spectra and likelihood
- Planck 2013 results. XVI. Cosmological parameters

Power Spectra, cosmological parameters

- Planck 2013 results. XVII. Gravitational lensing by large-scale structure
- Planck 2013 results. XVIII. The gravitational lensing-infrared background correlation
- Planck 2013 results. XIX. The integrated Sachs-Wolfe effect

Photon propagation effects

- Planck 2013 results. XX. Cosmology from Sunyaev- Zeldovich cluster counts
- Planck 2013 results. XXI. All-sky Compton-parameter map and characterization

The Sunyaev-Zeldovich effect

- Planck 2013 results. XXII. Constraints on inflation
- Planck 2013 results. XXIII. Isotropy and statistics of the CMB
- Planck 2013 results. XXIV. Constraints on primordial non-Gaussianity
- Planck 2013 results. XXV. Searches for cosmic strings and other topological defects
- Planck 2013 results. XXVI. Background geometry and topology of the Universe
- Planck 2013 results. XXVII. Special relativistic effects on the CMB dipole

Constraints on cosmology

- Planck 2013 results. XXVIII. The Planck Catalogue of Compact Sources
- Planck 2013 results. XXIX. The Planck catalogue of Sunyaev-Zeldovich sources
- Planck 2013 results. Explanatory supplement

Products

29 papers (+1 to come on CIB);
800+ pages
1 Explanatory Supplement
all products available online

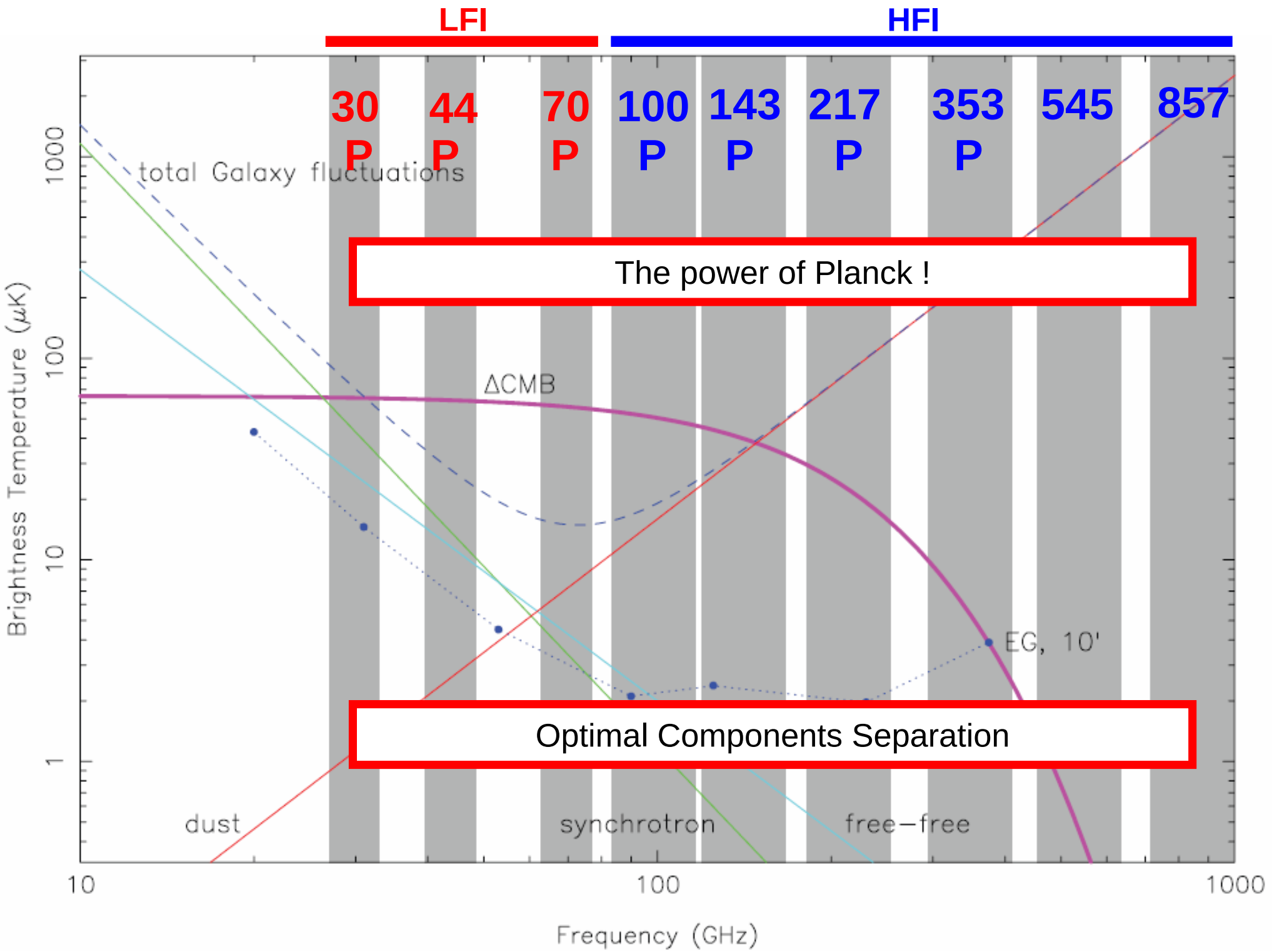
LFI
HFI
30
44
70
100
143
217
353
545
857
P
P
P
P
P
P
P
total Galaxy fluctuations
The power of Planck !
ΔCMB
EG, 10'
Optimal Components Separation
dust
synchrotron
free−free
Brightness Temperature (μK)
1000
100
10
1
10
100
1000
Frequency (GHz)

6x10^6 pixels (5')

Planck Legacy Maps

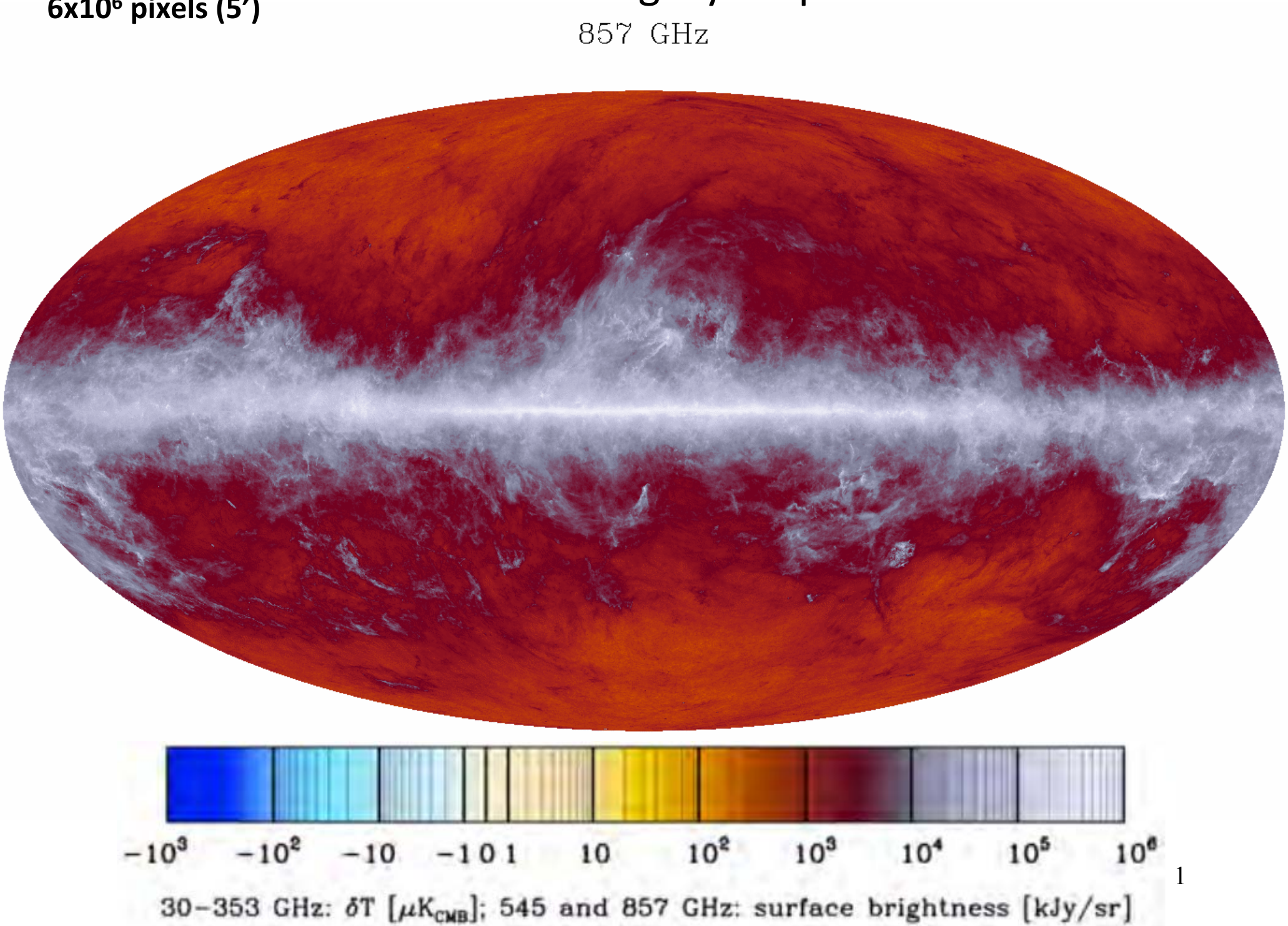

components separation

$$\Delta T(\nu_j,\ell,b) = \sum_k a_k(\nu_j,\ell,b) C_k(\ell,b)$$

Measured maps — physical components

k = CMB,dust,synchrotron,…

j = 33, 44, 70, 100, 143, 217, 353, 545, 857 GHz

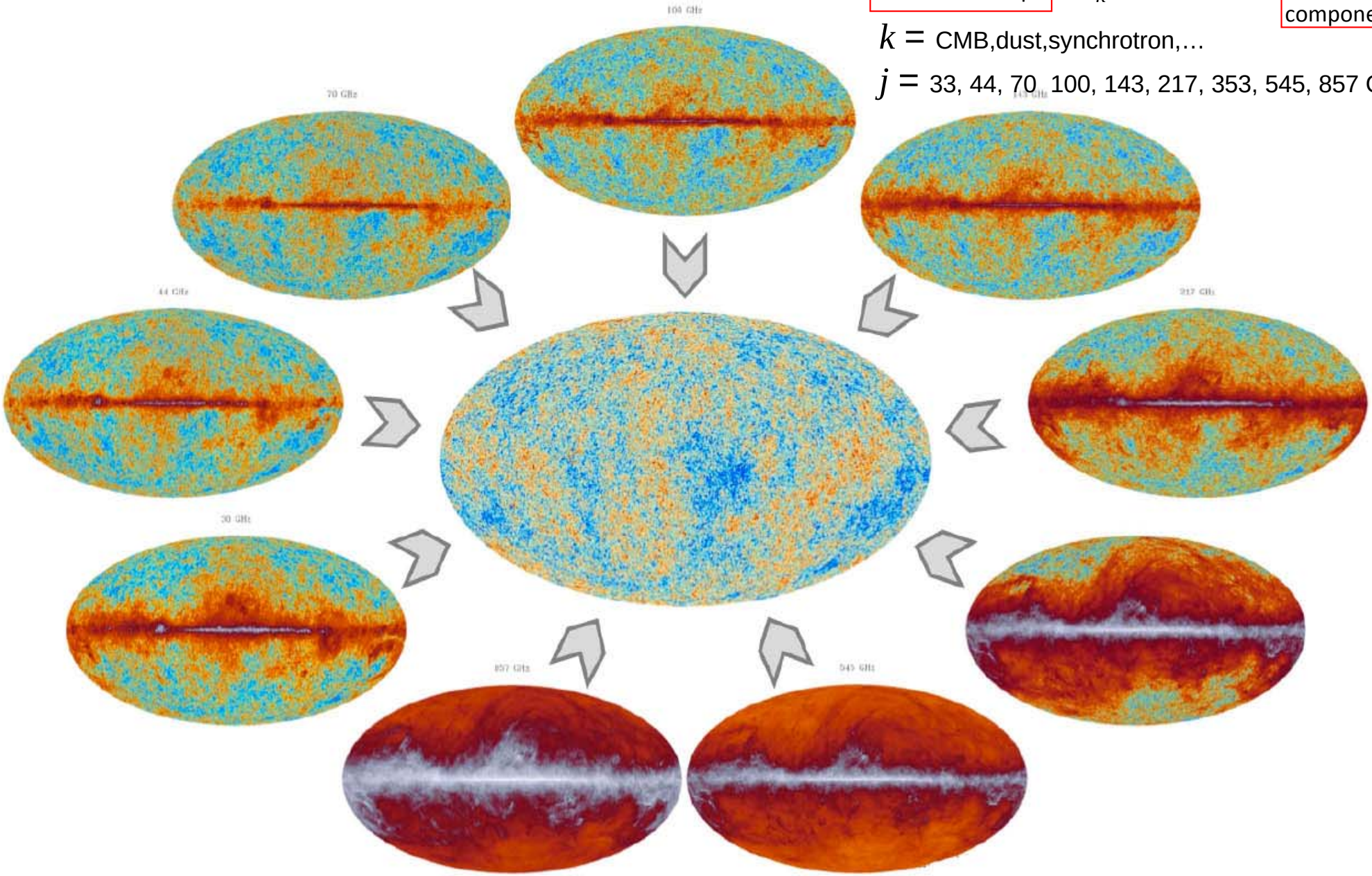

The CMB component

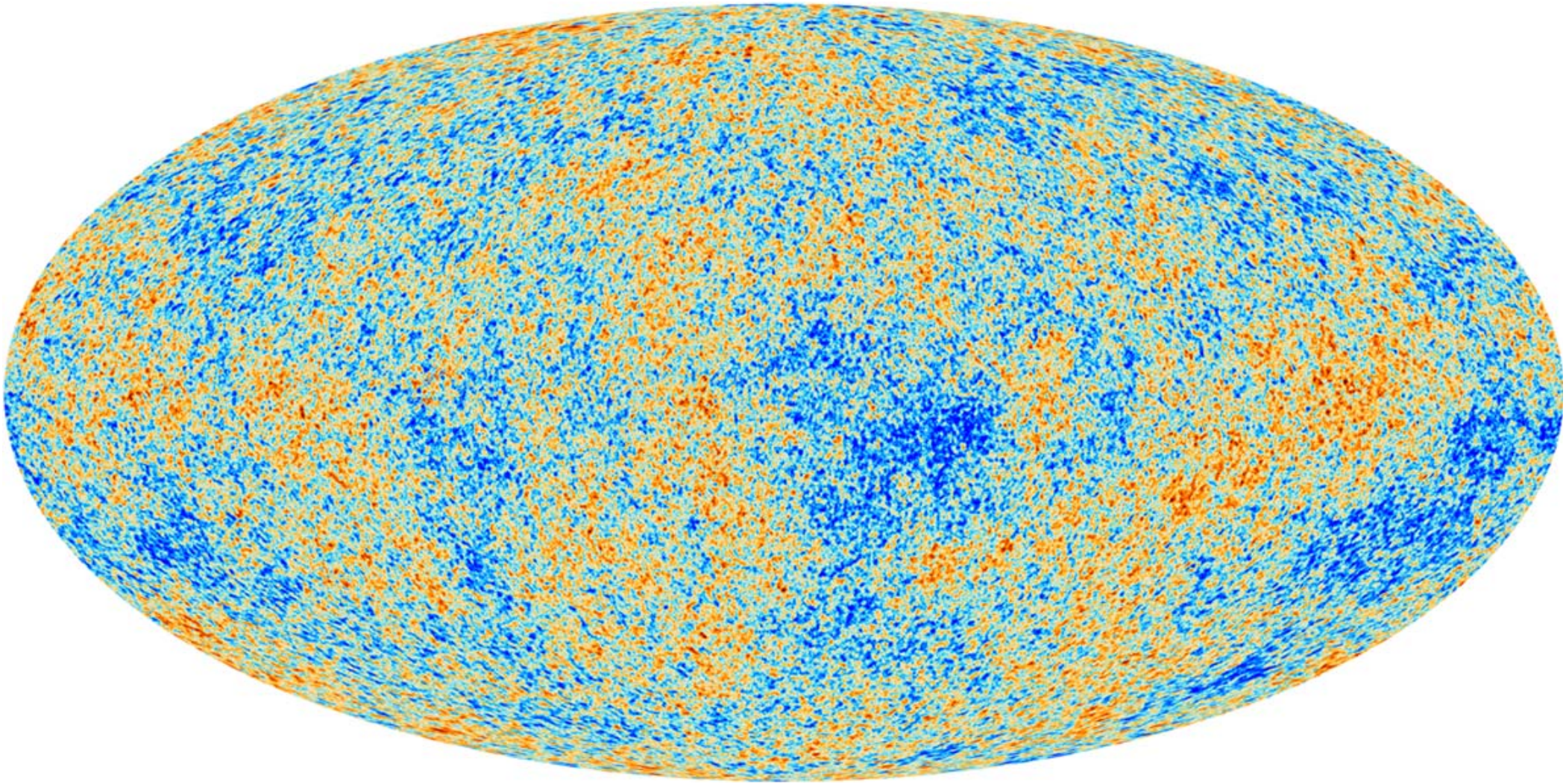

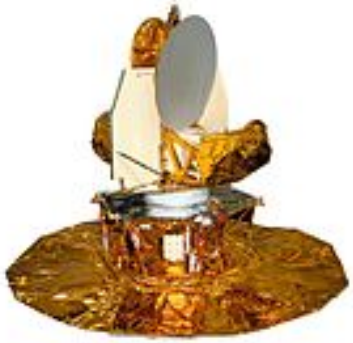

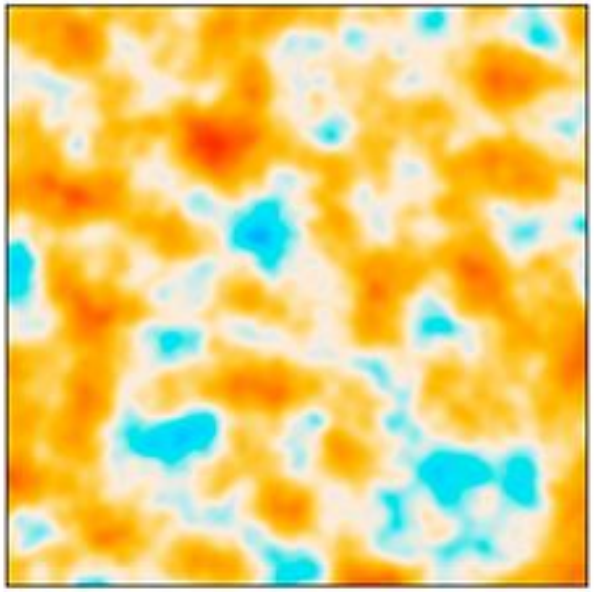

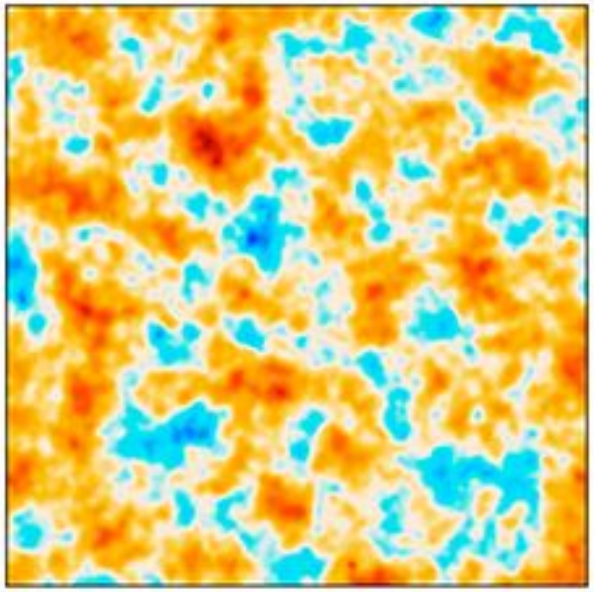

COBE

WMAP

Planck

Best angular resolution
Best control of foregorunds

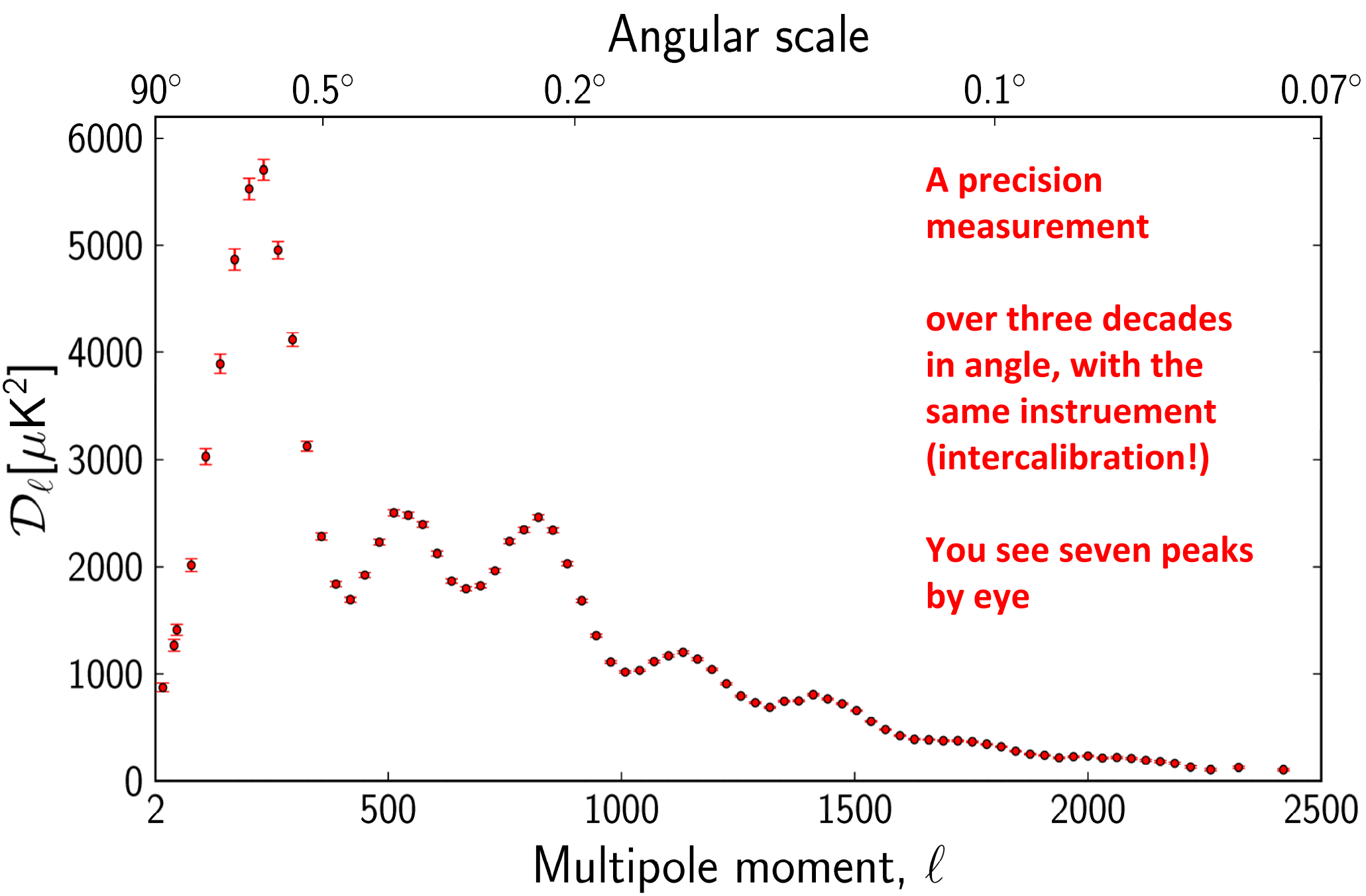
Angular scale
90°
0.5°
0.2°
0.1°
0.07°
6000
5000
4000
3000
2000
1000
0
$\mathcal{D}_\ell [\mu K^2]$
2
500
1000
1500
2000
2500
Multipole moment, ℓ
A precision measurement
over three decades in angle, with the same instruement (intercalibration!)
You see seven peaks by eye

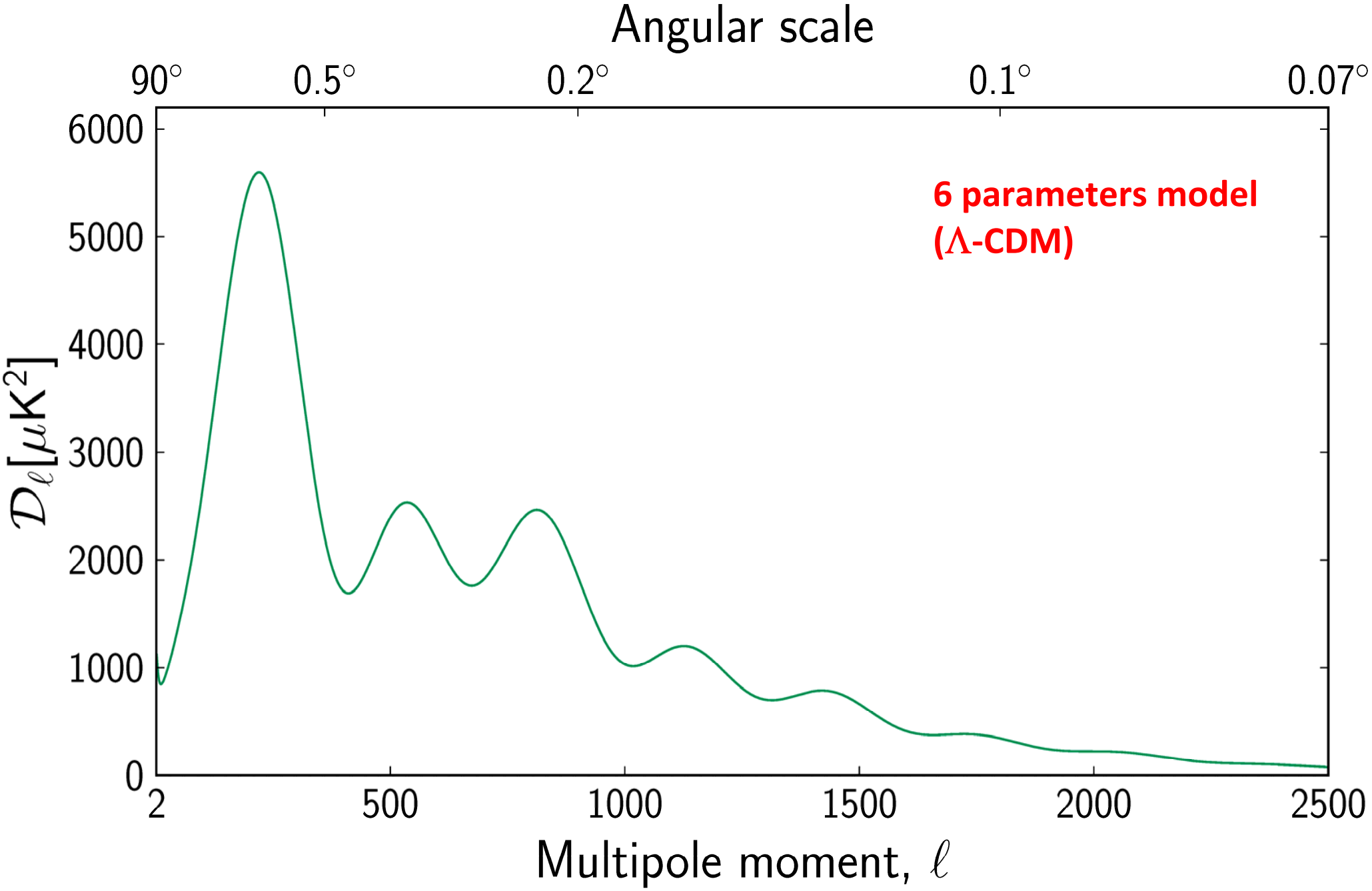
Angular scale
90°
0.5°
0.2°
0.1°
0.07°
6000
5000
4000
3000
2000
1000
0
$\mathcal{D}_\ell[\mu K^2]$
2
500
1000
1500
2000
2500
Multipole moment, ℓ
6 parameters model
(Λ-CDM)

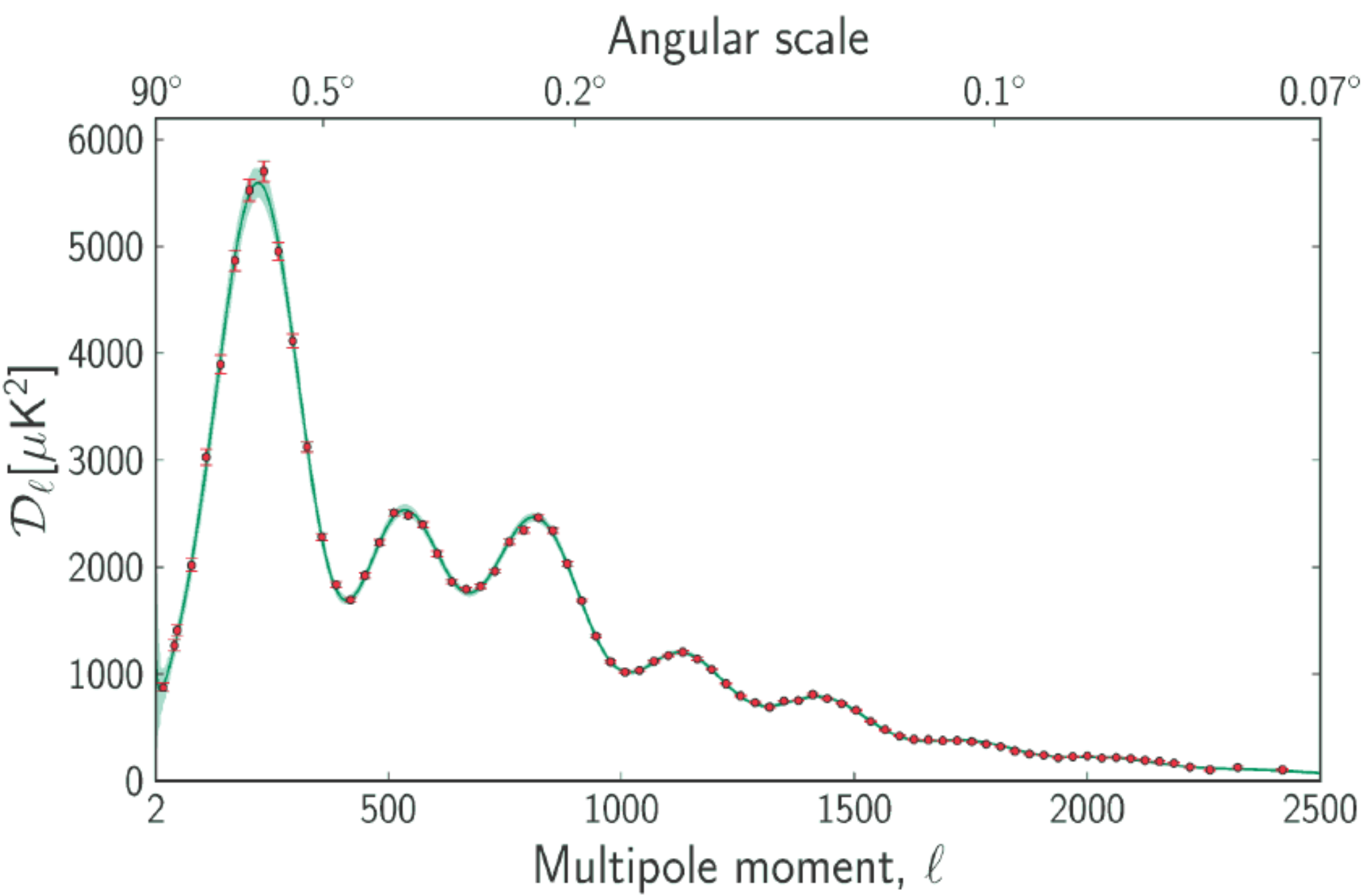
Angular scale
90°
0.5°
0.2°
0.1°
0.07°
6000
5000
4000
3000
2000
1000
0
$\mathcal{D}_\ell [\mu K^2]$
2
500
1000
1500
2000
2500
Multipole moment, ℓ

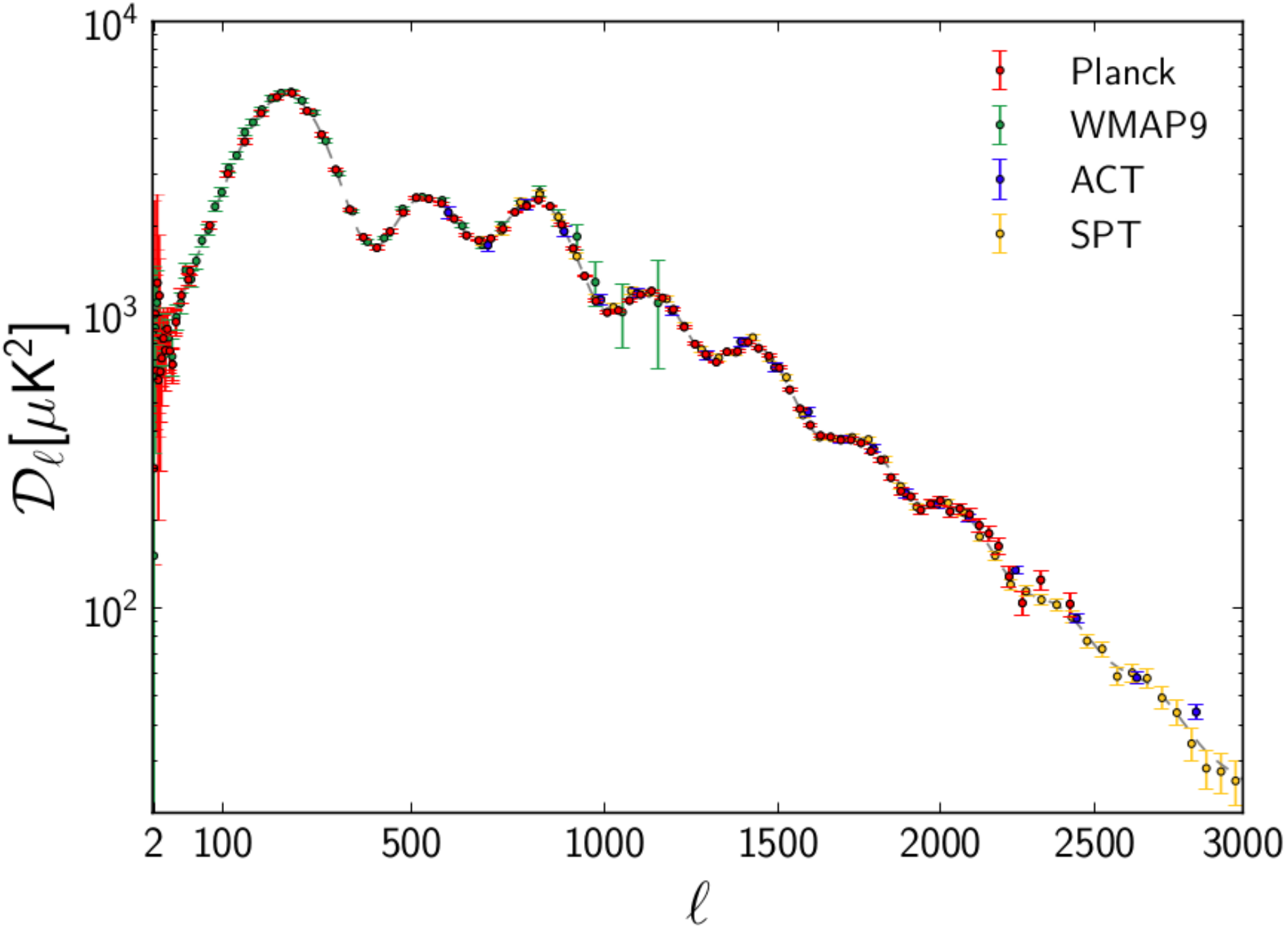
10^4
10^3
10^2
$\mathcal{D}_\ell[\mu K^2]$
Planck
WMAP9
ACT
SPT
2
100
500
1000
1500
2000
2500
3000
ℓ

Comological parameters base-model results

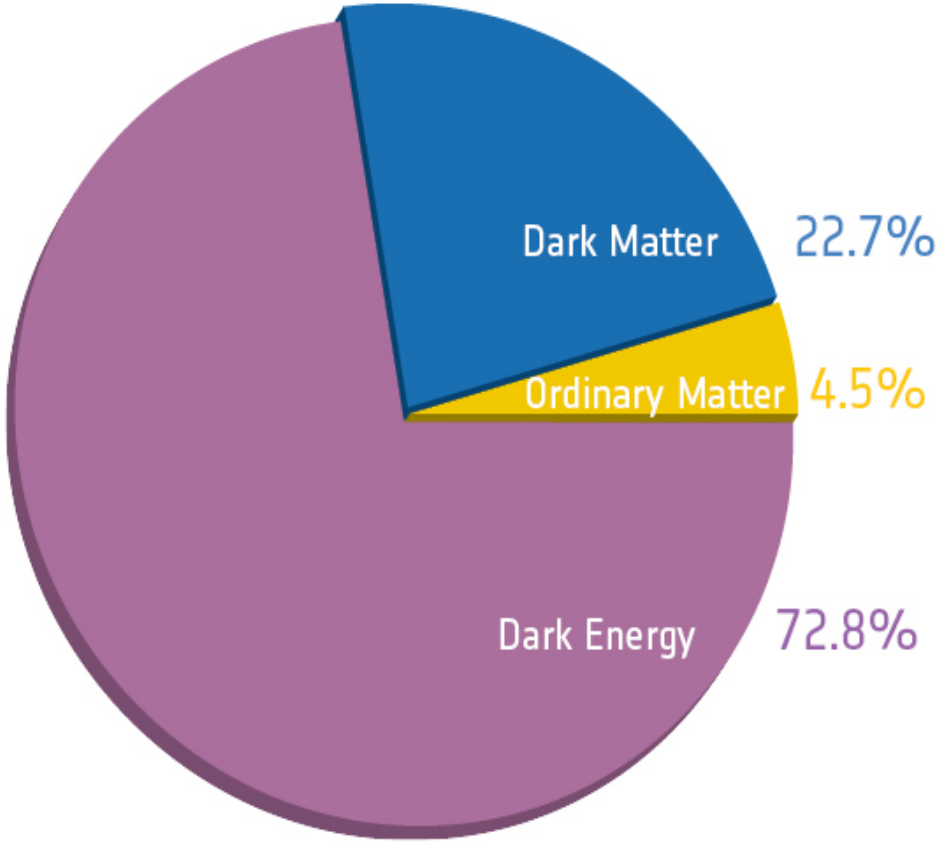

Before Planck

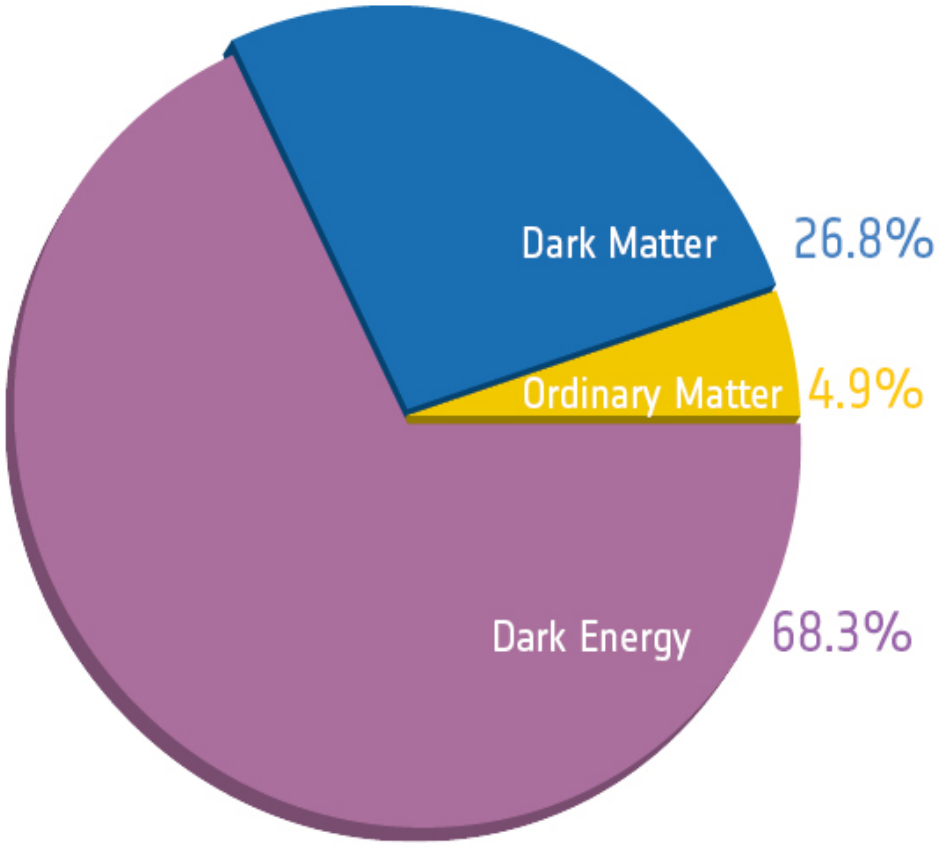

After Planck

Comological parameters
base-model results

baryon density

CDM density

sound horizon (rad)

reionization opacity

Primordial spectrum {

Assumed Curvature: 0

Parameter	*Planck* (CMB+lensing) Best fit	*Planck* (CMB+lensing) 68 % limits	*Planck*+WP+highL+BAO Best fit	*Planck*+WP+highL+BAO 68 % limits
$\Omega_b h^2$	0.022242	0.02217 ± 0.00033	0.022161	0.02214 ± 0.00024
$\Omega_c h^2$	0.11805	0.1186 ± 0.0031	0.11889	0.1187 ± 0.0017
$100\theta_{MC}$	1.04150	1.04141 ± 0.00067	1.04148	1.04147 ± 0.00056
τ	0.0949	0.089 ± 0.032	0.0952	0.092 ± 0.013
n_s	0.9675	0.9635 ± 0.0094	0.9611	0.9608 ± 0.0054
$\ln(10^{10} A_s)$	3.098	3.085 ± 0.057	3.0973	3.091 ± 0.025
Ω_Λ	0.6964	0.693 ± 0.019	0.6914	0.692 ± 0.010
σ_8	0.8285	0.823 ± 0.018	0.8288	0.826 ± 0.012
z_{re}	11.45	$10.8^{+3.1}_{-2.5}$	11.52	11.3 ± 1.1
H_0	68.14	67.9 ± 1.5	67.77	67.80 ± 0.77
Age/Gyr	13.784	13.796 ± 0.058	13.7965	13.798 ± 0.037
$100\theta_*$	1.04164	1.04156 ± 0.00066	1.04163	1.04162 ± 0.00056
r_{drag}	147.74	147.70 ± 0.63	147.611	147.68 ± 0.45
$r_{drag}/D_V(0.57)$	0.07207	0.0719 ± 0.0011		

All-sky map of dark matter

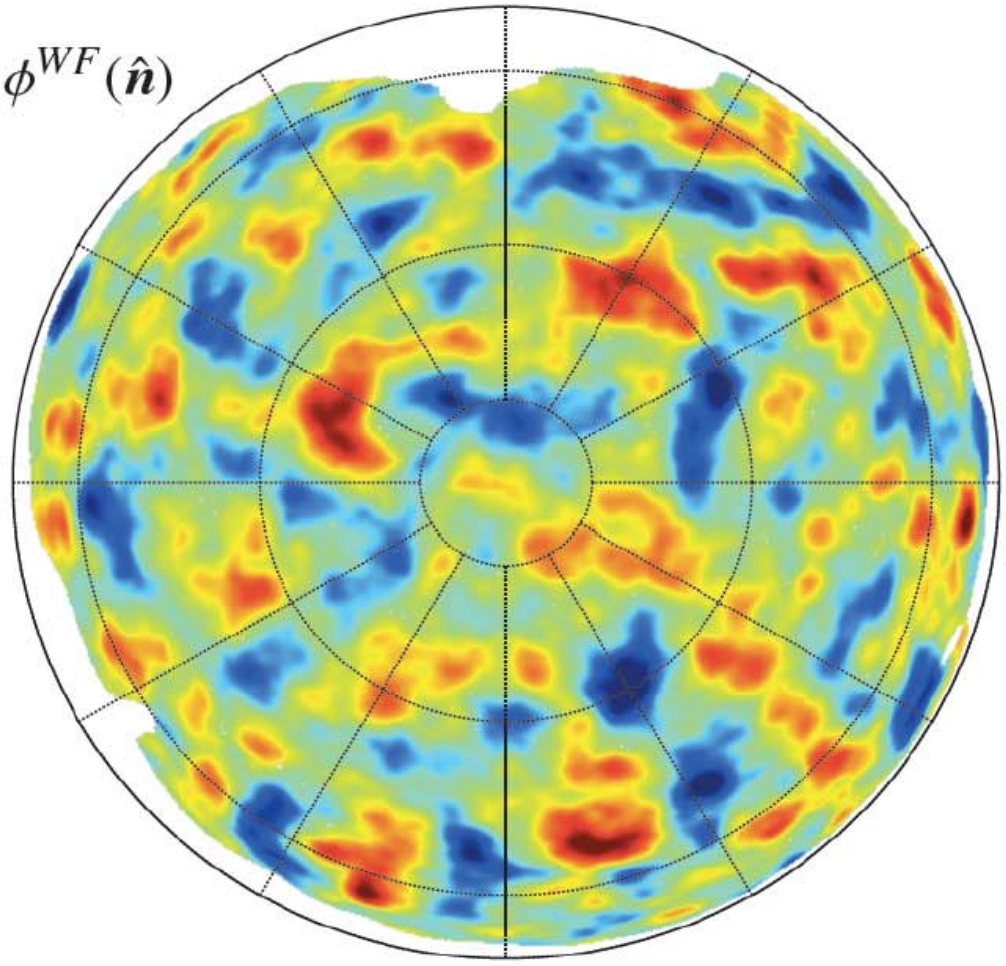

Galactic North

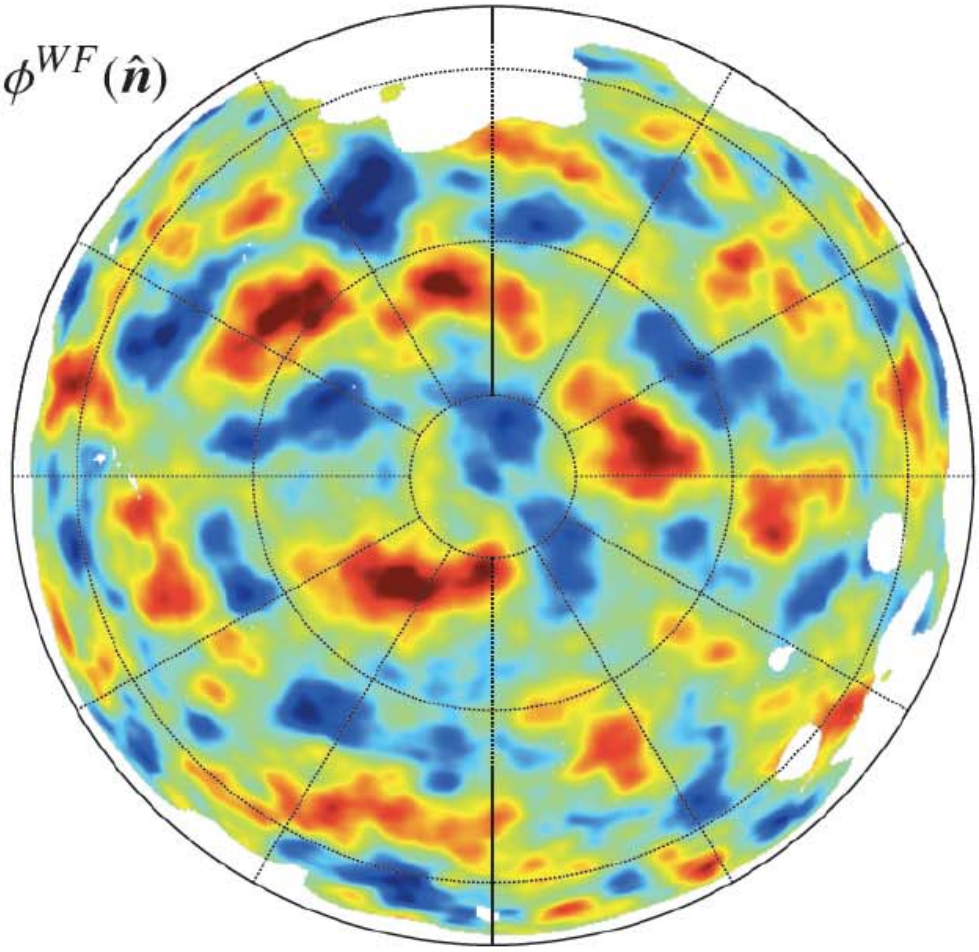

Galactic South

Dark Matter IS THERE !

- Robust and multiple evidence in astrophysics and cosmology.
- Only hints about its nature.
- Next step: what is it ? Direct and indirect searches of particles, theory, LHC ….
- Hear coming talks !